SRI International

Final Report • December 1997

CHARACTERIZATION OF HYDROGEN INGRESS IN HIGH-STRENGTH ALLOYS

B. G. Pound
Electrochemical and Polymer Technology Center

SRI Project PYU-7495

Prepared for:

Office of Naval Research, ONR 332
800 N. Quincy Street
Arlington, VA 22217-5660

Attn: Dr. A. J. Sedriks, Program Officer

Contract No. N00014-95-C-0313

Approved:

S. Narang, Director
Electrochemical and Polymer Technology Center

David M. Golden
Senior Vice President
Chemicals, Energy, and Materials

REPORT DOCUMENTATION PAGE

Form Approved OMB No. 0704-0188

1. AGENCY USE ONLY *(Leave blank)*	2. REPORT DATE	3. REPORT TYPE AND DATES COVERED
	Nov 97	Final 20 Sept 95-19 Sept 97

4. TITLE AND SUBTITLE
Characterization of Hydrogen Ingress in High-Strength Alloys

5. FUNDING NUMBERS
N00014-95-C-0313

6. AUTHOR(S)
Bruce G. Pound

7. PERFORMING ORGANIZATION NAME(S) AND ADDRESS(ES)
SRI International
333 Ravenswood Ave.
Menlo Park, CA 94025

8. PERFORMING ORGANIZATION REPORT NUMBER
PYU-7495

9. SPONSORING/MONITORING AGENCY NAME(S) AND ADDRESS(ES)
Office of Naval Research, ONR 332
800 N. Quincy St.
Arlington, VA 22217-5000

10. SPONSORING/MONITORING AGENCY REPORT NUMBER

11. SUPPLEMENTARY NOTES

12a. DISTRIBUTION/AVAILABILITY STATEMENT
Approved for public release - distribution unlimited

12b. DISTRIBUTION CODE

13. ABSTRACT *(Maximum 200 words)*

The effect of heat treatment on irreversible hydrogen trapping was investigated for high-strength steels (4340, 18Ni (250), and AerMet 100), alloy K-500, and precipitation-hardened alloys (X-750 and 18Ni (250) steel), with the goal of providing insight into the factors governing the intrinsic susceptibility to hydrogen embrittlement (HE). A potentiostatic pulse technique was used to determine irreversible trapping constants (k), which were compared with changes in strength and microstructure. Irreversible trapping in AerMet 100 is associated with two types of carbide, depending on the aging temperature. 4340 steel also undergoes a change in its principal type of irreversible trap with decreasing yield strength. The type of heat treatment for alloy K-500 can produce differences in trapping. Annealing increases k considerably, whereas aging has a negligible effect for the annealed alloy but can result in an increase for the unannealed alloy. 18Ni steel and alloy X-750 both show an increase in k with aging. Carbonitride particles provide the principal irreversible traps in the unaged alloys and appear to be one of the principal traps in aged X-750 but not in the aged steel. The order of the k values for AerMet 100, 4340, 18Ni (250), and two previously studied steels—H11 and 18Ni (300)—inversely parallels their threshold stress intensities for stress corrosion cracking. A correlation was found between k and the observed resistance to HE also for annealed/aged and direct-aged alloy K-500, alloys X-750 and 718, and 18Ni (250) steel and alloy 718.

14. SUBJECT TERMS
High strength steels, Alloy K-500, Ni-base Alloys, Heat Treatment, Aging, Potentiostatic Pulse, Hydrogen Trapping, Hydrogen Embrittlement

15. NUMBER OF PAGES
92

16. PRICE CODE

17. SECURITY CLASSIFICATION OF REPORT	18. SECURITY CLASSIFICATION OF THIS PAGE	19. SECURITY CLASSIFICATION OF ABSTRACT	20. LIMITATION OF ABSTRACT
UNCLASSIFIED	UNCLASSIFIED	UNCLASSIFIED	SAR

PREFACE

This final report describes work performed for the Office of Naval Research in a continuation of our program (Contract No. N00014-95-C-0313) to investigate hydrogen ingress into various high-strength alloys. The work focused on irreversible hydrogen trapping, with a view to characterizing its role in determining the susceptibility of the alloys to hydrogen embrittlement. A potentiostatic pulse technique was used to obtain anodic current transients for the alloys in 1 mol L^{-1} acetic acid/1 mol L^{-1} sodium acetate, and the transients were analyzed using a diffusion/trapping model under interface control conditions to evaluate the trapping constant and hydrogen entry flux in each case.

The report is presented as an Executive Summary followed by five papers that will be published in journals or in conference proceedings:

1. "Hydrogen Trapping in High-Strength Steels," submitted to *Acta Metallurgica et Materialia.*

2. "The Ingress of Hydrogen into Alloy A-286 and 2Be-Cu," submitted to *Corrosion Science.*

3. "The Relationship Between Heat Treatment and Hydrogen Trapping in Alloy K-500," submitted to *Corrosion.*

4. "The Effect of Aging on Hydrogen Trapping in Precipitation-Hardened Alloys," submitted to *Corrosion Science.*

5. "The Effect of Heat Treatment on Hydrogen Trapping in AerMet 100 and Alloy K-500," in *Proceedings of the 1997 Tri-Service Conference on Corrosion* (Wrightsville Beach, NC, 1997), in press.

The first paper covers three high-strength steels: AerMet 100 and AISI 4340 and H11. The next paper concerns a Be-Cu alloy and a stainless steel, A-286, while the third concerns a Ni-Cu alloy, K-500. The fourth paper deals with two precipitation-hardened alloys: 18Ni (250) maraging steel and X-750. The final paper reviews the effect of heat treatment on two of these alloys—AerMet 100 and K-500.

CONTENTS

EXECUTIVE SUMMARY

High-performance alloys often must possess a combination of properties such as strength, toughness, and corrosion resistance. However, their resistance to hydrogen embrittlement (HE) remains a concern in many situations. Microstructural heterogeneities in these and other alloys provide potential trapping sites for hydrogen and so can play a crucial role in determining an alloy's intrinsic susceptibility to HE. However, whether embrittlement will actually occur is also affected by other factors, including the amount of hydrogen entering the alloy. Consequently, alloys need to be characterized in terms of both trapping capacity and the rate of hydrogen entry to assess their likelihood of embrittlement.

This report describes work performed during a continuation of our program with the Office of Naval Research to investigate hydrogen ingress in various alloys. The work focused on irreversible trapping, with a view to characterizing its role in determining the susceptibility of the alloys to HE. A potentiostatic pulse technique was used to obtain anodic current transients for the alloys in 1 mol L^{-1} acetic acid/1 mol L^{-1} sodium acetate containing 15 ppm As_2O_3. The transients were analyzed using a diffusion/trapping model under interface control conditions to evaluate the apparent trapping constant (k_a) and hydrogen entry flux (J) in each case. k_a was then used to determine the irreversible trapping constant (k) and, where possible, the density of irreversible traps.

The first part of this work dealt with the trapping behavior of three high-strength steels: AerMet 100 and AISI 4340 and H11. The order of the k values for these three steels and two 18Ni maraging steels (see the fourth part of this work) inversely parallels their threshold stress intensities for stress corrosion cracking (K_{ISCC}). Irreversible trapping in AerMet 100 varies with aging temperature and appears to be associated with Fe_3C particles at low aging temperatures and M_2C particles at high aging temperatures. For 4340 steel, k can be correlated with K_{ISCC} over a range of yield strengths (1034-1792 MPa). The change in k is consistent with a change in the principal type of irreversible trap from matrix boundaries at high yield strengths to incoherent Fe_3C at lower yield strengths. The principal irreversible traps in H11 at high yield strengths are thought to be similar to those in 4340 steel.

The second part of the study involved a precipitation-hardened stainless steel, alloy A-286, and a precipitation-hardened Cu alloy, 2Be-Cu. The values of k were compared with those for three other precipitation-hardened alloys—718, 925, and 18Ni (250) steel—examined previously. The k values for alloy A-286 and 2Be-Cu were intermediate between those for the two Ni-base

alloys (718 and 925) and were considerably lower than that for the 18Ni steel. The k values of the 18Ni steel, 2Be-Cu, and alloys 718 and A-286 are consistent with test data for their relative resistances to HE.

The next part of the work addressed alloy K-500. Valuws of k and J were obtained for annealed, annealed and aged (AA), and 12-h and 16-h direct aged (DA) specimens of cold drawn Alloy K-500 that had been used earlier to provide as-received (unannealed, cold drawn) and 8-h DA specimens. The type of heat treatment can produce marked differences in irreversible trapping. The intrinsic susceptibility to HE, as defined by k, is increased considerably by annealing. Aging has a negligible effect on the intrinsic susceptibility for the annealed alloy but can result in a sizable increase for the unannealed alloy if performed for extended times. The intrinsic susceptibilities for the AA and DA alloys can be correlated with the observed resistances to HE, implying that the previously reported decrease in the resistance to HE produced by annealing is caused to a large extent, if not entirely, by a change in the irreversible traps.

The final part of the work was concerned with two precipitation-hardened, nickel-containing alloys: 18Ni maraging steel and alloy X-750. Aging causes an increase in k for both alloys. The value of k for aged alloy X-750 is higher than the values for three other hardened Ni-base alloys (625, 718, and 925) but is considerably lower than the value for the aged 18Ni steel. A correlation was found between k and the observed resistance to HE for three groups of aged alloys: X-750 and 718; 18Ni (250) and 718; and 18Ni (250), 18Ni (300), and 4340 steels. Carbonitride particles appear to provide the principal irreversible traps in unaged alloy X-750 and 18Ni (250) steel. They also appear to be one of the principal irreversible traps in aged alloy X-750, with additional trapping resulting from at least one other microstructural heterogeneity that could be grain boundary carbides. For the aged 18Ni steel, however, carbonitrides make only a small contribution to irreversible trapping, the main contribution coming from some other heterogeneity that possibly involves intergranular S.

HYDROGEN TRAPPING IN HIGH-STRENGTH STEELS*

Abstract—Hydrogen trapping in three high-strength steels—AerMet 100 and AISI 4340 and H11—was studied using a potentiostatic pulse technique. Values of the irreversible trapping constant (k) and the hydrogen entry flux were determined for these alloys in 1 mol L^{-1} acetic acid/1 mol L^{-1} sodium acetate. The order of the k values for the three steels and two 18Ni maraging steels previously studied inversely parallels their threshold stress intensities for stress corrosion cracking (K_{ISCC}). Irreversible trapping in AerMet 100 varies with aging temperature and appears to be associated with Fe_3C particles at low aging temperatures and M_2C particles at high aging temperatures. For 4340 steel, k can be correlated with K_{ISCC} over a range of yield strengths (1034-1792 MPa). The change in k is consistent with a change in the principal type of irreversible trap from matrix boundaries at high yield strengths to incoherent Fe_3C at lower yield strengths. The principal irreversible traps in H11 at high yield strengths are thought to be similar to those in 4340 steel.

INTRODUCTION

Various steels are used for aircraft components such as landing gear and arresting hooks because of their high-strength characteristics. However, these steels must meet stringent requirements with respect not only to strength but also to fracture toughness and resistance to environmentally assisted cracking. AISI 4340 steel has been used extensively for high-strength aircraft components but becomes highly susceptible to hydrogen embrittlement (HE) as its yield strength increases above 1379 MPa [1, 2]. A newer alloy developed for aerospace applications is a martensitic steel—AerMet 100—that is strengthened by precipitation of M_2C carbides (M = Mo and Cr, with Fe also being identified in one study) [3, 4]. This steel is reported to have a higher resistance to hydrogen-assisted cracking in 3.5% NaCl than 18Ni (250) maraging steel, 300M, and AISI 4340 and H11 steels [5-7]. However, precipitation-hardened martensitic steels as a group tend to be rather prone to HE [8-10].

The resistance of an alloy to HE is strongly affected by the interaction of hydrogen (H) with microstructural heterogeneities that act as H traps [11]. The type of heterogeneity can play a crucial role in determining an alloy's intrinsic susceptibility to HE, with large irreversible (high

* Submitted to *Acta Metallurgica et Materialia.*

binding energy) traps often imparting a high susceptibility [12, 13]. Hence, characterization of alloys in terms of irreversible trapping can allow their intrinsic HE susceptibility to be assessed and provide a basis for examining the effect of traps on the observed resistance to HE.

Over the last few years, H entry and trapping in various high-strength alloys have been investigated by using a potentiostatic pulse technique [14-17]. The rates of H entry and rate constants (k) for irreversible trapping were determined. The results showed, for most of these alloys, a correlation between the intrinsic susceptibility, as represented by k, and the actual resistance to HE observed in mechanical tests.

In the present work, the pulse technique was used to investigate irreversible trapping in AerMet 100 and AISI H11 and 4340 steels. The variation in k was examined as a function of yield strength for AerMet 100 and 4340 steel. AerMet 100 and H11 extended the range of high-strength steels (4340 and 18Ni) examined to date [14, 15, 18], while the 4340 steel provided a comparison with specimens of this alloy that had already been studied at other yield strengths [14]. The results were used to characterize the intrinsic susceptibility of the steels to HE in terms of their irreversible trapping constants and to elucidate the influence of heat treatment on the resistance of these alloys to HE. The intrinsic susceptibilities were compared with results for the actual resistance to HE observed in tests by other workers. A further goal, where possible, was to identify the principal irreversible traps in each alloy.

EXPERIMENTAL PROCEDURE

Alloys

Table 1 shows the composition of each steel. The AerMet 100 and H11 steel were supplied in the form of rod with a diameter of 1.36 cm and 1.30 cm, respectively. The 4340 steel was supplied as 1.27-cm plate that was machined into two rods with a diameter of 1.27 cm and a length of 1.27 cm.

AerMet 100. The AerMet 100 was received in an overaged/annealed (677°C/16 h) condition. A section of rod was subsequently solution treated at 885°C for 1 h, air cooled to 66°C over 1-2 h, further cooled to -73°C for 1 h, and finally aged for 5 h at temperatures of 270°, 370°, and 482°C, which is the standard aging temperature.

The microstructure of AerMet 100 was not examined in this study, because it has been investigated in detail by other workers [3, 4]. This steel has an Fe-Ni lath martensite structure. Rod-shaped Fe_3C precipitates were observed by Novotny in the steel aged between 316° and 482°C but not at 204°C [4], which implies that the precipitates can begin to form at a temperature

somewhere in the range from 204° to 316°C. Aging at temperatures above 454°C causes precipitation of coherent M_2C carbides within the martensite, as noted above. Novotny did not detect these carbides in specimens aged at 454°C, but Ayer and Machmeier observed needle-shaped precipitates, which were too fine to be characterized [3]. Novotny found that the M_2C carbides produced by a 482°C/5 h age are well-dispersed, very fine, rod-shaped precipitates with an average length of 9.1 nm. Similar observations were made by Ayer and Machmeier, who reported the carbides as having a length of ~8 nm and a diameter of ~3 nm.

Ayer and Machmeier found that the M_2C carbides contained Cr, Mo, and Fe and that there was no Fe_3C, at least at the grain boundaries, in a 482°C-aged sample. In contrast, Novotny reported that only Mo and Cr constituted the metallic components in the M_2C carbides and that Fe_3C precipitates were still present after aging at 482°C but were smaller (40 nm long × 5 nm wide) than those formed at aging temperatures from 316° to 454°C. AerMet 100 also contains ~3 vol% austenite, as quenched and when aged for 5 h at temperatures from 93° to 468°C. Aging at 482°C increased the amount of austenite slightly to 4 vol%. The austenite is present as a thin film (~3 nm) at the martensite lath boundaries.

H11. The H11 steel was obtained in an annealed condition with a hardness of HRC 20. The steel was heat treated in accordance with the procedure recommended by the producer: 1010°C for 0.5 h, Ar (instead of air) cool, followed by three treatments at 538°C for 2.5 h with an Ar cool between each treatment. The resulting yield strength of the hardened alloy was 1661 MPa. Only the hardened alloy was tested in the present work. The steel was examined under the scanning electron microscope and found to be free of sulfide inclusions, at least at the micrometer level.

4340. The as-received 4340 plate was produced from an argon-oxygen-decarburized heat and was vacuum-arc remelted (VAR) before being forged, rolled, and annealed. After the plate was machined into rods, two specimens of the steel were heat treated as shown in Table 2 to give yield strengths of 1034 MPa (150 ksi) and 1379 MPa (200 ksi). The two specimens are denoted as 4340 (150) and 4340 (200), respectively, in accordance with the nomenclature used to identify a grade of maraging steel by its nominal yield strength (ksi) in parentheses. Table 2 also lists the heat treatments and yield strengths for the previous specimens, which are denoted 4340 (175) and 4340 (260).

The inclusion content had been examined previously [19], and the steel was found to contain ~10^5 m^{-2} MnS inclusions randomly distributed through it. The inclusions were ellipsoidal with the major axis transverse to the rolling direction. However, they were treated as spherical to

determine the volume density, which was calculated to be 2×10^9 m^{-3}. The mean radius of the inclusions averaged over the transverse and parallel directions was 9.2 μm.

Electrochemical tests

Details of the electrochemical cell and instrumentation have been given previously [14]. The test electrodes of each steel consisted of a 1.27-cm length of rod (as-supplied or machined) press-fitted into a polytetrafluoroethylene sheath so that only the planar end surface was exposed to the electrolyte. The surface was polished before each experiment with SiC paper followed by 0.05-μm alumina powder. The electrolyte contained 1 mol L^{-1} acetic acid and 1 mol L^{-1} sodium acetate (pH 4.8) with 15 ppm As_2O_3 and was deaerated continuously with argon before and throughout data acquisition. The potentials were measured with respect to a saturated calomel electrode (SCE). All tests were performed at 22° ± 1°C.

The test electrode was cathodically charged with H at a potential E_c for a time t_c, after which the potential was stepped anodically to a value 10 mV negative of the open-circuit potential E_{oc}. Anodic current transients were obtained over a range of charging times, typically from 5 to 60 s, at different overpotentials ($\eta = E_c - E_{oc}$). The open-circuit potential of the test electrode was measured immediately before each charging time and was also used to monitor the stability of the alloy surface.

RESULTS

The current transients were analyzed using a diffusion/trapping model based on a constant entry flux at the surface [14, 20]. According to the model, the anodic charge (C m^{-2}) is given by

$$q'(\infty) = FJt_c\{1 - e^{-R}/(\pi R)^{1/2} - [1 - 1/(2R)]\mathrm{erf}(R^{1/2})\} \quad (1)$$

where F is the Faraday constant, J is the ingress flux in mol m^{-2} s^{-1}, $R = k_a t_c$, and k_a is an apparent trapping constant measured for irreversible traps in the presence of reversible traps. The charge $q'(\infty)$ is equated to the charge (q_a) passed during the experimental anodic transients. q_a can be associated entirely with absorbed H, because the adsorbed charge is almost invariably negligible. k_a is related to the irreversible trapping constant by kD_a/D_L, where D_a is the apparent diffusivity and D_L is the lattice diffusivity of H. The magnitude of k depends on the density of particles or defects (N_i) providing irreversible traps, the radius (d) of the trap defects, the diameter (a) of the metal atom, and D_L [21]:

$$k = 4\pi d^2 N_i D_L / a \quad (2)$$

The term d^2N_i can be used to represent the trapping capacity and thus provides a basis for proposing k as an index of an alloy's intrinsic susceptibility to HE. The correlation observed between k and the actual resistance to HE suggests that k contains enough key parameters to be effective as an index of susceptibility for the alloys studied to date at their respective yield strengths. The use of k as an index of susceptibility has been discussed in more detail elsewhere [17].

For aged AerMet 100, and H11 and 4340 steels, equation (1) could be fitted to the experimental data for q_a to obtain values of k_a and J, where J was constant over the range of charging times at each potential. For overaged AerMet 100, q_a increased linearly with t_c, indicating that $k_a = 0$ and therefore that irreversible trapping was negligible. Tables 3 through 5 show the number of tests and range of overpotentials used for each steel. Also listed are the number of k_a values and the mean k_a obtained for each test.

The values of k_a for aged AerMet 100 are presented in Fig. 1. In all the tests, k_a was independent of charging potential, as is required for the diffusion/trapping model to be valid, because the trapping characteristics should be unaffected by electrochemical conditions unless the traps become filled to a significant extent. The aged alloy, in contrast to the overaged alloy, exhibited moderately high values of k_a, which indicated pronounced irreversible trapping. However, raising the aging temperature from 270° to 370°C did not have a significant effect on k_a, whereas it was increased considerably by aging at the standard temperature of 482°C. The overall mean value of k_a for each aging temperature is given in Table 6, which shows that k_a for the 482°-aging is 50% higher than the value for the two lower aging temperatures.

The values of k_a for H11 and 4340 steel are given in Fig. 2. k_a was independent of charging potential also for these two steels. The values for the 4340 (150) specimen were a little more scattered than for the 4340 (200) specimen but appeared to be slightly higher. Table 6 indicates that the mean values of k_a for these two specimens could differ to a small extent but that the difference is within experimental error.

The H11 steel usually exhibited a few blue/black tarnish spots at the end of each test. The presence of these spots is not desirable, because the surface conditions for H entry may be affected in those areas during the test. A further issue was that values of k_a could be obtained only over a narrow potential range that was limited by the rate of H entry at lower overpotentials and by bubble formation at high overpotentials. Despite these two issues, the values of k_a were surprisingly consistent between tests for H11.

DISCUSSION

Irreversible trapping constants

Irreversible trapping constants (k) were calculated from the mean values of k_a by correcting for the effect of reversible traps. The correction is made using diffusivity data for the "pure" alloy to obtain the lattice diffusivity (D_L) and for the actual alloy to obtain the apparent diffusivity (D_a), so that the ratio of D_L to D_a can be determined. From the viewpoint of diffusivity, the "pure" alloys were assumed to be Fe-11Ni-3Cr for AerMet 100, Fe-5Cr for H11, and Fe for 4340 steel. Co is a prominent alloying element in AerMet 100, but it is regarded as an anti-trap in Fe [11] and has been shown to have little effect on the diffusivity [22]. Minor elements in the actual alloys were treated as reversible traps and in fact were assumed to be primarily responsible for reversible trapping.

For body-centered cubic Fe, elements such as Cr can have a marked effect on the diffusivity of H [23]. For example, the addition of 5 at% Cr to Fe decreases the diffusivity by over two orders of magnitude at 27°C. Although AerMet 100 differs in having a martensitic lattice and in Cr being considered one of its major elements, minor elements that act as reversible traps could also be expected to have significant but smaller effects in this alloy. Based on the case of Cr, even these reduced effects are likely to be large enough to dominate those of microstructural defects such as dislocations. The austenite present at lath boundaries may provide reversible traps in the actual alloy, but the small amount (3-4 vol%) suggests that the effect of the austenite should be small enough to ignore, particularly for a martensitic lattice. The contribution of the martensitic lattice itself is discussed below.

AerMet 100. The diffusivity was not available for martensitic Fe-11Ni-3Cr, so a value was estimated for D_L from data for ferritic Fe-3Cr [23]. The diffusivity for Fe-3Cr is $(7.5 \pm 0.5) \times 10^{-11}$ m^2 s^{-1}, which approaches the diffusivities for quenched and tempered martensitic steels (even with reversible traps) such as 4340 ($\sim 1 \times 10^{-11}$ m^2 s^{-1}) [24, 25] and thus suggests that the decrease caused by the Cr is enough to effectively incorporate that resulting from the martensitic lattice of AerMet 100. The effect of Ni on the diffusivity for Fe is much smaller than that of Cr; for example, 5Ni decreases the diffusivity by a factor of only 1.3 compared with ~140 for 5Cr [23, 26]. Hence, it was assumed that the effect of 11Ni on the diffusivity could be neglected. The presence of two phases (α and γ) in Fe-Ni alloys containing between 10% and 33% Ni [27, 28] was ignored for the purpose of estimating data for a martensitic steel. Thus, D_L was taken simply as the diffusivity for Fe-3Cr.

Diffusivity data were also not available for AerMet 100. However, the diffusivity for another high-strength steel—D6AC with a yield strength of 1550 MPa—has been studied [24] and, although this steel contains only 1.08 Cr, was considered to provide the most appropriate value of D_a. The diffusivity obtained from electrochemical permeation measurements for D6AC is $(7.8 \pm 0.5) \times 10^{-12}$ m^2 s^{-1}. Thus, a value of 9.6 was obtained for D_L/D_a and was used to calculate values of k for AerMet 100, as given in Table 6. The same value of D_L/D_a was assumed to apply to the overaged alloy and the partially and standard (482°C) aged alloy, because the Fe_3C and M_2C particles precipitated during aging were considered irreversible traps [29] (discussed below) and therefore should not affect D_a as measured when only reversible traps are effective (irreversible traps being saturated).

H11 Steel. The diffusivity for Fe-5Cr is $(1.3 \pm 0.1) \times 10^{-11}$ m^2 s^{-1} [23]. The diffusivity for H11 has been determined from permeation measurements and is $(3.0 \pm 0.2) \times 10^{-13}$ m^2 s^{-1} [24]. Hence, the value of D_L/D_a was calculated to be 43.3 ± 6.2 for H11.

4340 Steel. Diffusivity data for pure iron show considerable variation, but a value of 5×10^{-11} m^2 s^{-1} at 25°C appears to be reliable to use for D_L [30-32]. Some data have been reported for 4340 steel but only at high strengths. Kargol and Paul obtained a value of ~10^{-11} m^2 s^{-1} for electroslag remelted (ESR) 4340 steel with a hardness of HRC 50 [25], which was in good agreement with the value of 1.4×10^{-11} m^2 s^{-1} obtained by Kortovich and Steigerwald for 4340 steel with a yield strength of 1427 MPa [24]. Beck et al. obtained a slightly higher value of 2.7×10^{-11} m^2 s^{-1} for 4340 steel with a tensile strength of 1792 MPa [33]. Kargol and Paul's value was the most suitable for the 4340 (260) steel because their ESR steel, like the VAR specimens used in this work, was produced by a remelting process and because it was similar in hardness to the VAR steel (HRC 53).

Diffusivities for 4340 steel at the other yield strengths (1034 to 1379 MPa) were estimated from data for comparable steels. Radhakrishnan and Shreir used permeation measurements to determine the diffusivity for R.S. 140 steel (0.4C, 0.6Mn, 1.0Mo, 0.3Ni, 0.2Si, <0.01S, <0.015P) at different tempering temperatures [34]. This steel has a similar composition to 4340 steel and was austenized under similar conditions of 850°C for 45 min. The tempering time was 1 h, which was also used for the 4340 (175) steel but was less than the time for the 4340 (150) and 4340 (200) specimens (2 h) and the 4340 (260) specimen (80 min). The diffusivity for R.S. 140 was independent of tempering temperature up to 400°C and had a value of ~1.8×10^{-11} m^2 s^{-1}, which is commensurate with the values for 4340 steel at high yield strengths. Yield strengths were not given for the R.S. 140, but data are available for 4340 steel austenized at 870°C for 1 h and tempered for 1 h at various temperatures; 320°C gives a yield strength of 1379 MPa and 400°C gives 1206 MPa [35]. Thus, the 4340 steel used in the present work was assumed to have a

constant diffusivity at yield strengths down to at least 1379 MPa, allowing for the differences in heat treatment.

Radhakrishnan and Shreir did not specify whether the diffusivity for R.S. 140 was obtained from the first permeation transient or subsequent transients and hence whether it was affected by irreversible trapping. However, they discussed the variation in diffusivity within the context of microstructural changes, including carbide precipitation. When the steel is tempered at ≥400°C, the carbides, which become irreversible traps in iron and steels as they become less coherent [29], grow enough to be resolved at high magnification [34]. (In 4340 steel, carbides have been identified as irreversible traps for tempering temperatures of ≥400°C, or yield strengths of ≤1206 MPa [35]). The implication is that the diffusivity data obtained by Radhakrishnan and Shreir for R.S. 140 tempered above 400°C is affected by irreversible traps as well as reversible traps, whereas the values required to obtain k from k_a should reflect only reversible trapping.

Because of the lack of diffusivity data for 4340 steel at different yield strengths, the diffusivity was assumed in our previous work to be the same for the 4340 (175) and 4340 (260) specimens. However, a subsequent comparison with other steels indicated that acceptable diffusivity data for 4340 steel at yield strengths below 1379 MPa (200 ksi) can be estimated from measurements made by Kim and Loginow on a Ni-Cr-Mo steel containing 0.13C, 0.29Mn, 0.011S, 2.97Ni, 1.60Cr, and 0.51Mo [36]. Although this steel has a lower C content than 4340 steel, and the diffusivities were obtained at yield strengths from 655 to 1034 MPa, Kim and Loginow considered the diffusivity in terms of reversible trapping alone. Fig. 3 shows their data together with measurements for 4340 steel at a yield strength of 1379 MPa. Although the D_a values for 4340 steel were obtained for higher yield strengths, they can be used for 1379 MPa because, as discussed above, D_a was assumed to be constant down to this yield strength. The diffusivities for the Ni-Cr-Mo steel empirically show a logarithmic dependence on yield strength, and extrapolation to 1379 MPa gives a diffusivity that is within the range of values reported for 4340 steel. Accordingly, it was assumed that the diffusivity for 4340 steel at yield strengths of 1034 MPa and 1206 MPa can be approximated reasonably well by values obtained from the empirical dependence for the Ni-Cr-Mo steel: 6.3×10^{-11} m^2 s^{-1} for 1034 MPa and 3.5×10^{-11} m^2 s^{-1} for 1206 MPa.

Susceptibility to HE

Table 6 compares the trapping constants for AerMet 100, H11, and 4340 together with 18Ni (250) and 18Ni (300) steels [18]. AerMet 100 (partially and standard aged) has the lowest k value and was therefore considered to have the lowest intrinsic susceptibility to HE of the five steels. The order of the k values for these steels at the highest strengths used in this work

inversely parallels typical values of the steels' threshold stress intensities for stress corrosion cracking (K_{ISCC}) in 3.5% NaCl [5, 10] (Fig. 4); that is, a lower value of *k* corresponds to a higher value of K_{ISCC}. This trend is underscored by the similarity in *k* values matching the similarity in K_{ISCC} values for the two most susceptible steels—4340 and H11. The *k* values indicate that the intrinsic susceptibility may actually be a little lower for H11. The order of this difference is consistent with test results showing that, for these two steels in distilled water, the failure times at various applied stress intensities were longer for H11 [37]. Furthermore, the value of *k* for H11 is consistent with that for 18Ni (250) steel in terms of the degree of embrittlement observed in electrolytic charging tests [38].

The inverse parallel between *k* and K_{ISCC} supports the general view that H plays the predominant role in stress corrosion cracking of martensitic steels [39]. Thus, for these four steels, *k* can be correlated with the observed resistance to HE, as represented by K_{ISCC}. This correlation provides additional support for the concept of *k* as an index of intrinsic susceptibility for high-strength alloys. In addition, it implies that the intrinsic susceptibility, as defined by *k*, is a principal factor determining the observed resistance of these high-strength steels to HE.

AerMet 100. Fig. 5 compares the dependence of *k* on aging temperature with a typical dependence of yield strength, as reported by the alloy producer [40]. *k* clearly follows the general trend in yield strength, exhibiting an initial increase before leveling off and then increasing more sharply. The changes in the two curves match reasonably well with respect to aging temperature, bearing in mind that the yield strength curve is not specific to either the form or size of alloy used in these tests. The increase in *k* with aging temperature, particularly between 370° and 482°C, implies that the observed resistance to HE should decrease based on the correlation between *k* and K_{ISCC}. Such a decrease would be consistent with the decreases in HE resistance observed for 4340 steel and 18Ni maraging steel as their yield strengths are increased [1, 2, 10]. Bernstein and Thompson have shown, however, that the resistance to HE is more directly an effect of microstructure than of strength [39, 41]. Thus, *k* would not necessarily be expected to show a correlation with yield strength. Clearly, the more appropriate comparison is between *k* and the microstructural changes that occur during aging.

Fig. 6 shows the variation in *k* and carbide size with aging temperature. The increase in *k* occurs in two stages. The first stage corresponds to Fe_3C precipitation and the second stage corresponds to M_2C precipitation. The arrest in *k* between 270° and 370°C coincides with the aging temperature range where the Fe_3C particles do not change in size. Furthermore, the subsequent steep increase in *k* occurs with the transition in carbides from Fe_3C to M_2C and evidently reflects the sharp increase in size of the M_2C particles. The lath boundary austenite may provide irreversible traps and hence the higher *k* at 482°C may have resulted from the increase in

austenite. However, the austenite increased only from 3 vol% to 4 vol%, and also k~0 for the unaged alloy with its 3 vol% austenite.[1] Another possibility is that impurities such as S and P segregate to grain boundaries during aging, thereby causing an increase in the irreversible trapping capability. Nevertheless, the M_2C particles remain most likely responsible for the increased k at 482°C. Thus, irreversible trapping in AerMet 100 appears to involve the carbides primarily, with Fe_3C particles providing the principal traps for lower aging temperatures and M_2C particles filling that role for higher aging temperatures.

The M_2C particles in AerMet 100 aged at 454°C are coherent with the matrix,[2] but at least some of them appear to lose coherency at 482°C [3]. Trapping at these particles is therefore expected to become more irreversible with higher aging temperatures [29]. Lee and Waldman have shown that stress corrosion cracking in AerMet 100 aged at 482°C is predominantly intergranular [42, 43], which implies that the loss of coherency must occur preferentially at grain boundaries, if the resistance to HE is governed, at least partly, by irreversible trapping (as indicated by the correlation with k) and if the less coherent M_2C particles are the principal irreversible traps produced by aging at 482°C.

4340 Steel. Fig. 7 shows the dependence of $1/k$ and K_{ISCC} on yield strength. $1/k$, being the inverse of k, can be regarded as a measure of the intrinsic *resistance* to HE and so provides a ready comparison with the observed parameter, K_{ISCC}. Data for K_{ISCC} were taken from studies by Peterson et al. on 4340 steel in flowing seawater [1] and by Sandoz on the steel in 3.5% NaCl [2]. $1/k$ follows the trend in K_{ISCC} as the yield strength increases, showing a steep decrease before leveling off at approximately 1380 MPa. The good agreement between the trends of $1/k$ and K_{ISCC} is further evidence of the role of H in stress corrosion cracking of martensitic steels.

The change in the value of k with decreasing yield strength suggests a change in either the density or size, or even the type, of principal irreversible trap and therefore in $N_i d^2$. Sulfide inclusions are important irreversible traps in 4340 steel, as shown by thermal desorption results [44] and by differences in H absorption and outgassing between different grades of 4340 steel [25]. However, incoherent Fe_3C and high angle lath boundaries and grain boundaries can also act as irreversible traps, although their presence depends on the tempering conditions [35]. MnS inclusions were found to act as traps in a low alloy steel (0.34C-1Cr) tempered at 300°C, with precipitates coming into play in specimens tempered at 600°C [45]. Hence, sulfide inclusions may provide the predominant irreversible traps in 4340 steel at very high yield strengths (where there is

---

[1] Any additional reversible trapping caused by the slightly higher level (1 vol%) of austenite in the standard aged alloy would decrease D_a and thereforee increase k. Hence, the effect of aging would appear even more pronounced.
[2] Coherent particles are likely to be more reversible in terms of trapping [29]. If the coherent M_2C particles were reversible traps, D_a would be expected to decrease as the aging temperature is increased above 454°C, and so k would increase still more sharply with aging temperature.

negligible Fe_3C) and another heterogeneity (such as Fe_3C) may become the principal trap as the yield strength is decreased.

In our previous work, it was reported that k and hence N_i did not change significantly for yield strengths of 1206 MPa and 1792 MPa, but this conclusion was based on the rough approximation that D_a for 4340 steel, as noted above, did not vary significantly with heat treatment [14]. The apparent lack of change in N_i suggested that sulfide inclusons could be the principal irreversible traps. In addition, the trap density calculated on the basis of sulfide inclusions differed from the actual concentration of inclusions by a factor of 10, which was regarded as being reasonably close. However, this difference may imply that the inclusions are not the principal irreversible traps in 4340 steel, even at high yield strengths.

For high yield strength (≥1379 MPa) 4340 steel, the other irreversible traps are high-angle austenite grain boundaries, unrecovered lath boundaries, lath colony boundaries, and any microcracks [35]. High strength 4340 steel tends to exhibit primary and secondary crack paths along these irreversible traps. Some secondary cracks have also been observed to intersect and run along inclusions, but they were not a major occurrence, even in 4340 steel containing a significant level (0.013 wt%) of S [35]. In view of this observation and the k-K_{ISCC} correlation linking H trapping to cracking, inclusions can probably be discounted as the principal irreversible traps at high (and low) yield strengths.

The decrease in k with yield strength for 4340 steel below 1379 MPa indicates a decrease in the irreversible trapping capacity and coincides with a marked rise in K_{ISCC}. The inverse relationship between trapping capacity and K_{ISCC} at these yield strengths is consistent with other work [35] in which it was found that 4340 steel with a yield strength of ≤1206 MPa does not contain a high enough density of large irreversible traps to promote a large fraction of interfacially aligned fracture paths.

Incoherent Fe_3C and any microcracks have been identified as the irreversible traps in 4340 steel at yield strengths of 1206 MPa and lower [35]. Lath boundaries present at higher strengths undergo a high-to-low angle transformation. In addition, as the yield strength decreases below 1206 MPa, the Fe_3C coarsens, which causes a decrease in the carbide-ferrite interfacial area. This decrease coupled with the lath boundary transformation coincides with the decrease in k, which suggests that the principal irreversible traps are associated with Fe_3C in 4340 steel with yield strengths ≤ 1206 MPa. The incoherent Fe_3C tends to accumulate at low angle lath boundaries, which provide a secondary H-assisted crack path [35]. Thus, H trapping at Fe_3C appears to enhance fracture in lower-yield strength (≤1206 MPa) 4340 steel by inducing cracking at lath boundaries.

The primary crack path in the lower-yield strength 4340 steel was found to be transgranular, involving approximately equal amounts of ductile tearing and transgranular cleavage [35]. Both fracture modes were observed in the uncharged steel, but the proportion of transgranular cleavage was smaller. Whether irreversible traps also play a role in increasing the fraction of transgranular cleavage is unknown. On the other hand, the correlation between k and K_{ISCC} suggests that the higher K_{ISCC} values at lower yield strengths could be due, at least partly, to the change in H trapping from sites that affect primary cracking to sites that just affect secondary cracking.

H11 Steel. Irreversible trapping in H11, as in other quenched and tempered steels, might be expected to occur at particle-matrix interfaces associated with sulfide inclusions and carbide precipitates, and at high-angle grain boundaries [29]. However, as noted above, the steel is essentially free of sulfide inclusions, and it does not contain Ti, which is a prominent irreversible trap as a carbide. H11 does contain the carbide-formers Cr and Mo, but specimens heated to 1010°C, air-quenched, and double-tempered at 510°C exhibit only a small amount of very fine carbide [46]. Hence, the irreversible traps in H11 at a yield strength of 1661 MPa are speculated to be similar to that in 4340 steel at high yield strengths (≥1379 MPa), being principally matrix boundaries with carbides making only a minor contribution.

SUMMARY

- AerMet 100 in its standard aged (482°C) condition has the lowest value of k among the five high-strength steels, whereas H11 and 4340 steel have the highest values. Hence, AerMet 100 is considered to have the lowest intrinsic susceptibility to HE of the five steels, whereas H11 and 4340 steel are the most susceptible.
- For the five steels, the observed resistance to HE, as represented by K_{ISCC}, can be correlated with the intrinsic susceptibility defined by k. This correlation implies that the intrinsic susceptibility is a principal factor determining the observed resistance of these high-strength steels to HE.
- The intrinsic susceptibility (as represented by k) of AerMet 100 to HE increases with aging temperature, particularly from 370° to 482°C. AerMet 100 exhibited a large difference in k between overaged (annealed) and aged specimens. In contrast to the overaged alloy, the partially and standard aged alloy displayed significant irreversible trapping, which appears to be associated with Fe_3C particles at low aging temperatures and M_2C particles at high aging temperatures.

- For 4340 steel, the variation in k with yield strength matches that for K_{ISCC}, which further illustrates the correlation between intrinsic susceptibility and observed resistance to HE of martensitic steels. The decrease in k with yield strength indicates a decrease in the irreversible trapping capacity and is consistent with a change in the principal type of irreversible trap from matrix boundaries at high yield strengths to increasingly coarse Fe_3C at lower yield strengths.
- The principal irreversible traps in H11 at high yield strengths were assumed to be associated with matrix boundaries, with carbides making only a minor contribution. However, the role of these heterogeneities as the principal traps in H11 has not been verified.

ACKNOWLEDGEMENT

Financial support of this work by the U.S. Office of Naval Research under Contracts N00014-91-C-0263 and N00014-95-C-0313 is gratefully acknowledged.

REFERENCES

1. Peterson, M. H., Brown, B. F., Newbegin, R. L. and Groover, R. E., *Corrosion*, 1967, **23**, 142.
2. Sandoz, G., *Metall. Trans.*, 1972, **3**, 1169.
3. Ayer, R. and Machmeier, P. M., *Metall. Trans.*, 1993, **24A**, 1943.
4. Novotny, P. M., in *Proc. Gilbert R. Speich Symposium: Fundamentals of Aging and Tempering in Bainitic and Martensitic Steel Products*. ISS, Warrendale, PA, 1992, p. 215.
5. McCaffrey, T. J., *Advanced Maters. Processes*, 1992, **9**, 47.
6. Novotny, P. M. and Dahl, J. M., in *Proc. 32nd Conf. on Mechanical Working and Steel Processing*, Vol. XXVIII. ISS, Warrendale, PA, 1991, p. 275.
7. Neu, C. E., Lee, E. U., Lee, E. W., Boodey, J. B., Kozol, J., Morris, J. W. and Waldman, J., in *Proc. of the 40th Sagamore Army Materials Research Conference: Metallic Materials for Lightweight Applications*, 1993, p. 389.
8. Thompson, A. W., *Metall. Trans.*, 1973, **4**, 2819.
9. Thompson, A. W., in *Fracture 1977: Proc. Fourth Int. Conf. on Fracture*, ed. D.M.R. Taplin, Vol. 2. University of Waterloo Press, Waterloo, Ontario, Canada, 1977, p. 237.
10. Dautovich, D. P. and Floreen, S., in *Proc. Conf. on Stress Corrosion Cracking and Hydrogen Embrittlement of Iron-Base Alloys*, ed. R. W. Staehle, J. Hochman, R. D. McCright, and J. E. Slater. NACE, Houston, TX, 1977, p. 798.
11. Bernstein, I. M. and. Pressouyre, G. M, in *Hydrogen Degradation of Ferrous Alloys*, ed. R. A. Oriani, J. P. Hirth, and M. Smialowski. Noyes Publications, Park Ridge, NJ, 1985, p. 641.

12. Pressouyre, G. M. and Bernstein, I. M., *Metall. Trans.*, 1978, **9A**, 1571.

13. Pressouyre, G. M. and Bernstein, I. M., *Acta Metall.*, 1979, **27**, 89.

14. Pound, B. G., *Corrosion*, 1989, **45**, 18.

15 Pound, B. G., *Acta Metall.*, 1990, **38**, 2373.

16. Pound, B. G., *Acta Metall.*, 1991, **39**, 2099.

17. Pound, B. G., in *Proc. Fifth Int. Conf. on Hydrogen Effects on Material Behavior*, ed. N. R. Moody and A. W. Thompson. TMS, Warrendale, PA, 1996, p. 115.

18. Pound, B. G., "Characterization of Hydrogen Ingress in High-Strength Alloys," Final Report to Office of Naval Research, Contract No. N00014-95-C-0313 (1997).

19. Shockey, D. A., Curran, D. R. and Seaman, L., "Development of Improved Dynamic Failure Models," Final Report, U.S. Army Research Office, Contract No. DAAG-29-81-K0123, 1985.

20. McKibbin, R., Harrington, D. A., Pound, B. G., Sharp, R. M. and Wright, G. A., *Acta Metall.*, 1987, **35**, 253.

21. Pound, B. G., Sharp, R. M. and Wright, G. A., *Acta Metall.*, 1987, **35**, 263.

22. Lange, K. W. and Koning, H. J., in *Proc. Second Int. Conf. on Hydrogen in Metals*, ed. P. Azou. 1973, paper 1A5.

23. Bockris, J. O'M., Genshaw, M. A. and Fullenwider, M., *Electrochim. Acta*, 1970, **15**, 47.

24. Kortovich, C. S. and Steigerwald, E. A., *Eng. Fract. Mech.*, 1972, **4**, 637.

25. Kargol, J. A. and Paul, L. D., in *Proc. 1st Int. Conf. on Current Solutions to Hydrogen Problems in Steels*, ed. C. G. Interrante and G. M. Pressouyre. ASM, Materials Park, 1982, p. 91.

26. Beck, W., Bockris, J. O'M., Genshaw, M. A. and Subramanyan, P. K., *Met. Trans.*, 1971, **2**, 883.

27. Hanson, D. and Freeman, J. R., *J. Iron Steel Inst.*, 1923, **154**, 301.

28. Ogilvie, R. E., *Trans. TMS-AIME*, 1965, **223**, 2083.

29. Pressouyre, G. M., *Metall. Trans.*, 1979, **10A**, 1571.

30. Oriani, R. A., *Acta Met.*, 1970, **18**, 147.

31. Kumnick, A. J. and Johnson, H. H., *Met. Trans.*, 1974, **5**, 1199.

32. Pound, B.G., in *Modern Aspects of Electrochemistry*, No. 25, ed. J. O'M. Bockris, B. E. Conway, and R. E. White. Plenum Press, New York, NY, 1993, p. 63.

33. Beck, W., Bockris, J. O'M., McBreen, J. and Nanis, L., *Proc. Royal. Soc.*, 1966, **290A**, 220.

34. Radhakrishnan, T. P. and Shreir, L. L., *Electrochim. Acta*, 1967, **12**, 889.

35. Gibala, R. and DeMiglio, D. S., in *Proc. 3rd Int. Conf. on Effect of Hydrogen on Behavior of Materials*, ed. I. M. Bernstein and A. W. Thompson. TMS, Warrendale, PA, 1980, p. 113.

36. Kim, C. D. and Loginow, A. W., *Corrosion*, 1968, **24**, 313.

37. Benjamin, W. D. and Steigerwald, E. A., *Metall. Trans.*, 1971, **2**, 606.

38. Groeneveld, T. P., Fletcher, E. E. and Elsea, A. R., *A Study of Hydrogen Embrittlement of Various Alloys*, Summary Report, Contract No. NAS8-20029. NASA, Marshall Space Flight Center, Huntsville, AL, 1966.

39. Thompson, A. W. and Bernstein, I. M., in *Advances in Corrosion Science and Technology*, ed. R. W. Staehle and M. Fontana. Plenum Press, New York, 1979, p. 53.

40. Alloy Data: AerMet 100 Alloy, Alloy Steels 6. Carpenter Tech. Corp., Reading, PA, 1992.

41. Bernstein, I. M. and Thompson, A. W., *Int. Met. Rev.*, 1976, **21**, 269.

42. Lee, E. U. and Waldman, J., *Naval Engrs. J.*, Nov. 1994, p. 77.

43. Lee, E. U., *Metall. Mater. Trans.*, 1995, **26A**, 1313.

44. Lee, J. Y., Lee, J. L. and Choo, W. Y., in *Proc. 1st Int. Conf. on Current Solutions to Hydrogen Problems*, ed. C. G. Interrante and G. M. Pressouyre. ASM, Materials Park, OH, 1982, p. 423.

45. Asaoka, T., in *Proc. JIMIS-2*, "Hydrogen in Metals," Minakami. Jpn. Inst. Met., 1980, p. 161.

46. *Metals Handbook*, 9th Ed., Vol. 9. ASM International, Materials Park, OH, 1985, p. 271.

Table 1. Alloy composition (wt%)

Element	AerMet 100	H11	4340
Al	0.005		0.031
C	0.24	0.41	0.42
Co	13.47		
Cr	3.00	4.88	0.89
Cu		0.03	0.19
Fe	71.00	bal	bal
Mn	0.01	0.30	0.46
Mo	1.19	1.32	0.21
N	<0.0010		0.005
Ni	11.07	0.04	1.74
O	<0.0010		0.001
P	0.002	0.011	0.009
S	<0.0005	0.003	0.001
Si	<0.01	0.88	0.28
Ti	0.009		
V		0.45	

Table 2. Heat treatment and yield strength for 4340 Steel

Specimen	Heat Treatment*		Yield strength	
	Austenize	Temper	MPa	ksi
4340 (150)	845°C for 45 min	585°C for 2 h	1034	150
4340 (175)	830°C for 45 min	450°C for 1 h	1206	175
4349 (200)	845°C for 45 min	425°C for 2 h	1379	200
4340 (260)	850°C for 45 min	180°C for 80 min	1792	260

*Quenched in oil after austenizing and quenched in water after tempering.

Table 3. Apparent trapping constants for aged AerMet 100

T_{age} (°C)	Test no.	η range (V)	No. of k_a values	k_a (s^{-1})
270	1	-0.05 to -0.20	4	0.044 ± 0.005
	2	-0.10 to -0.25	2	0.044 ± 0.001
	3	-0.10 to -0.15	2	0.049 ± 0.002
	4	-0.10 to -0.20	2	0.049 ± 0.002
370	1	-0.10 to -0.20	3	0.045 ± 0.005
	2	-0.05 to -0.20	4	0.047 ± 0.002
482	1	-0.10 to -0.25	4	0.069 ± 0.006
	2	-0.20 to -0.25	2	0.069 ± 0.001

Table 4. Apparent trapping constants for hardened H11 steel

Test no.	η range (V)	No. of k_a values	k_a (s^{-1})
1	-0.15 to -0.175	2	0.083 ± 0.001
2	-0.20	1	0.083
3	-0.20	1	0.080
4	-0.20	1	0.070

Table 5. Apparent trapping constants for hardened 4340 steel

Test no.	η range (V)	No. of k_a values	k_a (s^{-1})
4340 (150)			
1	-0.10 to -0.20	3	0.010 ± 0.002
2	-0.10 to -0.20	3	0.011 ± 0.004
4340 (200)			
1	-0.15 to -0.20	2	0.009 ± 0.001
2	-0.10 to -0.25	4	0.009 ± 0.001
3	-0.15 to -0.25	3	0.080 ± 0.001

Table 6. Trapping parameters for high-strength steels

Alloy	Condition	k_a (s^{-1})	D_L/D_a	k (s^{-1})
AerMet 100	Annealed	0.000 ± 0.001	9.6 ± 1.3	0.00
	270°C-aged	0.046 ± 0.003	9.6 ± 1.3	0.44 ± 0.09
	370°C-aged	0.046 ± 0.004	9.6 ± 1.3	0.44 ± 0.10
	482°C-aged	0.069 ± 0.004	9.6 ± 1.3	0.66 ± 0.13
4340 (150)	1034 MPa	0.011 ± 0.003	79.4 ± 10	0.87 ± 0.35
4340 (175)	1206 MPa	0.008 ± 0.001	147 ± 18	1.2 ± 0.3
4340 (200)	1379 MPa	0.008 ± 0.001	500 ± 60	4.0 ± 1.0
4340 (260)	1792 MPa	0.008 ± 0.001	500 ± 60	4.0 ± 1.0
H11	HRC 51	0.080 ± 0.004	43.3 ± 6.2	3.5 ± 0.7
18Ni (250)*	482°C-aged (6 h)	0.006 ± 0.001	167 ± 45	1.00 ± 0.43
18Ni (300)*	482°C-aged (4 h)	0.005 ± 0.002	294 ± 76	1.47 ± 0.97

* Ref. 18.

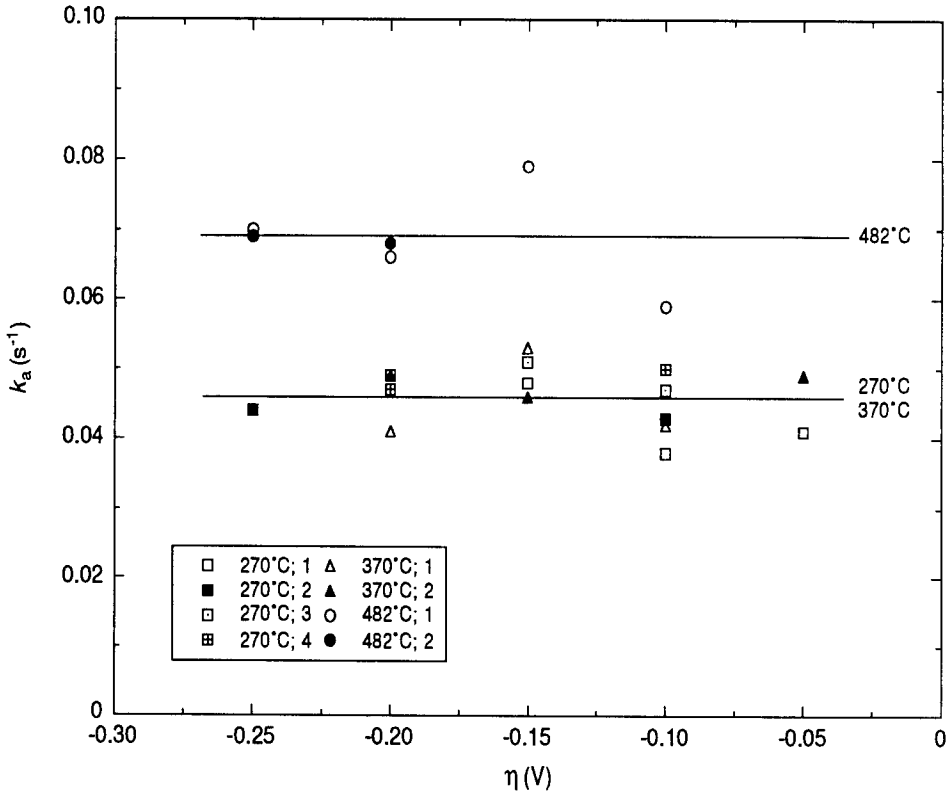

Figure 1. Values of k_a for aged AerMet 100 at various overpotentials. Each symbol is identified by the aging temperature and a test number for that temperature.

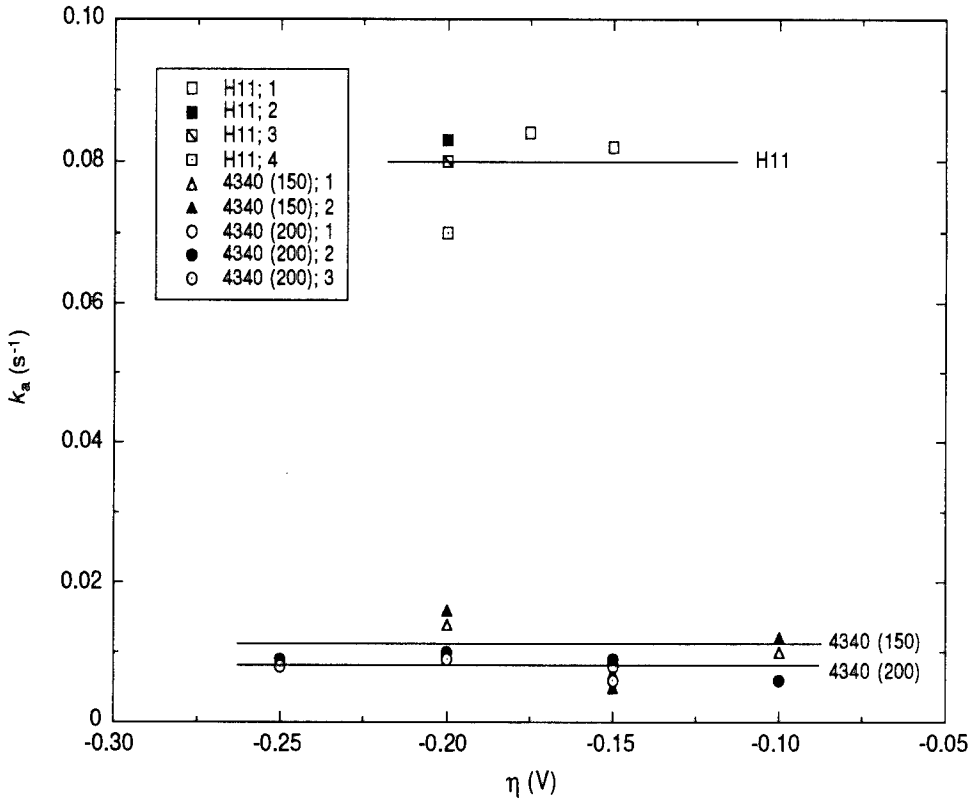

Figure 2. Values of k_a for hardened AISI 4340 and H11 steels at various overpotentials.
Each symbol is identified by the steel and a test number for that steel.

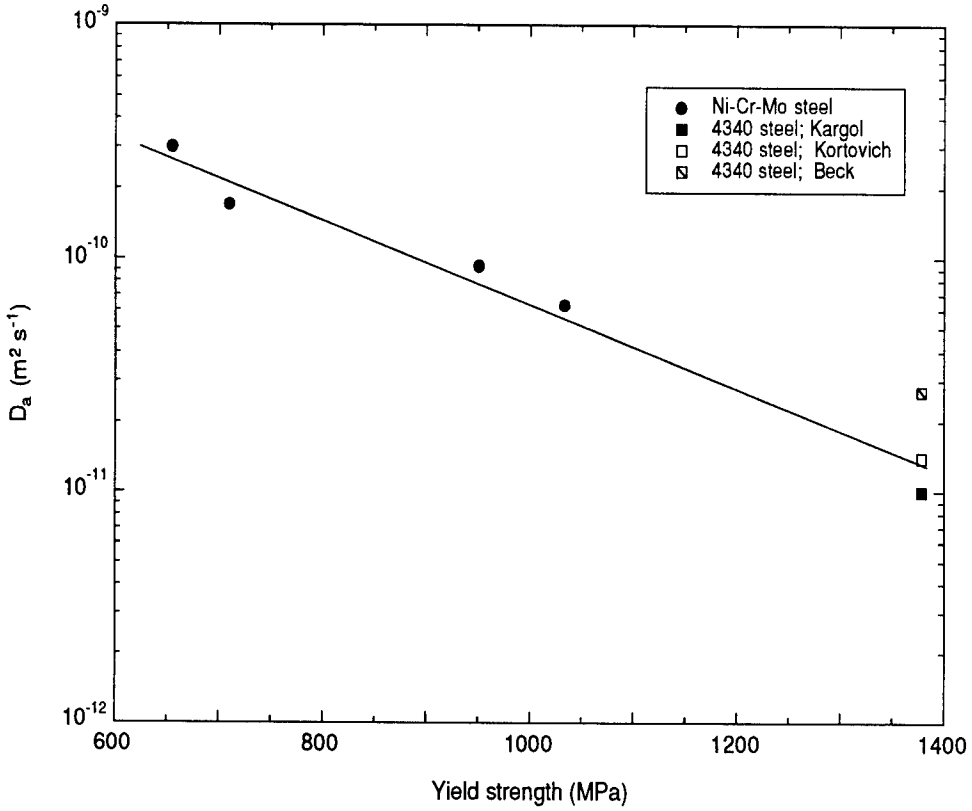

Figure 3. Variation in hydrogen diffusivity with yield strength for Ni-Cr-Mo steel and 4340 steel.
Data were taken from Ref. 36 for Ni-Cr-Mo steel and from Refs. 24-26 for 4340 steel.

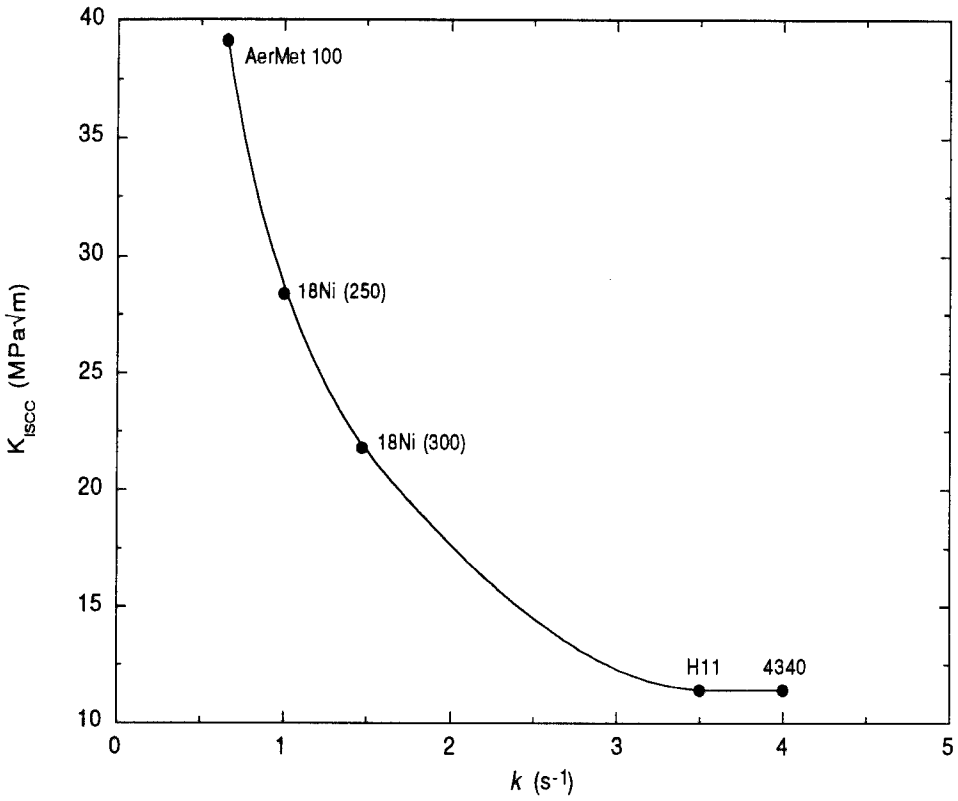

Figure 4. Variation of typical K_{ISCC} values with k for high-strength steels. The K_{ISCC} data were taken from Ref. 10 for 18Ni steel and from Ref. 5 for the other steels.

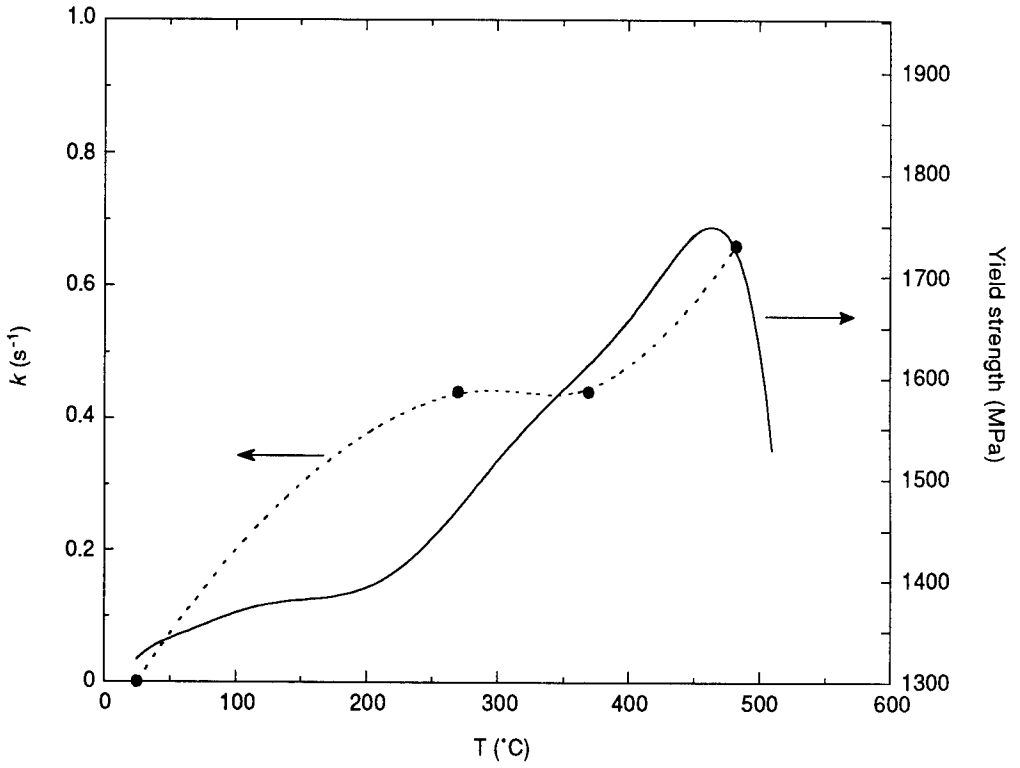

Figure 5. Variation of k and yield strength with aging temperature for AerMet 100.

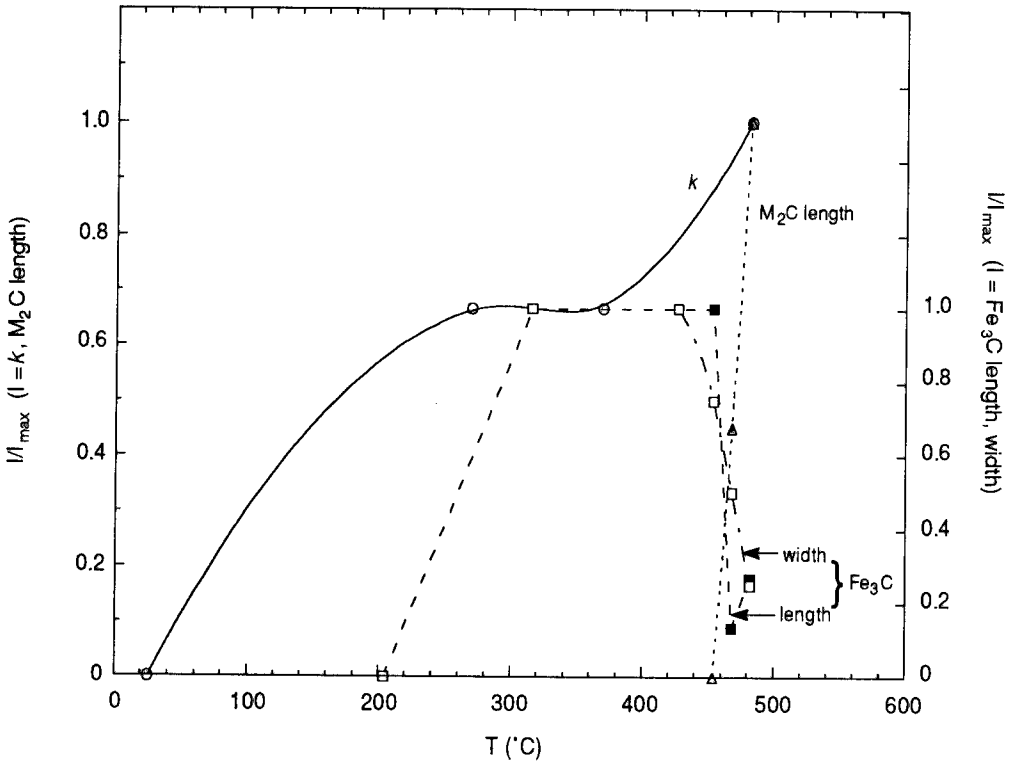

Figure 6. Variation of *k* and carbide size with aging temperature for AerMet 100.
The dimensions of the carbides were obtained from the study by Novotny (Ref. 4).

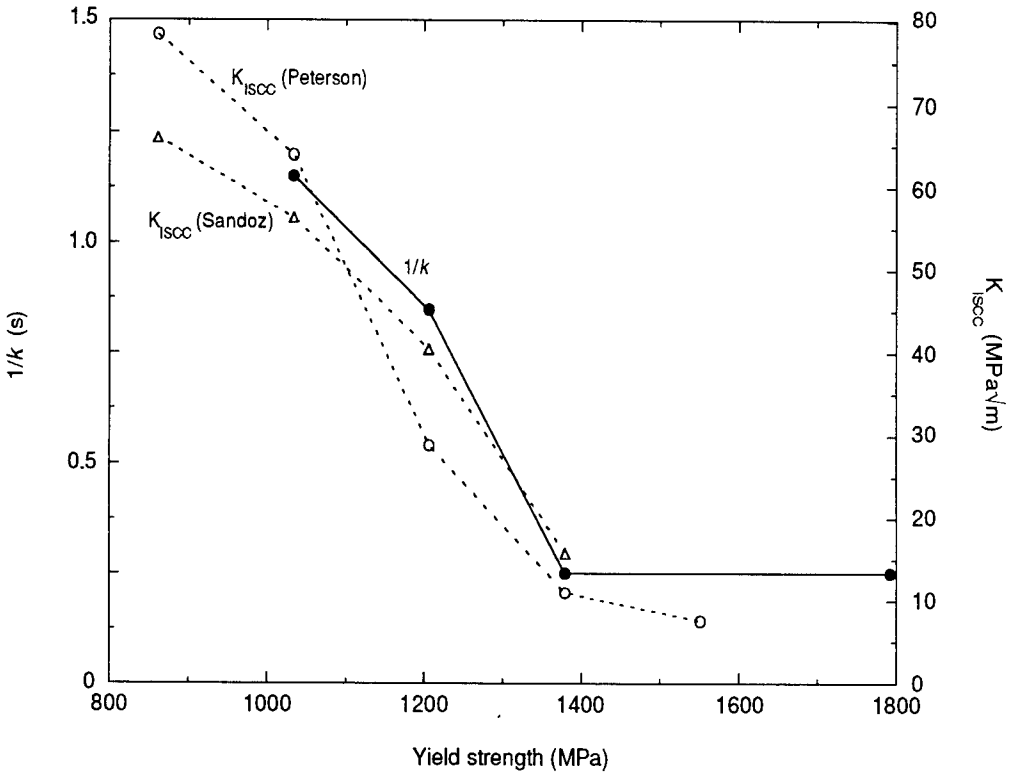

Figure 7. Variation of $1/k$ and K_{ISCC} with yield strength for 4340 steel. Data for K_{ISCC} were taken from Refs. 1 and 2.

THE INGRESS OF HYDROGEN INTO ALLOY A-286 AND 2Be-Cu*

Abstract—The ingress of hydrogen into two precipitation-hardened alloys, alloy A-286 and 2Be-Cu, was studied using a potentiostatic pulse technique. Values of the irreversible trapping constant (k) and the hydrogen entry flux were determined for the alloys in 1 mol L^{-1} acetic acid/ 1 mol L^{-1} sodium acetate. The values of k were compared with those for three other precipitation-hardened alloys—718, 925, and 18Ni (250) steel—examined previously. The values for aged alloy A-286 and 2Be-Cu were intermediate between those for the two Ni-base alloys (718 and 925) and were considerably lower than that for the 18Ni steel. The k values for the 18Ni steel, 2Be-Cu, and alloys 718 and A-286 were consistent with test data for their relative resistances to hydrogen embrittlement.

INTRODUCTION

Austenitic iron-base alloys such as A-286 (UNS S66286), in which the strength is imparted by precipitation of the γ' phase composed of $Ni_3(Al,Ti)$, have been found to undergo hydrogen embrittlement (HE).[1-3] Thompson and Brooks rationalized the effect of hydrogen (H) on alloy A-286 in terms of the effects of second-phase particles on ductile fracture.[3,4] The misfit between the γ' precipitates and the austenite was thought to affect the strain at which the precipitates lose coherency and begin to accumulate H at the precipitate/matrix interface.

Various copper-containing alloys can also be precipitation-hardened to high yield strengths. Be-Cu alloys, for example, are strengthened by precipitation of (Cu,Co)Be in the α-Cu matrix.[5] The ability of these alloys to be aged allows them to be used in a wide range of applications, but tensile tests have shown that the alloys can display some vulnerability to HE under certain conditions.[6]

In the present work, a potentiostatic pulse technique was used to explore the entry and trapping of H in two precipitation-hardened alloys: A-286 and 2Be-Cu (UNS C17200). The technique was used previously to determine the rates of H entry and rate constants (k) for irreversible trapping in various high-strength alloys.[7-10] For most of these alloys, a correlation was observed between the intrinsic susceptibility, as represented by k, and the actual resistance to HE observed in mechanical tests.

---

* To be submitted to *Corrosion Science*.

2Be-Cu and alloy A-286 provided a comparison with two precipitation-hardened nickel-base superalloys, 718 and 925, and a precipitation-hardened maraging steel, 18Ni (250), that have also been studied.[8,11] The research was aimed at characterizing the intrinsic susceptibility of 2Be-Cu and alloy A-286 to HE in terms of their irreversible trapping constants. The intrinsic susceptibilities were then compared with those for the previous alloys and with results for the resistance to HE observed in tests by other workers.

EXPERIMENTAL PROCEDURE

The Be-Cu alloy contained 1.8-2.0 wt% Be and was supplied as rod with a diameter of 6.35 mm. This alloy was received in an unaged condition with a Rockwell C hardness [HRC] of 17-18 and a corresponding yield strength of 585-613 MPa. A section of alloy was aged at 315°C for 2 h in Ar to give an HRC of 36 and a corresponding yield strength of ~860 MPa. The unaged alloy was examined under the scanning electron microscope and found to be free of any particles, although some microvoids were present. Aged Be-Cu, as noted above, contains (Cu,Co)Be precipitates, which are small, mainly spheroidal, and uniformly dispersed.[5]

Table 1 gives the composition of alloy A-286. The alloy was supplied as rod with a diameter of 1.27 cm and was used as-received in the solution-annealed (900°C/2 h) and aged (720°C/16 h) condition. The yield strength of the aged alloy was 848 MPa. In addition to the γ' phase precipitated during aging, the alloy contained Ti-rich carbide particles. The characteristic dimension of the particles was determined as the mean of the linear dimensions in the exposed plane and had a value of approximately 3 μm. The concentration of MC carbides was calculated to be 6.6×10^{13} m^{-3} on the basis of a spherical shape, with the radius taken as half the characteristic dimension.

Details of the electrochemical cell and instrumentation have been given previously.[7] The test electrodes consisted of a 1.27-cm length of alloy rod press-fitted into a polytetrafluoroethylene sheath so that only the planar end surface was exposed to the electrolyte. The surface was polished before each experiment with SiC paper followed by 0.05-μm alumina powder. The electrolyte contained 1 mol L^{-1} acetic acid and 1 mol L^{-1} sodium acetate (pH 4.8) with 15 ppm As_2O_3 and was deaerated continuously with argon before and throughout data acquisition. The potentials were measured with respect to a saturated calomel electrode (SCE). All tests were performed at 22 ± 1°C.

The test electrode was cathodically charged with hydrogen at a constant potential E_c for a time t_c, after which the potential was stepped in the positive direction to a value 10 mV negative of the open-circuit potential E_{oc}. Anodic current transients were obtained over a range of charging

times, typically from 5 to 60 s, at different overpotentials ($\eta = E_c - E_{oc}$). The open-circuit potential of the test electrode was measured immediately before each charging time and was also used to monitor the stability of the alloy surface.

RESULTS

The current transients were analyzed using a diffusion/trapping model based on a constant entry flux at the surface.[7,12] According to the model, the total anodic charge (C m^{-2}) is given by

$$q'(\infty) = FJt_c\{1 - e^{-R}/(\pi R)^{1/2} - [1 - 1/(2R)]\mathrm{erf}(R^{1/2})\} \quad (1)$$

where F is the Faraday constant, J is the ingress flux in mol m^{-2} s^{-1}, $R = k_a t_c$, and k_a is an apparent trapping constant measured for irreversible traps in the presence of reversible traps. The charge $q'(\infty)$ is equated to the charge (q_a) passed during the experimental anodic transients. q_a can be associated entirely with absorbed H, because the adsorbed charge is almost invariably negligible. k_a is related to the irreversible trapping constant by kD_a/D_L, where D_a is the apparent diffusivity and D_L is the lattice diffusivity of H. The use of k as an index of susceptibility has been discussed elsewhere.[10]

For both alloys, equation (1) could be fitted to the experimental data for q_a to obtain values of k_a and J, where J was constant over the range of charging times at each potential. Table 2 shows the number of tests and range of overpotentials used for each alloy. Also listed are the number of k_a values and the mean k_a obtained for each test. In all the tests, k_a was independent of overpotential. The mean values of k_a for each group of tests were 0.073 ± 0.005 s^{-1} for alloy A-286, 0.045 ± 0.006 s^{-1} for unaged 2Be-Cu, and 0.042 ± 0.009 s^{-1} for aged 2Be-Cu. Clearly, k_a for 2Be-Cu is not significantly affected by aging.

The H entry flux for each alloy increased as the charging potential was made more negative (Fig. 1). This increase was to be expected because of the dependence of J on the surface coverage of adsorbed H. Aging has a small effect on the entry flux for 2Be-Cu, such that the changes in surface chemistry make J less dependent on potential.

DISCUSSION

Irreversible Trapping Constants

Evaluation of k from k_a requires that the effect of reversible trapping be taken into account. The effect of reversible trapping is determined using the values of D_L and D_a, corresponding to the diffusivity for the "pure" alloy (or metal in some cases) and for the actual alloy, respectively. From the viewpoint of diffusivity, the pure alloy/metal was assumed to be Fe-24Ni-14Cr for alloy A-286 and Cu for 2Be-Cu. Minor elements in the actual alloy were treated as reversible traps and in fact were assumed to be primarily responsible for reversible trapping. For face-centered cubic alloys, defects such as vacancies or edge dislocations are unlikely to contribute significantly to reversible trapping, because the binding energy of H to such defects is considerably (a factor of 4) smaller than the activation energy for diffusion.[13, 14] Thus, reversible trapping in 2Be-Cu and alloy A-286 (solution annealed and aged) with its austenitic lattice should be influenced more by composition than by microstructural defects.

Alloy A-286. Diffusivity data were not available for either Fe-24Ni-14Cr or alloy A-286. However, data have been obtained for other austentic stainless steels (301, 304, and 310) at temperatures from 100° to 350°C.[15] Diffusivities for these alloys at 25°C were estimated by extrapolation and are given in Table 3. The values shown indicate that the differences in diffusivity between the three alloys are relatively small, which is consistent with other work indicating that H transport in austenitic stainless steels is essentially independent of the austenite composition.[16] Accordingly, the minor elements were assumed to have a negligible effect on the diffusivity and so the ratio of D_L to D_a for alloy A-286 was taken to be 1.0 ± 0.1. (The uncertainty was estimated on the basis of the maximum deviation from the median diffusivity, 3.49×10^{-16} m^2 s^{-1}, for the stainless steels in Table 3). Thus, k was equal to k_a, with a value of 0.073 ± 0.012 s^{-1}.

2Be-Cu. The diffusivity of H in α-Cu has been determined over the temperature range 47°-657°C,[17] and extrapolation to 25°C gave a value of 2.1×10^{-14} m^2 s^{-1}. In transition metals, defects that introduce an electron vacancy will attract H.[18] On this basis, Be is unlikely to attract H in Cu and therefore unlikely to significantly affect the diffusivity. Hence, D_a for unaged Be-Cu was assumed to be similar in value to D_L, and so k was approximated to k_a.

No data were available for the diffusivity for the aged alloy. However, in the case of another aged high-Cu alloy—K-500 (65Ni-30Cu)—the intermetallic particles appear to have little effect on D_a compared with that of the minor alloying elements in solid solution: D_a for the aged alloy was only about a factor of 2 smaller than D_L.[17, 19] Because most solutes introducing an

electron vacancy provide reversible traps that could largely account for this factor, the intermetallics must be presumed to add little to the effect of the minor elements. Hence, it was assumed that the intermetallic particles in 2Be-Cu have only a small effect on D_a and that the value of D_L/D_a for aged alloy K-500 represented the upper limit of this ratio for aged 2Be-Cu. k was therefore estimated to be $\leq 0.084 \pm 0.021\ s^{-1}$.

Susceptibility to HE

Table 4 compares the trapping constants for alloy A-286, 2Be-Cu, and those for three other precipitation-hardened alloys, consisting of two Ni-base types (718 and 925)[8] and 18Ni (250) steel.[11] The values of k for aged alloy A-286, 2Be-Cu, and the Ni-base alloys are presented graphically in Fig. 2 to highlight differences between them. Alloy A-286 and 2Be-Cu were intermediate in their k values between alloys 718 and 925, so they can be considered intrinsically less susceptible than alloy 718 but more susceptible than alloy 925.

Measurements of the reduction of notch tensile strength and of ductility in gas-phase charging tests at room temperature have shown that alloy 718 undergoes extreme HE whereas alloy A-286 exhibits negligible embrittlement.[6] Corresponding measurements have been made in cathodic charging tests on alloys 718 and A-286 aged to strengths that, relative to each other, were similar to those used in the present work.[20] As in the gas-phase tests, alloy 718 underwent a greater decrease in notch strength and ductility than alloy A-286. Thus, irrespective of the type of charging, the intrinsic susceptibility parallels the relative resistance to HE for these two alloys.

Fig. 3 compares the irreversible trapping constants for alloys A-286, 718, and 2Be-Cu, as well as for 18Ni (250) steel, with the reduction of notch strength determined for these alloys in gaseous hydrogen.[6] Clearly, there is a correlation between k and the reduction of strength for the four alloys. Alloy A-286 has the lowest value of k and so is regarded as having the lowest intrinsic susceptibility, which fits the reduction-of-strength data indicating that alloy A-286 is the most resistant to HE, followed by 2Be-Cu, alloy 718, and then the 18Ni steel. Electrolytic charging tests[21] have likewise shown that the degree of embrittlement decreases in the order 18Ni (250) steel, 718, and, by implication (based on the cathodic tests above) A-286. Thus, the values of k for the four alloys are consistent with their relative resistances to HE observed in tests.

The cathodic charging tests[20] and the correlation above suggest that the stronger the alloy, the greater the decrease in strength and ductility as a result of absorbed hydrogen. The observed resistance to HE, however, can be considered more directly an effect of microstructure than of strength.[22,23] The trapping constants for the 18Ni steel, 2Be-Cu, and alloys 718 and A-286

parallel their mechanical properties, so quite possibly the microstructure, through its traps, is the key factor for these alloys.

Identification of irreversible traps

A-286. The presence of the γ′ phase precipitated during aging appears to be critical to the H-induced losses in ductility of alloy A-286.[3,4] As noted above, the misfit between the γ′ particles and the austenitic matrix was believed to affect the strain at which the particles lose coherency and begin to accumulate H at the particle/matrix interface. Thus, the γ′ particles may provide irreversible traps in alloy A-286, although intermetallic precipitates in alloys such as maraging steels tend to be reversible traps.[8,24]

Although the γ′ phase has been implicated in the HE of alloy A-286, the possibility was considered that the Ti-rich particles observed in this alloy might be key irreversible traps, because Ti carbide and carbonitride particles have been identified as the principal irreversible traps in various other alloys.[10] The density of particles or defects (N_i) providing irreversible traps can be calculated from k_a according to equation (2):

$$N_i = k_a a/(4\pi d^2 D_a) \qquad (2)$$

where a is the diameter of the metal atom and d is the trap radius.[7,25] The value of a for an alloy is taken as the mean of the atomic diameters weighted in accordance with the atomic fraction of each element. The trap radius was estimated from the size of the Ti-rich particles. The value of D_a for alloy A-286 with its 24Ni-14Cr was taken as the median diffusivity, $\sim 3.5 \times 10^{-16}$ m^2 s^{-1}, for the stainless steels in Table 3. Thus, by using $d = 1.5 \times 10^{-6}$ m and $a = 250 \times 10^{-12}$ m, N_i was found to be $(1.8 \pm 0.4) \times 10^{15}$ m^{-3}, whereas the actual concentration of Ti-rich particles was only 6.6×10^{13} m^{-3}. The factor of 27 difference in the two values indicates that these particles are probably not the principal traps, even allowing for the uncertainty in D_a. This finding is consistent with the results of Thompson and Brooks,[4] who found that the TiC phase could not be correlated with the overall H-induced ductility loss of alloy A-286.

Since the Ti-rich particles are discounted as the *principal* irreversible traps, the γ′ precipitates may fill this role in alloy A-286. However, the role of these precipitates as the principal irreversible traps is speculative and has not been verified.

2Be-Cu. Although particles were absent in the unaged alloy, the presence of some microvoids could account for part of the irreversible trapping. However, the principal irreversible traps were probably associated with some other heterogeneity, possibly grain boundaries, that was more numerous than the microvoids.

The aged alloy, as noted above, contains small, uniformly dispersed (Cu,Co)Be precipitates. Small particles tend to be coherent with the matrix, and trapping becomes more reversible as the coherency of a particle increases.[18] Consequently, the (Cu,Co)Be precipitates are unlikely to be irreversible traps. Thus, the principal irreversible traps in aged 2Be-Cu, as in the unaged alloy, may be associated with grain boundaries.

SUMMARY

- The values of k for alloy A-286 and 2Be-Cu are intermediate between those for the two Ni-base alloys, 718 and 925, and are considerably lower than that for 18Ni (250) steel. Thus, alloy A-286 and 2Be-Cu are intrinsically less susceptible to HE than alloy 718 and the 18Ni steel but more susceptible than alloy 925.
- The intrinsic susceptibilities (defined by k) of 18Ni (250) steel, 2Be-Cu, and alloys 718 and A-286 are consistent with their observed resistances to HE. The results for alloy A-286 and 2Be-Cu therefore extend the previously reported correlation[10] between k and HE resistance to include these alloys.
- The principal irreversible traps in alloy A-286 do not appear to involve TiC particles but may be provided by the γ' particle/austenite matrix interfaces. In the case of 2Be-Cu, the principal traps may be associated with grain boundaries for both the unaged and aged alloy.

ACKNOWLEDGEMENT

Financial support of this work by the U.S. Office of Naval Research under Contract N00014-91-C-0263 is gratefully acknowledged.

REFERENCES

1. J. Papp, R. F. Hehemann, and A. R. Troiano, in *Hydrogen in Metals*, ed. I. M. Bernstein and A. W. Thompson, p. 657, ASM, Materials Park, OH (1974).
2. J. LeGrand, M. Caput, C. Couderc, R. Broudeur, and J.-P. Fidelle, *Mem. Sci. Rev. Met.* **68**, 861 (1971).
3. A. W. Thompson, in *Hydrogen in Metals*, ed. I. M. Bernstein and A. W. Thompson, p. 91, ASM, Materials Park, OH (1974).
4. A. W. Thompson and J. A. Brooks, *Metall. Trans.* **6A**, 1431 (1975).
5. Metals Handbook, Vol. 2: Properties and Selection: Nonferrous Alloys and Pure Metals, 9th ed, p. 303, ASM, Materials Park, OH, (1979).
6 R. J. Walter, R. P. Jewett, and W. T. Chandler, *Mater. Sci. Eng.* **5**, 98 (1969/70).

7. B. G. Pound, *Corrosion* **45**, 18 (1989).
8. B. G. Pound, *Acta Metall.* **38**, 2373 (1990).
9. B. G. Pound, *Acta Metall.* **39**, 2099 (1991).
10. B. G. Pound, in *Proc. Fifth Int. Conf. on Hydrogen Effects on Material Behavior*, ed. N. R. Moody and A. W. Thompson, p. 115, TMS, Warrendale, PA (1996).
11. B. G. Pound, "Characterization of Hydrogen Ingress in High-Strength Alloys," Final Report to the Office of Naval Research, Contract No. N00014-95-C-0313 (1997).
12. R. McKibbin, D. A. Harrington, B. G. Pound, R. M. Sharp, R. M. and G. A. Wright, *Acta Metall.* **35**, 253 (1987).
13. W. D. Wilson and S. C. Keeton, in *Advanced Techniques for Characterizing Hydrogen in* Metals, ed. N. F. Fiore and B. J. Berkowitz, p. 3, TMS AIME, Warrendale, PA (1981).
14. J. Y. Lee and S. M. Lee, *Metall. Trans.* **17A**, 181 (1986).
15. T.-P. Perng and C. J. Altstetter, *Acta Metall.* **34**, 1771 (1986).
16. M. R. Louthan, Jr. and R. G. Derrick, *Corrosion Sci.* **15**, 565 (1975).
17. H. Hagi, *Trans. Jpn. Inst. Metals* **27**, 233 (1986).
18. G. M. Pressouyre, *Metall. Trans.* **10A**, 1571 (1979).
19. J. A. Harris, R. C. Scarberry, and C. D. Stephens, *Corrosion* **28**, 57 (1972).
20. P. D. Hicks and C. J. Alstetter, in *Proc. Fourth Int. Conf. on Hydrogen Effects on Material Behavior*, ed. N. R. Moody and A. W. Thompson, p. 613, TMS, Warrendale, PA (1990).
21. T. P. Groeneveld, E. E. Fletcher, and A. R. Elsea, *A Study of Hydrogen Embrittlement of Various Alloys*, Summary Report, Contract No. NAS8-20029, NASA, Marshall Space Flight Center, Huntsville, AL (1966).
22. A. W. Thompson and I. M. Bernstein, in *Advances in Corrosion Science and Technology*, ed. R. W. Staehle and M. Fontana, p. 53, Plenum Press, New York (1979).
23. I. M. Bernstein and A. W. Thompson, *Int. Met. Rev.* **21**, 269 (1976).
24. V. I. Sarrak, G. A. Filippov, and G. G. Kush, *Phys. Met. Metall.* **55**, 94 (1983).
25. B. G. Pound, R. M. Sharp, and G. A. Wright, *Acta Metall.* **35**, 263 (1987).

Table 1. Composition (wt%) of alloy A-286

Al	C	Cr	Fe	Mn	Mo	Nb+Ta	Ni	P	S	Si	Ti	Other*
0.13	0.024	14.02	57.08	0.28	1.37	5.30	24.38	0.019	0.001	0.22	2.09	0.20 V

* 0.0046 B; 0.10 Cu; 0.08 Co.

Table 2. Apparent trapping constants

Alloy	Test no.	η range (V)	No. of k_a values	k_a (s^{-1})
A-286	1	-0.15 to -0.30	4	0.077 ± 0.005
	2	-0.15 to -0.30	3	0.071 ± 0.006
	3	-0.15 to -0.25	3	0.071 ± 0.004
Unaged 2Be-Cu	1	-0.55 to -0.70	4	0.047 ± 0.006
	2	-0.45 to -0.70	5	0.044 ± 0.006
Aged 2Be-Cu	1	-0.50 to -0.70	5	0.038 ± 0.007
	2	-0.55 to -0.70	3	0.045 ± 0.008
	3	-0.50 to -0.70	4	0.046 ± 0.007

Table 3. Diffusivities for austenitic stainless steels

Alloy	Ni	Cr	D_a ($m^2 s^{-1}$)
301	7	17	3.09×10^{-16}
304	9	18	3.49×10^{-16}
310	20	25	3.67×10^{-16}

Table 4. Trapping constants for precipitation-hardened alloys

Alloy	Yield Strength (MPa)	k_a (s^{-1})	D_L/D_a	k (s^{-1})
18Ni (250)	1873	0.006 ± 0.001	167 ± 45	1.00 ± 0.43
718	1238	0.031 ± 0.002	4.0 ± 0.5	0.124 ± 0.024
Be-Cu aged	860	0.042 ± 0.009	≤2	≤0.084 ± 0.021
A-286	848	0.073 ± 0.005	1.0 ± 0.1	0.073 ± 0.012
Be-Cu unaged	600	0.045 ± 0.006	~1	0.045 ± 0.006
925	758	0.006 ± 0.003	5.6 ± 0.6	0.034 ± 0.004

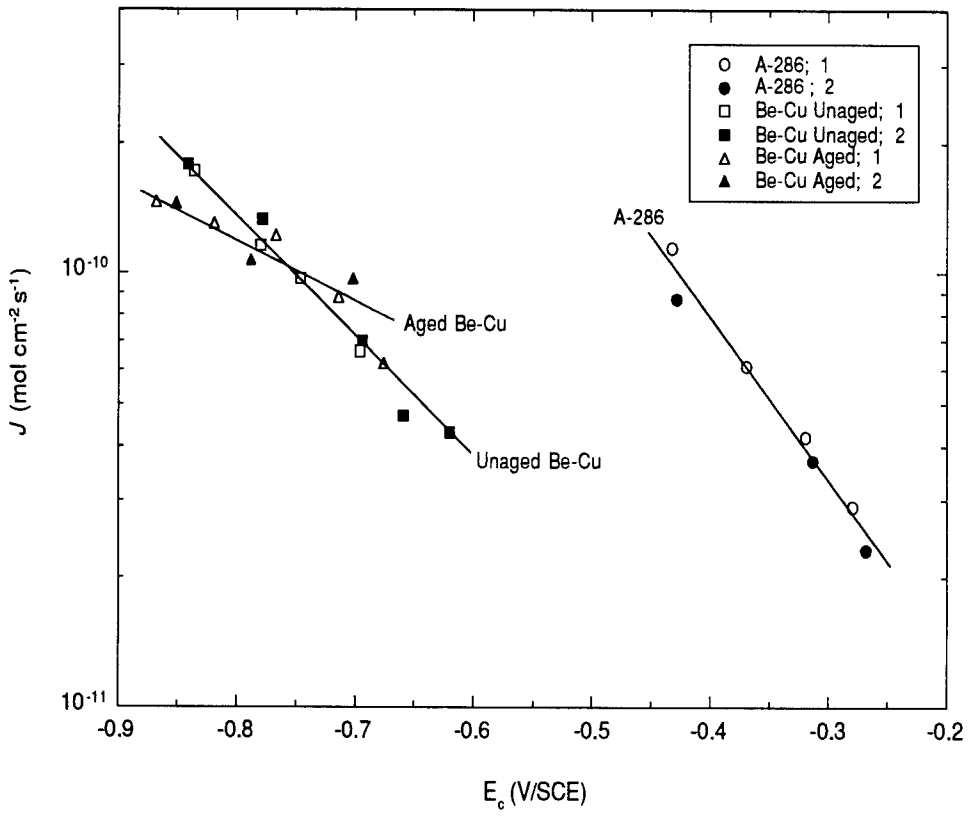

Figure 1. Dependence of H entry flux on charging potential for alloy A-286 and 2Be-Cu. Each symbol is identified by the alloy and a test number.

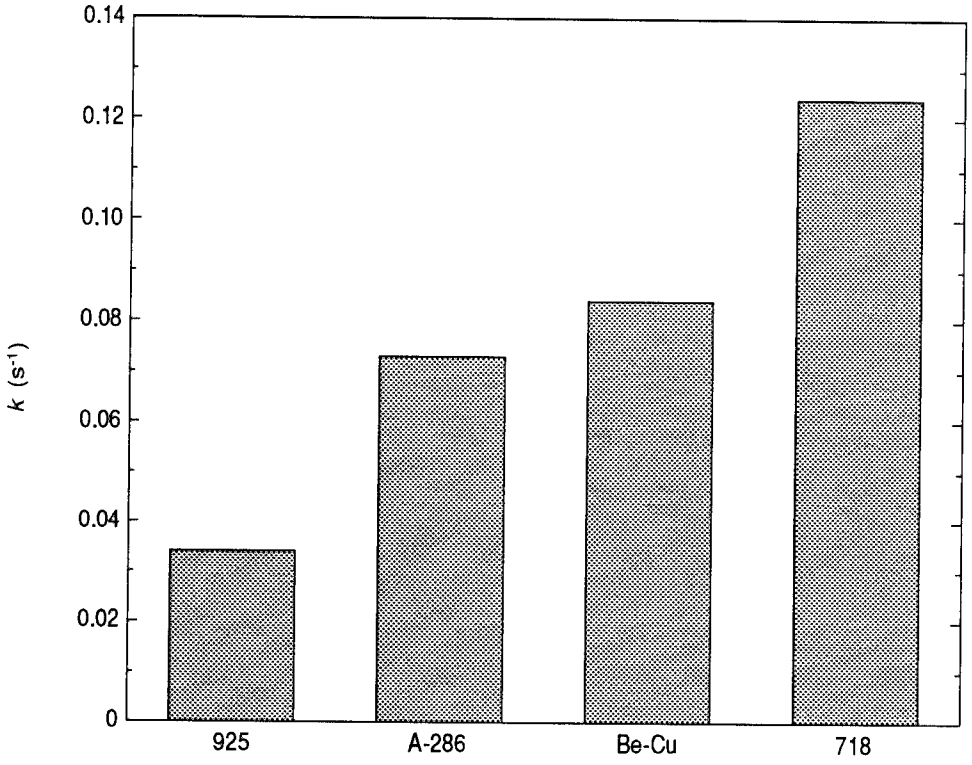

Figure 2. Variation in k for precipitation-hardened alloys.
k shown for Be-Cu is the upper limit.

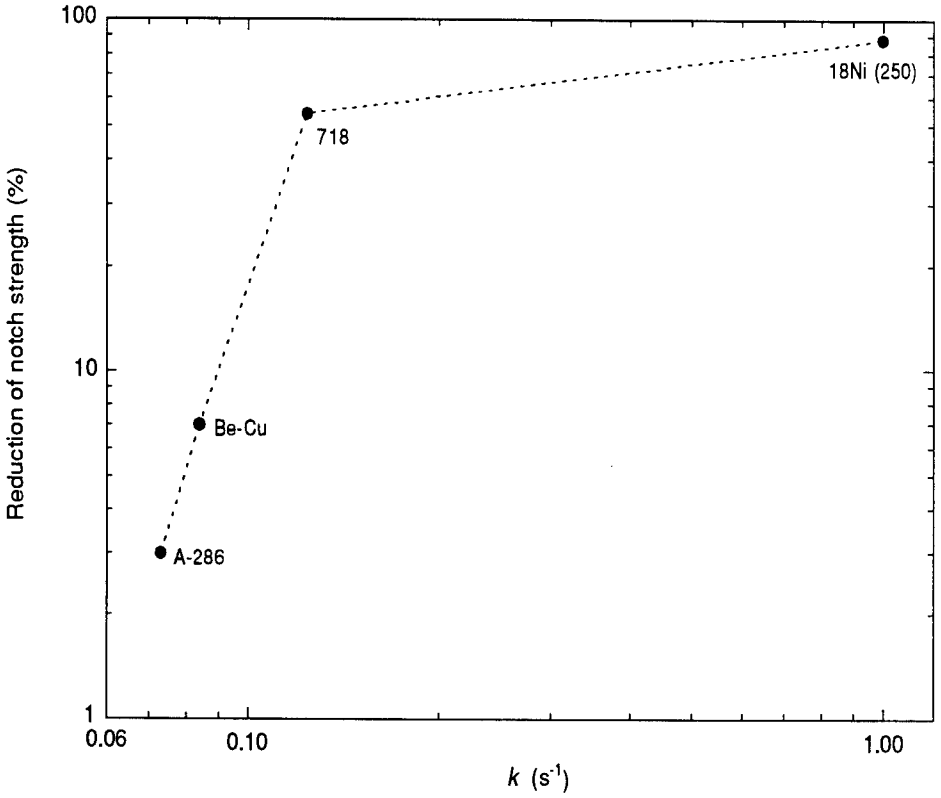

Figure 3. Variation in reduction of notch strength with *k* for precipitation-hardened alloys.
k shown for Be-Cu is the upper limit. Data for reduction of notch strength were taken from Ref. 6.

The Relationship Between Heat Treatment and Hydrogen Trapping in Alloy K-500*

ABSTRACT

The effect of heat treatment on irreversible hydrogen (H) trapping was investigated for Alloy K-500 [UNS N05500], with the goal of providing a more detailed insight into the factors governing the intrinsic susceptibility to hydrogen embrittlement (HE). A potentiostatic pulse technique was used to determine irreversible trapping constants (k) and H entry fluxes for annealed, annealed and aged (AA), and 12-h and 16-h direct aged (DA) specimens of cold drawn Alloy K-500 that had been used earlier to provide as-received (unannealed, cold drawn) and 8-h DA specimens. The type of heat treatment can produce marked differences in irreversible trapping. The intrinsic susceptibility to HE, as defined by k, is increased considerably by annealing. Aging has a negligible effect on the intrinsic susceptibility for the annealed alloy but can result in a sizable increase for the unannealed alloy if performed for extended times. The intrinsic susceptibilities for the AA and DA alloys can be correlated with the observed resistances to HE, implying that the previously reported decrease in the resistance to HE produced by annealing is caused to a large extent, if not entirely, by a change in the irreversible traps.

INTRODUCTION

The age-hardenable Ni-Cu alloy, K-500 [UNS N05500], is used extensively for seawater applications where strength is a critical factor. However, aging can render the alloy more susceptible to hydrogen embrittlement (HE), depending on the type of heat treatment.[1] Tests on cold worked Alloy K-500 have shown that the ultimate tensile strength of annealed and aged (AA) specimens which were cathodically precharged for 16 days decreased by 37.5%, whereas the strength of the direct aged (DA) alloy actually increased slightly. Thus, alloys, such as K-500, that are of interest in their aged condition present some concern with respect to the possibility of HE.

In recent work at SRI International, the type of heat treatment was also found to have a marked effect on the irreversible trapping of hydrogen (H) in Alloy K-500.[2] A potentiostatic pulse technique was used to determine the rate constants for irreversible trapping (k) for Alloy K-500 in the cold drawn (CD) and DA condition (yield strength of 1096 MPa) and the AA condition (yield strength of ~700 MPa). k was found to be more than twice as large for the AA alloy as it was for the DA alloy. The order of the k values for the two types of aged Alloy K-500 correlated with their

* To be submitted to *Corrosion*.

observed resistance to HE, based on the tensile strength tests. Thus, the effect of heat treatment on the HE resistance of Alloy K-500 appeared to involve, at least partly, irreversible H traps.

The main differences in heat treatment between the DA and AA alloy were the annealing step and the aging time (16 h for AA compared with 8 h for DA). Prolonged exposure of Ni 200 (≤0.15 C) between 425° and 650°C can cause graphite precipitation,[3] which Lee and Latanison have observed to occur at grain boundaries in specimens that were solution annealed and then aged for 24 h at 450° to 650°C.[4] Thus, the difference in aging time for Alloy K-500 may have been a key factor between the DA and AA specimens with respect to graphite precipitation. On the other hand, annealing may play the crucial role, because AA specimens with different annealing times have been found to exhibit different levels of graphitic C at grain boundaries.[5,6] Thus, it is unclear whether the higher k for the AA alloy resulted from the longer aging time or from inclusion of the annealing step.

In the present work, the potentiostatic pulse technique was used to examine irreversible trapping in Alloy K-500 as a function of heat treatment (direct aging versus annealing and aging) to determine whether aging time or annealing is responsible for irreversible trapping differences observed between the AA and DA alloys. Values of k were obtained for annealed, AA, and 12-h and 16-h DA specimens of the CD Alloy K-500 that had been used earlier to provide as-received (unannealed, CD) and 8-h DA specimens. These values were compared with results for the alloy in the unannealed and the DA conditions as well as for the earlier AA specimens, which were obtained elsewhere.† The results were intended to elucidate whether heat treatment is a critical factor in Alloy K-500's resistance to HE and, if so, which is the key aspect of the heat treatment.

EXPERIMENTAL PROCEDURE

Table 1 gives the compositions of the CD Alloy K-500 and the AA alloy (in two heats, denoted as AA-1 and AA-2) used previously. AA-1 and AA-2 were supplied as sections of bar that had been solution-annealed and aged at 607°C for 16 h to give a yield strength in the range 689-724 MPa. The alloys had a similar bulk composition, but the AA-2 alloy exhibited a moderate amount (~20%) of graphitic C at the grain boundaries, whereas the AA-1 alloy contained only a small amount (1%-3%) of grain boundary C.[5,6]

The CD alloy was supplied as a 1.27-cm-diameter rod, which was direct aged in the previous work to give a yield strength of about 1096 MPa. The aging treatment followed the procedure recommended for CD rods ≤3.8 cm in diameter: Heat at 600°C for 8 h and then cool to 480°C at a rate of 11°C/h.[7] In the present work, the CD alloy was annealed at 982°C and, where

† Provided by Dr. M. Natishan, formerly at the David Taylor Research Center, Department of the Navy, and now at the University of Maryland.

relevant, aged at 600°C. The alloy was tested in six conditions, involving different annealing times (t_{ann}) and aging times (t_{age}), as given in Table 2 together with the notations used for these conditions. During aging, γ' particles of $Ni_3(Ti,Al)$ are precipitated throughout the matrix of Alloy K-500.[7]

Details of the electrochemical cell and instrumentation have been given previously.[8] The test electrodes of Alloy K-500 consisted of a 1.27-cm length of rod (as-supplied or machined) press-fitted into a polytetrafluoroethylene sheath so that only the planar end surface was exposed to the electrolyte. The surface was polished before each experiment with SiC paper and then 0.05-μm alumina powder. The electrolyte (pH 4.8) contained 1 mol L^{-1} acetic acid (CH_3COOH) and 1 mol L^{-1} sodium acetate (CH_3COONa) with 15 ppm As_2O_3 and was deaerated continuously with Ar before and throughout data acquisition. The potentials were measured with respect to a saturated calomel electrode (SCE). All tests were performed at 22° ± 1°C.

The test electrode was cathodically charged with H at a potential E_c for a time t_c, after which the potential was stepped anodically to a value 10 mV negative of the open-circuit potential E_{oc}. Anodic current transients were obtained over a range of charging times, typically from 5 to 60 s, at different overpotentials ($\eta = E_c - E_{oc}$). The open-circuit potential of the test electrode was measured immediately before each charging time and was also used to monitor the stability of the alloy surface.

ANALYSIS

The current transients were analyzed using a diffusion/trapping model based on a constant entry flux of H at the surface.[8,9] According to the model, the anodic charge (C m^{-2}) is given by

$$q'(\infty) = FJt_c\{1 - e^{-R}/(\pi R)^{1/2} - [1 - 1/(2R)]\mathrm{erf}(R^{1/2})\} \qquad (1)$$

where F is the Faraday constant, J is the ingress flux in mol m^{-2} s^{-1}, $R = k_a t_c$, and k_a is an apparent rate constant for irreversible trapping measured in the presence of reversible traps. The charge $q'(\infty)$ is equated to the charge (q_a) passed during the experimental anodic transients. q_a can be associated entirely with absorbed H, since the adsorbed charge is almost invariably negligible. k_a is related to the irreversible trapping constant (k) by kD_a/D_L, where D_a is the apparent diffusivity and D_L is the lattice diffusivity of H. The value of k_a and therefore of k depends on the density (N_i) and radius (d) of particles or defects providing irreversible traps according to Equation (2):

$$N_i = k_a a/(4\pi d^2 D_a) \quad (2)$$

where a is the diameter of the metal atom.[10, 11]

k has been used in our previous work as an index for characterizing an alloy's intrinsic susceptibility to HE.[12, 13] It has long been recognized that the susceptibility is affected by a wide range of factors, but some of them would be expected to exert a greater influence than others and so be primarily responsible for determining the susceptibility. The correlation observed between k and the actual resistance to HE for Alloy K-500 and other high-strength alloys[12, 13] suggests that k contains enough key parameters to be effective as an index of susceptibility for the alloys studied at their respective yield strengths.

RESULTS

For the constant flux model to be applicable, it must be possible to determine a value of k_a for which J is constant over the range of charging times at each potential. Equation (1) could in fact be fitted to the experimental data for q_a to obtain values of k_a and J that satisfy this requirement. Table 3 shows the number of tests and range of overpotentials used for each condition of Alloy K-500. Also listed are the number of k_a values and the mean k_a obtained for each test.

The values of k_a for Alloy K-500 in each condition are given in Fig. 1. In all the tests, k_a was independent of charging potential, as is also required for the model to be valid. Annealing increased k_a, with the unannealed DA alloy having the lowest values, followed by the 0.25-h annealed alloy and then the 0.5-h annealed alloy. The overall mean values of k_a are listed in Table 4, which shows that k_a for the 8-h aged alloy is more than doubled by a 0.25-h anneal before aging and is tripled by a 0.5-h anneal. The 16-h aged alloy showed a smaller but still considerable (50%) increase in k_a if annealed for 0.5 h before aging. k_a for the 0.5-h annealed alloy was essentially unaffected by aging, whereas it increased for the DA alloy when the aging time was extended from 8 h to 12-16 h.

The entry flux generally increased to some extent with overpotential, which was to be expected because of the dependence of J on the surface coverage of adsorbed H. The flux did not show a significant difference between the various heat treatments.

DISCUSSION

Irreversible Trapping Constants

Irreversible trapping constants (k) were calculated from the mean values of k_a by correcting for the effect of reversible traps. The correction is made using diffusivity data for the "pure" alloy to obtain the lattice diffusivity (D_L) and for the actual alloy to obtain the apparent diffusivity (D_a), so that the ratio of D_L to D_a can be determined. From the viewpoint of diffusivity, the "pure" Alloy K-500 was taken as 65Ni-35Cu. Minor elements (either in their atomic form or as fine intermetallic particles precipitated during aging) in the actual alloy were treated as reversible traps and in fact were assumed to be primarily responsible for reversible trapping. For face-centered cubic (fcc) alloys, defects such as vacancies or edge dislocations were presumed to make a negligible contribution to reversible trapping, because the binding energy of H to such defects is considerably smaller than the activation energy for diffusion.[14-16] Thus, reversible trapping in Alloy K-500, which has an fcc lattice, should be influenced more by composition than by microstructural defects.

The lattice diffusivity was determined by interpolation of data for a range of binary Cu-Ni alloys and was found to be $(3.0 \pm 0.1) \times 10^{-14}$ m^2 s^{-1} for 65Ni-35Cu at 25°C.[17] The level of Cu differs slightly between the 65Ni-35Cu alloy and actual Alloy K-500 (30Cu), but the error in using the diffusivity of the 35Cu alloy for D_L was considered negligible. The apparent diffusivity for AA-16h Alloy K-500 (assumed to be at ambient temperature) is 1.90×10^{-14} m^2 s^{-1}, compared with 1.48×10^{-14} m^2 s^{-1} for the DA-16h alloy.[1] Thus, the respective values of D_L/D_a are 1.6 and 2.0, which were used to calculate values of k, as given in Table 4.

No diffusivity data were available for the other conditions, so D_a in these cases was estimated from the values for the 16-h aged alloys. The intermetallic particles precipitated during aging appear to have little effect on D_a compared with that of the minor alloying elements in solid solution: D_a for the 16-h-aged alloys was only a factor of ≤ 2 smaller than D_L. Because most solutes introducing an electron vacancy provide reversible traps that could largely account for this factor, the intermetallics must be presumed to add little to the effect of the minor elements. In addition, the CD alloy with its high initial hardness of HRC 23 is expected to reach full hardness (HRC 35) in 8 h,[7] so any precipitation of γ' particles occurring over longer aging times should be relatively small. Hence, D_a for the CD, DA-8h, and DA-12h alloys was approximated to that for the DA-16h alloy, and D_a for the annealed and AA-8h alloys was approximated to that for the AA-16h alloy. By using these values and the D_L above, k was calculated for the CD, annealed, and <16h-aged alloys (Table 4).

Susceptibility to HE

The values of k for the different heat treatments are presented graphically in Fig. 2. Clearly, Alloy K-500 can exhibit a marked difference in irreversible trapping, depending on the type of heat treatment. Annealing caused a large increase in k for CD Alloy K-500 and thus can be considered to greatly heighten the instrinsic susceptibility of this alloy. In fact, the values of k for all the 0.5-h-annealed specimens—unaged or aged—were more than twice as large as that obtained for the 8-h DA specimen. Even halving the annealing time to 0.25 h resulted in a k double that of the 8-h DA alloy and only about 20% lower than the value obtained for the full (0.5-h) annealing time. Addition of the 0.5-h annealing step before aging the CD alloy gave virtually the same k values as those for the annealed and (16-h) aged alloy (AA-1 and AA-2) that was obtained from two other heats and tested previously.[2]

Aging for 8 h had a negligible effect on k for the annealed alloy and only a relatively small effect for the unannealed alloy. However, a considerable difference was observed between the alloys when the aging time was doubled to 16 h, with k showing no change for the annealed alloy but almost doubling for the unannealed alloy. Even an intermediate aging time of 12 h for the unannealed alloy had a marked effect on k. In fact, the value of k for a 12-h age was higher than that for the 16-h age, but this order is probably an artifact caused by assuming that D_a is similar for both aging times. D_a should tend to increase as the aging time is reduced (less γ' precipitation), and in fact it would need to be only slightly higher (1.9×10^{-14} m^2 s^{-1}) for k to have similar values for the 12-h and 16-h DA specimens.

The results show that differences in irreversible trapping observed previously between the DA-8h specimens and the AA-1 and AA-2 specimens resulted from the differences in heat treatment. Moreover, they indicate that annealing has a pronounced effect on the irreversible trapping characteristics of Alloy K-500. Two key points emerge from the results: the k value obtained by annealing for 0.5 h is unaffected by subsequent aging for 16 h, and the k value obtained by direct aging for 16 h is somewhat lower than those for the annealed specimens—aged or unaged. These points suggest that the annealing step rather than the aging time is the primary factor in the previous differences.

Tensile tests on Alloy K-500, as discussed above, showed a difference in ultimate tensile strength between DA and AA specimens (aged for 16 h) cathodically precharged for 16 days.[1] The previous comparison between k and the reduction of strength was made using k values for DA-8h and AA-1/AA-2 (16h-aged) specimens.[2] The new data enable a more appropriate comparison to be made based on the same aging time (16 h) and the same CD alloy. Fig. 3 shows k and the reduction of strength for the two types of aged alloy. The decrease in strength of the AA alloy together with the small increase for the DA alloy indicated that the AA alloy is less resistant to HE.

Thus, the order of the k values for the 16-h aged alloys correlates with the observed resistances to HE. The correlation confirms the one reported previously and implies that the decrease in the resistance to HE produced by annealing is caused, at least in part, by changes in the irreversible H traps.

The yield strength of Alloy K-500 also varies with the type of heat treatment and should therefore be considered as a possible factor in the resistance to HE. However, the order of the yield strengths for the AA specimens (689-724 MPa) and the DA specimen (1096 MPa) was opposite that of their k values, which suggests that the difference in HE susceptibility does not result from yield strength.

Identification of Irreversible Traps

In the previous work on Alloy K-500, the differences in thermomechanical processing were presumed to be responsible for differences in the species at grain boundaries. The principal irreversible trap in the DA alloy was thought to be grain boundary S for several reasons: (1) the intergranular HE of Ni[18-20] and Ni-Co alloys[21] is assisted by S segregated at grain boundaries, and H also probably segregates to the grain boundaries as in Ni[20]; (2) S has been identified as the critical segregant among three species (S, P, and Sb) in the intergranular HE of Ni because of its large enrichment at the grain boundaries[19]; (3) the calculated trap densities for two other high-Ni alloys, C-276 [UNS N10276] and MP35N [UNS R30035], were in close agreement with the amount of grain boundary S and P distributed per unit volume of the alloy[13]; (4) the sequence of the calculated trap densities for DA Alloy K-500 and a 77Cu-15Ni alloy was consistent with the levels of grain boundary segregants, based on the S-P contents of the alloys[22*]; and (5) the small increase in k for Alloy K-500 with direct aging for 8 h is consistent with a reduced volume diffusion of S thought to result from the addition of Cu to Ni.[23]

The present results indicate that annealing considerably changes the number, size, or type of irreversible traps in Alloy K-500. Extended aging times (>8 h) can also cause such changes in unannealed specimens. Lee and Latanison, as noted above, found that Ni 200 (≤0.15 C) solution annealed and then aged for 24 h at 450° to 650°C undergoes graphite precipitation at grain boundaries.[4] Recent work by Natishan et al. suggests that intergranular cracking of AA Alloy K-500 may be associated with grain boundary C.[5, 6, 24] The two AA heats used by these workers were the same as AA-1 and AA-2 in the present study. High-resolution, scanning Auger electron spectroscopy showed graphitic C to be located on the intergranular facets and within grain boundaries.[5] The AA-1 and AA-2 specimens differed in heat treatment only with respect to

* The intergranular concentration of S in Ni increases with total S content,[23] and it seems reasonable to expect similar behavior for Ni-Cu alloys.

annealing time yet exhibited different levels of grain boundary graphite, which implies that annealing renders Alloy K-500 more prone to graphite precipitation during aging. Thus, the increase in k with annealing time appears to result from an increase in grain boundary graphite; that is, the k values for the AA alloys are determined by the amount of grain boundary C.

The similarity in the values of k for the annealed (unaged) alloy and AA alloys suggests that graphite precipitation may actually initiate during annealing in the case of Alloy K-500. On the other hand, k for the DA alloy shows a sizable increase when the aging time is increased from 8 to ≥12 h, which suggests that graphite precipitation may also occur in these specimens and therefore that annealing is not essential for graphite to be precipitated. Alternatively, the increase in k with annealing (with or without aging) and with extended direct aging times may reflect a change in some other microstructural feature and not, in fact, graphite precipitation.

Lee and Latanision found that the effect of S segregation on intergranular HE of Ni was most prominent when the grain boundaries were free of graphite precipitates.[4] Accordingly, in the case of Alloy K-500, it is postulated that S governs HE of the DA-8h alloy but C predominates in the AA and DA-12/16h alloys. If the respective critical species are S and C, k might be expected to be higher for the specimens with precipitated C, because the total content of C is over two orders of magnitude greater than that of S. This rationale is consistent with the actual results showing that k is higher for the annealed (aged or unaged) alloy and the DA-12/16h alloy, which thus supports the conjecture that k reflects irreversible trapping at graphite precipitates in these alloys.

SUMMARY

- Irreversible trapping in CD Alloy K-500 can depend strongly on the type of heat treatment. Marked differences in k between unannealed and annealed specimens aged for the same time (8 h or 16 h) can be attributed to the annealing step.
- The intrinsic susceptibility to HE, as defined by k, is increased considerably by annealing. Aging has a negligible effect on the intrinsic susceptibility for the annealed alloy but can result in a sizable increase for the unannealed alloy if performed for extended times.
- The intrinsic susceptibilities for AA and DA Alloy K-500 can be correlated with the observed resistances to HE. Thus, the decrease produced in the HE resistance by annealing appears to result to a large extent, if not entirely, from a change in the irreversible traps.
- Differences in the grain boundary chemistry resulting from heat treatment could account for changes in the type of irreversible traps. The higher k values for the annealed (aged

or unaged) and the longer-DA alloy is consistent with the primary irreversible trap in these cases being grain boundary graphitic C.

ACKNOWLEDGMENT

Financial support of this work by the U.S. Office of Naval Research under Contract N00014-95-C-0313 is gratefully acknowledged.

REFERENCES

1. J. A. Harris, R. C. Scarberry, and C. D. Stephens, *Corrosion* **28**, 57 (1972).
2. B. G. Pound, *Corrosion*, submitted for publication.
3. Huntington Alloys Bulletin 10M2-79T-15, Huntington Alloys Inc., Huntington, WV (1979).
4. T.S.F. Lee and R. M. Latanision, *Metall. Trans.* **18A**, 1653 (1987).
5. M. E. Natishan, E. R. Sparks, and M. L. Tims, in ISTFA '90: Proceedings of the International Symposium for Testing and Failure Analysis, ASM International, Materials Park, OH, p. 385 (1990).
6. M. E. Natishan and W. C. Porr, Jr., "Issues Surrounding the Use of Nickel-Copper Alloy K-500 Fasteners in Seawater," CORROSION/94, paper no. 94-483, NACE, Houston, TX (1994).
7. Monel Nickel-Copper Alloys, 4th ed., Huntington Alloys Inc., Huntington, WV (1981).
8. B. G. Pound, *Corrosion* **45**, 18 (1989).
9. R. McKibbin, D. A. Harrington, B. G. Pound, R. M. Sharp, and G. A. Wright, *Acta Metall.* **35**, 253 (1987).
10. B. G. Pound, R. M. Sharp, and G. A. Wright, *Acta Metall.* **35**, 263 (1987).
11. B. G. Pound, *Acta Metall.* **38**, 2373 (1990).
12. B. G. Pound, in Proceedings of the Tri-Service Conference on Corrosion, The Army Materials Technology Laboratory, United States Army, p. 409 (1994).
13. B. G. Pound, in Proceedings of the Fifth International Conference on Hydrogen Effects on Material Behavior, eds. N. R. Moody and A. W. Thompson, The Minerals, Metals & Materials Society, Warrendale, PA, p. 115 (1994).
14. W. D. Wilson and S. C. Keeton, in Advanced Techniques for Characterizing Hydrogen in Metals, eds. N. F. Fiore and B. J. Berkowitz, The Metallurgical Society of AIME, Warrendale, PA, p. 3 (1981).
15. M. Uhlemann and B. G. Pound, "Diffusivity, Solubility, and Trapping Behavior of Hydrogen in Alloys 600, 690tt, and 800," *Corrosion Sci.*, accepted for publication.
16. J. Y. Lee and S. M. Lee, *Metall. Trans.*, **17A**, 181 (1986).
17. H. Hagi, *Trans. Jpn. Inst. Metals*, **27**, 233 (1986).
18. R. M. Latanision and H. Opperhauser, Jr., *Metall. Trans.* **5**, 483 (1974).
19. S. M. Bruemmer, R. H. Jones, M. T. Thomas, and D. R. Baer, *Metall. Trans.* **14A**, 223 (1983).

20. D. H. Lassila and H. K. Birnbaum, *Acta Metall.* **35**, 1815 (1987).

21. J. D. Frandsen, H. L. Marcus, and A. S. Tetelman, in Effect of Hydrogen on Behavior of Materials, eds. A. W. Thompson and I. M. Bernstein, The Metallurgical Society of AIME, Warrendale, PA, p. 299 (1976).

22. B. G. Pound, *Corrosion* **50**, 301 (1994).

23. C. Loier and J-Y. Boos, *Metall. Trans.* **12A**, 1223 (1981).

24. M. E. Natishan and W. C. Porr, Jr., "The Effect of Grain Boundary Carbon on the Hydrogen Assisted Intergranular Failure of Nickel-Copper Alloy K-500 Fastener Material," ASTM STP 1236 on Structural Integrity of Fasteners, ed. P. Toor, ASTM, Philadelphia, PA (1995).

TABLE 1
Alloy Composition (wt%)

Element	K-500 CD	K-500 AA-1	K-500 AA-2
Al	2.92	2.95	2.95
C	0.16	<0.17	<0.14
Cu	29.99	29.53	29.8
Fe	0.64	<0.85	<0.74
Mn	0.72	<0.70	<0.58
Ni	64.96	65.29	65.1
P			<0.002
S	0.001	<0.001	<0.001
Si	0.15	<0.05	<0.15
Ti	0.46	0.46	0.44

TABLE 2
Annealing and Aging Times Used for Alloy K-500

Notation	t_{ann} (h)	t_{age} (h)
DA-12h	-	12
DA-16h	-	16
0.25h-AA-8h	0.25	8
0.5h-A	0.5	-
0.5h-AA-8h	0.5	8
0.5h-AA-16h	0.5	16

TABLE 3
Apparent Trapping Constants for Alloy K-500

Condition	Test no.	η range (V)	No. of k_a values	k_a (s^{-1})
DA-12h	1	-0.35 to -0.40	2	0.047 ± 0.001
	2	-0.30 to -0.35	2	0.053 ± 0.001
	3	-0.25 to -0.30	2	0.047 ± 0.002
DA-16h	1	-0.30 to -0.40	2	0.039 ± 0.003
	2	-0.30 to -0.45	3	0.041 ± 0.003
	3	-0.30 to -0.40	2	0.041 ± 0.005
0.25h-AA-8h	1	-0.25 to -0.55	7	0.052 ± 0.004
	2	-0.25 to -0.50	3	0.051 ± 0.004
0.5h-A	1	-0.30 to -0.40	3	0.065 ± 0.002
	2	-0.30 to -0.45	4	0.063 ± 0.005
	3	-0.30 to -0.40	3	0.066 ± 0.001
0.5h-AA-8h	1	-0.25 to -0.45	5	0.064 ± 0.002
	2	-0.25 to -0.40	4	0.064 ± 0.004
0.5h-AA-16h	1	-0.30 to -0.40	3	0.061 ± 0.001
	2	-0.30 to -0.40	3	0.066 ± 0.003

TABLE 4
Irreversible Trapping Constants for Alloy K-500

Condition	k_a (s^{-1})	D_L/D_a	k (s^{-1})
CD-Unaged	0.017 ± 0.003	2.0 ± 0.1	0.034 ± 0.007
DA-8h	0.021 ± 0.003	2.0 ± 0.1	0.042 ± 0.007
DA-12h	0.049 ± 0.003	2.0 ± 0.1	0.098 ± 0.009
DA-16h	0.040 ± 0.003	2.0 ± 0.1	0.080 ± 0.009
0.25h-AA-8h	0.052 ± 0.004	1.6 ± 0.1	0.083 ± 0.009
0.5h-A	0.065 ± 0.003	1.6 ± 0.1	0.104 ± 0.008
0.5h-AA-8h	0.064 ± 0.003	1.6 ± 0.1	0.102 ± 0.008
0.5h-AA-16h	0.063 ± 0.003	1.6 ± 0.1	0.101 ± 0.008
AA-2 (aged 16 h)	0.063 ± 0.003	1.6 ± 0.1	0.099 ± 0.008
AA-1 (aged 16 h)	0.060 ± 0.006	1.6 ± 0.1	0.095 ± 0.013

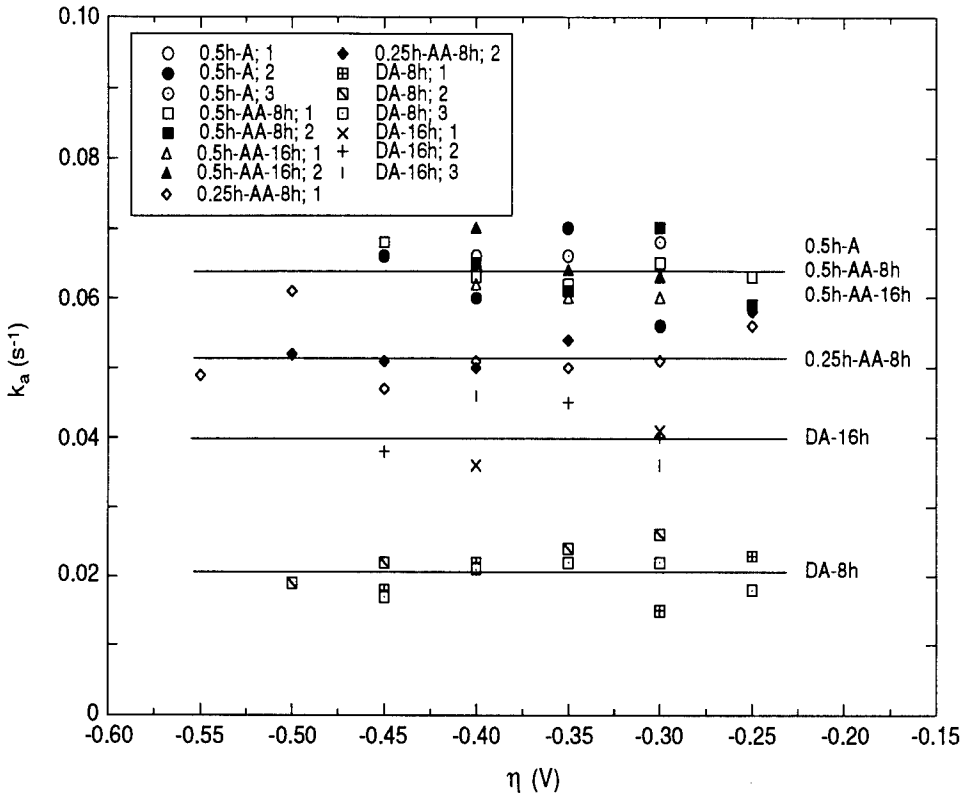

Figure 1. Values of k_a for Alloy K-500 at various overpotentials. Each symbol is identified by the heat treatment and a test number for that treatment. For clarity, data for the DA-12h and CD conditions are omitted.

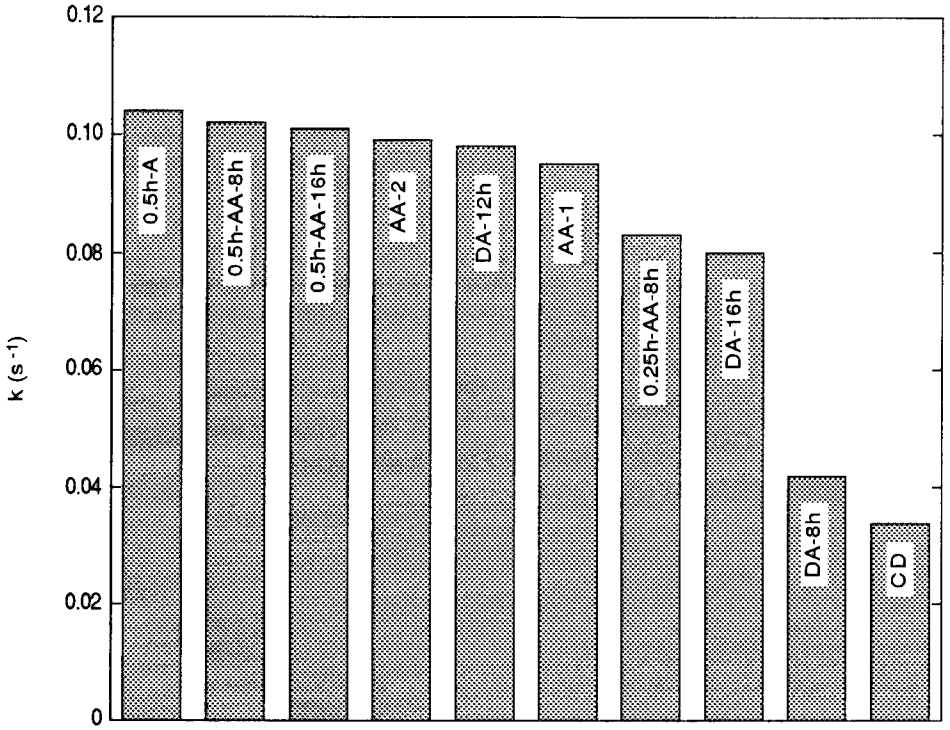

Figure 2. Variation in *k* for different heat treatments of Alloy K-500.

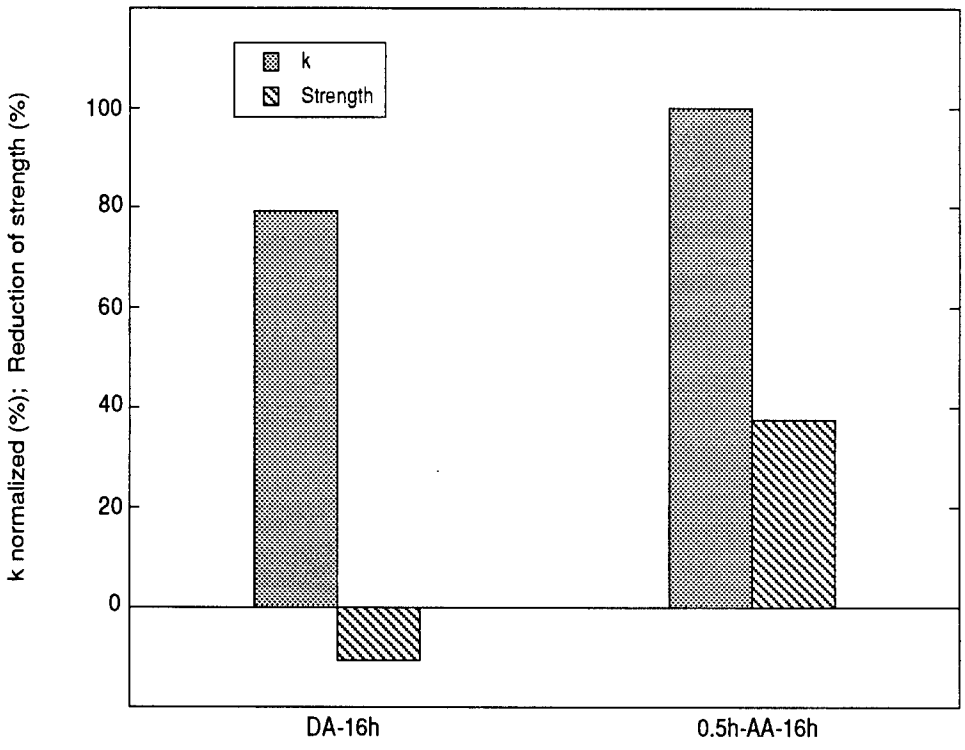

Figure 3. Comparison of *k* with reduction of strength for Alloy K-500. Data for reduction of strength were taken from Ref. 1. The DA alloy showed an increase in strength with H charging. k was normalized to a percentage of the value for the 0.5h-AA-16h alloy.

The Effect of Aging on Hydrogen Trapping in Precipitation-Hardened Alloys*

Abstract—Hydrogen trapping in two precipitation-hardened alloys—18Ni (250) maraging steel and alloy X-750—was studied using a potentiostatic pulse technique. Values of the irreversible trapping constant (k) and the hydrogen entry flux were determined for these alloys in 1 mol L^{-1} acetic acid/1 mol L^{-1} sodium acetate. Aging causes an increase in k for both alloys. The value of k for aged alloy X-750 is higher than the values for three other hardened Ni-base alloys (625, 718, and 925) but is considerably lower than the value for the aged 18Ni steel. A correlation was found between k and the observed resistance to HE for three groups of aged alloys: X-750 and 718; 18Ni (250) and 718; and 18Ni (250), 18Ni (300), and 4340 steels. Carbonitride particles appear to provide the principal irreversible traps in unaged alloy X-750 and 18Ni (250) steel. They also appear to be one of the principal irreversible traps in aged alloy X-750, with additional trapping resulting from at least one other microstructural heterogeneity that could be grain boundary carbides. For the aged 18Ni steel, however, carbonitrides make only a small contribution to irreversible trapping, the main contribution coming from some other heterogeneity that possibly involves intergranular S.

INTRODUCTION

Various studies have shown that precipitation-hardened alloys can be susceptible to hydrogen embrittlement (HE) but that the degree of susceptibility differs considerably between the alloys.[1-5] Stress-rupture tests during cathodic charging have shown that 18Ni (250) maraging steel† will undergo severe HE, whereas alloy 718 exhibits negligible embrittlement.[1] Likewise, room-temperature tensile tests in gaseous hydrogen showed from the reduction of notch strength that the maraging steel was less resistant than alloy 718, although the embrittlement in both cases was characterized as extreme.[2] Constant extension rate tests of cathodically charged specimens have shown that alloy 718 in the double-aged condition is also more resistant to intergranular cracking than aged or double-aged alloy X-750.[4,5]

---

* Submitted to *Corrosion Science*.

† The established nomenclature for the grade of maraging steel is nominal Ni content followed by nominal yield strength (ksi) in parentheses. Two grades referred to in this work have nominal yield strengths of 1723 MPa (250 ksi) and 2068 MPa (300 ksi).

The precipitation-hardened alloys typically contain Nb or Ti carbides and carbonitrides in the form of large particles (>1 μm and commonly several micrometers). TiC particles are known to provide irreversible traps for hydrogen in iron and ferritic steels and, if large enough (>1 μm), can be particularly conducive to HE.[6-8] Recent work using a potentiostatic pulse technique to determine rate constants (k) for irreversible trapping has indicated that carbides and carbonitrides also act as irreversible traps in 18Ni (300) maraging steel and various Ni-base alloys.[9-11] This finding is consistent with autoradiography studies that have shown hydrogen to be trapped at the carbonitride interfaces in maraging steels.[12,13]

The potentiostatic pulse work raised the question of whether carbides and carbonitrides make a large contribution to irreversible trapping in carbide/carbonitride-containing alloys in general. It also led to the question of whether these particles provide the principal irreversible traps in 18Ni maraging steels, because the irreversible trap density calculated for 18Ni (300) steel differed from the concentration of carbide/carbonitride particles by a factor of ~30.[9,11] The difference was considered to be reasonably close within the uncertainties of the calculations, but it remained to verify whether irreversible trapping in 18Ni steel is governed by these particles.

In the present work, the potentiostatic pulse technique was applied to alloy X-750 and 18Ni (250) maraging steel in the unaged and aged conditions. Alloy X-750 extended the group of carbide-containing Ni-base alloys (625, 925, and 718) examined previously,[9-11] while the 18Ni steel provided a comparison with other high-strength steels [4340, H11, AerMet 100, and 18Ni (300) steel] that have been studied.[9,14,15] The objectives of this work were to characterize the intrinsic susceptibility of each alloy to HE in terms of k and to determine whether k was consistent with the carbide/carbonitride content. The results could then be used to examine whether irreversible trapping provides a key link between the HE resistance and microstructure, particularly with respect to carbides and carbonitrides.

EXPERIMENTAL PROCEDURE

Table 1 gives the compositions of alloy X-750, 18Ni (250) steel, and for comparison, 18Ni (300) steel that was studied previously. Alloy X-750 was supplied in the stress-equalized (885°C for 24 h, air cool) condition, which after aging provides the highest yield strength and tensile ductility for this alloy at room temperature.[16] The alloy was obtained as 1.59-cm-diameter rod, which was aged at 704°C for 20 h to give a yield strength of 910 MPa. The 18Ni (250) steel was supplied in the annealed condition as 1.91-cm-diameter rod, which was aged at 482°C for 6 h to give a yield strength of 1873 MPa.

Both alloys were examined using scanning electron microscopy and were found to contain randomly distributed, intragranular, MC-type carbides. An energy dispersive X-ray analysis showed the particles to contain titanium and niobium in alloy X-750 and titanium in the 18Ni steel. Elliot has identified the particles in alloy X-750 as [Ti,Nb(C,N)] and has shown that the aged microstructure contains intergranular $Cr_{23}C_6$-type carbides in addition to intragranular γ' precipitates of $Ni_3(Ti,Al)$.[17] In the case of 18Ni steel, the precipitates formed during aging have been identified as Ni_3Mo and possibly Ni_3Ti or FeTi.[18]

The characteristic dimension of the MC carbides was determined as the mean of the linear dimensions in the exposed plane. It had values of approximately 2 μm for alloy X-750 and 4.4 μm for the 18Ni steel. The concentration of MC carbides was calculated on the basis of a spherical shape, with the radius being taken as half the characteristic dimension. The carbide concentration for alloy X-750 was $\sim 2 \times 10^{14}$ m^{-3}. For the 18Ni steel, the carbides were less numerous, with the concentration estimated to be on the order of 10^{11} m^{-3}.

Details of the electrochemical cell and instrumentation were given previously.[14] The test electrodes of each alloy consisted of a 1.27-cm length of rod press-fitted into a polytetrafluoro-ethylene sheath so that only the planar end surface was exposed to the electrolyte. The surface was polished before each experiment with SiC paper and then 0.05-μm alumina powder. The electrolyte contained 1 mol L^{-1} acetic acid and 1 mol L^{-1} sodium acetate with 15 ppm As_2O_3 and was deaerated continuously with Ar before and throughout data acquisition. The potentials were measured with respect to a saturated calomel electrode (SCE). All tests were performed at 22 $\pm$ 1°C.

The test electrode was cathodically charged with hydrogen at a constant potential E_c for a time t_c, which was varied from 5 to 60 s for each potential. The potential was then stepped in the positive direction to a value 10 mV negative of the open-circuit potential E_{oc}. Anodic current transients were obtained over the range of charging times at different overpotentials ($\eta = E_c - E_{oc}$). The transients, which resulted from the oxidation of hydrogen as it diffused back to the entry surface, were integrated to determine the anodic charge (q_a) corresponding to each charging time. The open-circuit potential of the test electrode was measured immediately before each charging pulse and was also used to monitor the stability of the alloy surface.

RESULTS

The current transients were analyzed using a diffusion/trapping model based on a constant entry flux at the surface.[14, 19] According to the model, the total anodic charge (C m^{-2}) depends on the charging time as follows:

$$q'(\infty) = FJt_c\{1 - e^{-R}/(\pi R)^{1/2} - [1 - 1/(2R)]\mathrm{erf}(R^{1/2})\} \quad (1)$$

where F is the Faraday constant, J is the ingress flux in mol m^{-2} s^{-1}, $R = k_a t_c$, and k_a is an apparent trapping constant measured for irreversible traps in the presence of reversible traps. The charge $q'(\infty)$ is equated to the charge (q_a) passed during the experimental anodic transients. The adsorbed charge is almost invariably negligible, so q_a can be associated entirely with absorbed H. k_a is related to the irreversible trapping constant by kD_a/D_L, where D_a is the apparent diffusivity and D_L is the lattice diffusivity of H. The use of k as an index of susceptibility has been discussed elsewhere.[11]

For both alloys in the unaged and aged conditions, equation (1) could be fitted to the experimental data for q_a to obtain values of k_a and J, where J was constant over the range of charging times at each potential. Tables 2 and 3 show the number of tests and range of overpotentials used for alloy X-750 and 18Ni (250) steel, respectively. Also listed are the number of k_a values and the mean k_a for each test.

The values of k_a for the two alloys are presented in Fig. 1. In all the tests, k_a was independent of charging potential, as is required for the diffusion/trapping model to be valid. Alloy X-750 showed no difference in k_a between the unaged and aged conditions, whereas the corresponding values of k_a for the 18Ni steel differed considerably. The overall mean value of k_a in each case is given in Table 4, which shows that aging decreased k_a for the 18Ni steel by a factor of 5. The corresponding values for 18Ni (300) steel and carbide-containing Ni-base alloys studied previously are shown for comparison. Aged alloy X-750 has the highest value of k_a among the four Ni-base alloys. The two grades of aged 18Ni steel have the same k_a values (within experimental uncertainty), which are among the lowest for all the alloys shown.

DISCUSSION

Irreversible trapping constants

Irreversible trapping constants (k) were calculated from the mean values of k_a by correcting for the effect of reversible traps. The correction is made using diffusivity data for the "pure" alloy to obtain the lattice diffusivity (D_L) and for the actual alloy to obtain the apparent diffusivity (D_a), so that the ratio of D_L to D_a can be determined.

From the viewpoint of diffusivity, the "pure" alloys were considered to be 71Ni-16Cr-8Fe for alloy X-750 and Fe-18Ni-8Co-5Mo for the 18Ni steel. Minor elements (either in their atomic form or as fine intermetallic particles precipitated during aging) in the actual alloys were treated as reversible traps and in fact were assumed to be primarily responsible for reversible trapping. For face-centered cubic (fcc) alloys, defects such as vacancies or edge dislocations are unlikely to contribute significantly to reversible trapping, because the activation energy of diffusion is estimated to be 38.6 kJ mol^{-1}, whereas the binding energy of hydrogen to such defects is about 9.6 kJ mol^{-1}.[20] Experimental data obtained over the range 150° to 500°C have shown that the activation energies of diffusion are even higher for alloys 718 (49.8 kJ mol^{-1}) and 903 (52.7 kJ mol^{-1}).[21]

Alloy X-750. The most appropriate diffusivity value for the pure Ni-Cr-Fe alloy is for 76Ni-16Cr-8Cr, for which D_L is $(7.9 \pm 1) \times 10^{-15}$ m^2 s^{-1}.[22] Latanision and Kurkela obtained a diffusivity of 5.6×10^{-15} m^2 s^{-1} for solution annealed alloy X-750,[23] so D_L/D_a is equal to 1.4 for the unaged alloy.

Turnbull et al. used the permeation technique to examine the effect of aging on hydrogen diffusion in alloy X-750 at 80°C and found that aging (704°C for 20 h) decreased the diffusivity by a factor of five.[4] They attributed this decrease to the presence of the γ' phase and, from the second permeation transient, obtained a binding energy of 32.8 kJ mol^{-1} for the γ' /matrix interface in alloy X-750. Moody et al. reported a much smaller binding energy of 19.3 kJ mol^{-1} for γ' in alloy 903,[24] but Turnbull and coworkers speculated that this difference could be associated with differences in γ' misfit strain between the alloys in the two studies.

On the other hand, the results obtained by Turnbull et al. raise some concern. First, their permeation tests involved alloy specimens without any coatings such as palladium, so the output surface, and possibly the input surface, would have been covered by a passive film, which can complicate the analysis of permeation data.[25] In contrast, Latanision and Kurkela coated the output side of their specimens with palladium. Second, Turnbull et al. assumed the boundary condition

for the input surface to be a constant concentration, implying that rapid equilibrium is obtained at the boundary. They justified this assumption by demonstrating that the permeation flux is independent of the normalized time, $\tau = Dt/a^2$, when the thickness (a) is varied. However, these workers overlooked the possibility that the a^2 relationship could instead indicate diffusion control with a constant rate of H entry; such a relationship is well recognized for both cases of diffusion control (constant concentration and constant entry rate) in the absence of trapping.[26] Finally, the composition of the passive film may differ between the unaged and aged conditions, particularly with the precipitation of $Ni_3(Ti,Al)$ during aging, and hence the rates of H entry may differ if a film is present on the input surface.

Because of these issues, the differences in binding energy between alloys X-750 and 903 may not be as great as reported. Moody et al. also used electrochemical charging and assumed that the input concentration was constant, but they analyzed the concentration profiles, so their results were not affected by concerns about the egress of H through a surface oxide. In addition, other results for trapping in fcc nickel, stainless steel, and superalloys have given binding energies typically between 4.8 and 14.5 kJ mol^{-1} for reversible traps such as dislocations and coherent precipitates.[27,28] Thus, the binding energy obtained by Turnbull et al. for alloy X-750 may be too high, possibly being nearer 19.3 kJ mol^{-1}, although misfit could still be an important factor. Hence, the effect of the γ' phase on the diffusivity at room temperature may be only a little more than that of the minor elements in the unaged alloy, particularly because two of the main minor elements—Ti and Al—are involved in the precipitates. Because $D_L/D_a = 1.4$ for the unaged alloy, the apparent diffusivity for the aged alloy is therefore estimated to be lower than that for the unaged alloy by a factor of ~1.5, or at most by a factor of 2. Based on this range from 1.5 to 2, D_a was taken as $(3.3 \pm 0.5) \times 10^{-15}$ m^2 s^{-1} for the aged alloy, and hence D_L/D_a was calculated to be 2.4 in this case.

18Ni Steel. Diffusivity data do not appear to be available for the pure Fe-Ni-Co-Mo alloy, but a simpler alloy can be considered. Although Co is a prominent alloying element in the 18Ni steel, it is regarded as an anti-trap in ferritic Fe[29] and has been shown to have little effect on the diffusivity.[30] Mo is another prominent element in the steel, but there is conflicting evidence about its effect on hydrogen, with some work indicating that it also is an anti-trap in Fe.[29] Thus, the most appropriate data for D_L were considered to be those for Fe-Ni alloys. The literature data were presented graphically as log D versus Ni content,[31] from which the diffusivity for 18% Ni was obtained as $(5 \pm 1) \times 10^{-11}$ m^2 s^{-1} at 27°C. This value differed slightly from that (3×10^{-11} m^2 s^{-1}) in the previous work on 18Ni (300) steel,[9] due to a more precise approach used to interpolate the literature data.

Diffusivity data were also unavailable for the unaged alloy. Accordingly, D_a was estimated by assuming that the diffusivity was affected principally by Ti, because it is the most prominent of the minor elements and, in contrast to Co and Mo, is known to be a reversible trap.[6, 29] The diffusivity for Fe containing up to 1.5% Ti is proportional to the density of Ti atoms.[32, 33] Thus, the presence of 0.47% Ti in Fe was estimated to decrease the diffusivity by a factor of 4, and it was assumed that a decrease of similar size occurs in a martensitic Fe-18Ni matrix.

The diffusivity for aged 18Ni (250) steel has been determined as a function of aging temperature.[34] Permeation measurements involving cathodic charging showed that the diffusivity decreases by a factor of ~3 when the aging temperature is increased from 400° to 500°C but that little change occurs above 500°C. Measurements, however, were not made for 482°C, which is in the region where the diffusivity begins to show little dependence on aging temperature. The next lowest temperature was ~435°C and the data at higher temperatures (505°-580°C) were scattered between 2.5×10^{-13} and 3.2×10^{-13} m^2 s^{-1}. Thus, the value of the diffusivity obtained from these measurements is uncertain for the steel aged at 482°C. Tison et al. used gas phase charging to determine the diffusivity of deuterium as a function of temperature from 55° to 138°C for 18Ni (250) steel aged at 480°C.[35] Extrapolation to 25°C gave 2.6×10^{-13} m^2 s^{-1}, which is at the lower end of the range of cathodic data obtained for aging temperatures of 505°C and higher. The diffusivity of hydrogen should be a little higher than that of deuterium and was therefore taken as 3×10^{-13} m^2 s^{-1} for the steel aged at 482°C. Thus, D_L/D_a was calculated to be 167.

The value of D_a was lowered from that used in the previous work for 18Ni (250) steel (3.7×10^{-13} m^2 s^{-1}),[9] as a result of a more extensive evaluation of the gas-phase data and permeation data. The value obtained previously was used at the time to estimate a D_a for the 300 grade, 1×10^{-13} m^2 s^{-1}, by taking into account differences in hardness and Ti content. In the present work, the estimate for 18Ni (300) steel was revised to reflect only the Ti content, because the difference in hardness between the 250 (HRC 51.6) and 300 (HRC 53.8) grades is relatively small and anyway should not directly affect diffusivity; microstructure is considered to play a more direct role because of reversible trapping. The revision to D_a for 18Ni (300) steel was based on the assumption that the inverse relationship between Ti content and diffusivity for Fe is applicable to the aged maraging steel. It was also assumed that the level of reversible trapping would be consistent with the Ti either in solution or as Ni_3Ti precipitates. Based on the nominal Ti contents of 0.4 in the 250 grade and 0.7 in the 300 grade, D_a was estimated to be $0.4/0.7 \times 3.0 \times 10^{-13}$ m^2 s^{-1}, or 1.7×10^{-13} m^2 s^{-1}, for the 18Ni (300) steel aged at 482°C. Hence, D_L/D_a for the aged 300 grade was calculated to be 294, which is only slightly lower than the previous value of 300 and hence caused little change in k.

Susceptibility to HE

The trapping constants for alloy X-750, and 18Ni (250) and 18Ni (300) steels are given with those for other precipitation-hardened alloys in Table 4. The values of k for the Ni-base alloys are compared in Fig. 2. Alloy X-750 showed an increase in k with aging, and in the aged condition, it has a higher value of k than alloys 718, 925, and 625. Hence, aged alloy X-750 is considered to be intrinsically more susceptible to HE than the other three alloys. Constant extension rate tests of cathodically charged specimens, as noted above, have shown that double-aged alloy 718 is more resistant to intergranular cracking than aged or double-aged X-750.[4,5] Thus, the intrinsic susceptibilities of these alloys parallel their relative resistances to HE observed in tests.

A similar parallel was found for 18Ni (250) steel and alloy 718. Aged 18Ni steel in either grade had a higher value of k than alloy 718. It can therefore be regarded as having a higher intrinsic susceptibility, and as discussed above, stress-rupture tests during cathodic charging and tensile tests during gas-phase charging have both shown that 18Ni (250) steel is less resistant than alloy 718 to HE.[1,2] Hence, irrespective of the type of charging, the k values for these two alloys are also consistent with their relative resistances to HE.

Fig. 3 compares the k values for the two grades of 18Ni steel and for AISI 4340 steel[14,15] with threshold stress intensities for stress corrosion cracking (K_{ISCC}) in 3.5% NaCl.[36,37] The k values indicate that the 18Ni (250) grade is intrinsically less susceptible than the 300 grade and that both grades are somewhat less susceptible than 4340 steel. The order of intrinsic susceptibilities follows the inverse of the K_{ISCC} values, which decrease as k increases. This correlation supports the view that hydrogen plays the predominant role in stress corrosion cracking of martensitic steels,[38] and it shows that the intrinsic susceptibilities, as represented by k, of the steels are matched by their observed resistances to HE.

Identification of irreversible traps

The density of particles or defects (N_i) providing irreversible traps can be calculated from k_a on the basis of a simple model involving spherical traps of radius d.[9,39] The model yields the following expression for N_i:

$$N_i = k_a a/(4\pi d^2 D_a) \qquad (2)$$

where a is the diameter of the metal atom. The value of a for an alloy is taken as the mean of the atomic diameters weighted in accordance with the atomic fraction of each element. The trap radius is estimated from the dimensions of heterogeneities that are potential irreversible traps, and trap

densities are then calculated for the different values of d. In this way, the principal irreversible trap can be identified by comparing the values of N_i with the actual concentrations of specific heterogeneities.[11]

Alloy X-750. Turnbull et al. did not observe a difference between the first and subsequent permeation transients for the solution-annealed alloy or the aged alloy.[4] As a result, they concluded that irreversible trapping was negligible in both cases and hence that any trapping at the [Ti,Nb(C,N)] particles must be reversible. On the other hand, Turnbull et al. recognized that the carbides may provide irreversible traps but were considered to be too few to have a significant effect on the transients. Another factor is that the permeation tests were performed at 80°C, which may have been high enough for traps that were irreversible at room temperature to become reversible.

The potentiostatic pulse technique involves relatively low currents and consequently is more sensitive to trapping than the permeation technique. In fact, the pulse results show that k is significant at room temperature and so indicate that irreversible traps are present in both unaged and aged alloy X-750. Hence, it is quite possible that the carbide particles are irreversible traps, as is the case in iron and steel,[7, 29] and that the increase in k with aging is associated with the $M_{23}C_6$ grain boundary carbides (the γ' phase, as noted above, appears to provide reversible traps[3]).

Turnbull et al. considered the grain boundary carbides to have little influence on trapping because these carbides contribute less than 10% to the total carbide content. However, the location of these carbides could allow them to play a more prominent role than expected simply on the basis of amount. H has been shown to segregate to the grain boundaries in Ni,[40] and the activation energy for diffusion along grain boundaries in Ni is estimated to be 25% lower than that for lattice diffusion.[41] Ni-base alloys are likely to be similar to Ni in terms of H segregation and grain boundary diffusion. Thus, even though the grain boundary carbides are present in a relatively small amount, their concentration on a favored diffusion path could allow them to make a sizable contribution to trapping, particularly if the activation energy for diffusion is significantly lower along grain boundaries.

The density of irreversible trap particles in unaged alloy X-750 was calculated from equation (2) on the basis of the Ti,Nb carbonitrides. Although the spherical trap shape assumed for this equation is an approximation for the carbonitride particles, a reasonable estimate can be obtained for the trap density. The trap radius was taken as half the characteristic dimension of the particles. By using $d = 1\ \mu m$, $a = 251.7$ pm, $D_a = 5.6 \times 10^{-15}\ m^2\ s^{-1}$, and $k_a = 0.057\ s^{-1}$, the density of irreversible trap particles was calculated to be $2.0 \times 10^{14}\ m^{-3}$, which is in agreement

with the actual concentration of carbonitrides, ~2×10^{14} m^{-3}. The [Ti,Nb(C,N)] particles therefore appear to provide the principal irreversible traps in unaged alloy X-750.

The k value for the unaged alloy X-750 constitutes more than half of that for the aged alloy, which indicates that the carbonitride particles must be one of the principal irreversible traps in the aged alloy. Clearly, at least one other microstructural heterogeneity must also be an important trap. This heterogeneity could well be the grain boundary carbides, as discussed above. The correlation between k and resistance to HE in fact implies that the key irreversible traps must be located at grain boundaries to be consistent with the intergranular cracking observed for alloy X-750.

18Ni (250) steel. Autoradiography has shown that hydrogen is strongly trapped at carbonitride interfaces in maraging steels, as noted above.[12, 13] The density of irreversible trap particles in unaged 18Ni (250) steel was therefore calculated from equation (2) on the basis of the Ti carbonitrides. The carbonitride particles were again treated as spherical traps, and the trap radius was assumed to be half the characteristic dimension of the particles. By using $d = 2.2$ μm, $a = 249.5$ pm, $D_a = 3 \times 10^{-13}$ m^2 s^{-1}, and $k_a = 0.006$ s^{-1}, the density of irreversible traps was calculated to be 8.2×10^{10} m^{-3}, which is of the same order of magnitude as the actual concentration estimated for the carbonitride particles, 10^{11} m^{-3}. Hence, the principal irreversible traps in the unaged alloy are probably provided by these particles.

Carbonitrides in the aged 18Ni steel, unlike alloy X-750, appear to make a relatively small contribution to irreversible trapping, based on the large difference in k values between the unaged and aged alloy. At least part of the increase in k with aging may result from segregation of S to grain boundaries. S has been found to accumulate at grain boundaries as a titanium sulfide or carbosulfide and is particularly detrimental to the stress corrosion resistance of maraging steels.[36] The titanium sulfides or carbosulfides are certainly likely to act as irreversible traps, but even elemental S may be effective, as in Ni where S was shown to be the critical segregant among three species (S, P, and Sb) in the intergranular HE of Ni because of its large enrichment at the grain boundaries.[42] Because stress corrosion cracking is predominantly intergranular in maraging steels, the grain boundary sites would in fact be expected to provide key traps in view of the correlation between k and K_{ISCC}.

SUMMARY

- Aging causes an increase in k for alloy X-750 and 18Ni (250) steel. The value of k for aged alloy X-750 is higher than the values for three other hardened Ni-base alloys (625, 718, and 925) but is considerably lower than the value for the aged 18Ni steel. Hence, aged X-750 is considered to be intrinsically more susceptible to HE than the other Ni-base alloys but less susceptible than the 18Ni steel.
- A correlation was found between the intrinsic susceptibility (k) and the observed resistance to HE for three groups of aged alloys: (1) the Ni-base alloys, X-750 and 718; (2) 18Ni (250) steel and alloy 718; and (3) the three steels, 18Ni (250), 18Ni (300), and 4340. This correlation implies that intrinsic susceptibility is a principal factor determining the observed resistance of these alloys to HE.
- [Ti,Nb(C,N)] particles appear to provide the principal irreversible traps in unaged alloy X-750. They also appear to be one of the principal irreversible traps in the aged alloy together with at least one other microstructural heterogeneity that could be grain boundary carbides. In view of the correlation between k and resistance to HE, the key irreversible traps must lie at grain boundaries to be consistent with the intergranular cracking of alloy X-750.
- The principal irreversible traps in unaged 18Ni (250) steel also seem to be associated with carbonitride particles. Although they contribute to irreversible trapping in the aged steel, the main contribution comes from some other heterogeneity that possibly involves S present at grain boundaries in the elemental form or as titanium sulfides or carbosulfides. The grain boundary sites would be expected to provide key traps because of the k/K_{ISCC} correlation and the fact that intergranular stress corrosion cracking is predominantly intergranular in maraging steels.

ACKNOWLEDGMENT

Financial support of this work by the U.S. Office of Naval Research under Contract N00014-95-C-0313 is gratefully acknowledged.

REFERENCES

1. T. P. Groeneveld, E. E. Fletcher, and A. R. Elsea, *A Study of Hydrogen Embrittlement of Various Alloys*, Summary Report, Contract No. NAS8-20029, NASA, Marshall Space Flight Center, Huntsville, AL (1966).
2. R. J. Walter, R. P. Jewett, and W. T. Chandler, *Mater. Sci. Eng.* **5**, 98 (1969/70).

3. P. D. Hicks and C. J. Alstetter, in *Proc. Fourth Int. Conf. on Hydrogen Effects on Material Behavior*, ed. N. R. Moody and A. W. Thompson, p. 613, The Minerals, Metals & Materials Society, Warrendale, PA (1990).
4. A. Turnbull, R. G. Ballinger, I. S. Hwang, M. M. Morra, M. Psaila-Dombrowski, and R. M. Gates, *Metall. Trans.* **23A**, 3231 (1992).
5. J. W. Prybylowski, Sc. D. Thesis, Massachusetts Institute of Technology, Cambridge, MA (1986).
6. G. M. Pressouyre, *Metall. Trans.* **10A**, 1571 (1979).
7. G. M. Pressouyre and I. M. Bernstein, *Metall. Trans.* **9A**, 1571 (1978).
8. G. M. Pressouyre and I. M. Bernstein, *Acta Metall.* **27**, 89 (1979).
9. B. G. Pound, *Acta Metall.* **38**, 2373 (1990).
10. B. G. Pound, *Acta Metall.* **39**, 2099 (1991).
11. B. G. Pound, in *Proc. Fifth Int. Conf. on Hydrogen Effects on Material Behavior*, ed. N. R. Moody and A. W. Thompson, p. 115, The Minerals, Metals & Materials Society, Warrendale, PA (1995).
12. M. Aucouturier, G. Lapasset, and T. Asaoka, *Metallography* **11**, 5 (1978).
13. P. Lacombe, M. Aucouturier, J. P. Laurent, and G. Lapasset, in *Proc. of Conf. on Stress Corrosion Cracking and Hydrogen Embrittlement of Iron-Base Alloys*, p. 423, NACE, Houston, Texas, (1973).
14. B. G. Pound, *Corrosion* **45**, 18 (1989).
15. B. G. Pound, "Characterization of Hydrogen Ingress in High Strength Alloys," Final Report, Office of Naval Research, Contract No. N00014-91-C-0263 (1995).
16. Alloy Data, Pyromet® Alloy X-750, Carpenter Technology Corporation, Reading, PA.
17. C. Elliott, Sc. D. Thesis, Massachusetts Institute of Technology, Cambridge, MA (1985).
18. S. Floreen, *Metall. Rev.* **13**, 115 (1968).
19. R. McKibbin, D. A. Harrington, B. G. Pound, R. M. Sharp, and G. A. Wright, *Acta Metall.* **35**, 253 (1987).
20. W. D. Wilson and S. C. Keeton, in *Advanced Techniques for Characterizing Hydrogen in Metals*, ed. N. F. Fiore and B. J. Berkowitz, p. 3, The Metallurgical Society of AIME, Warrendale, PA (1981).
21. W. M. Robertson, *Metall. Trans.* **10A**, 489 (1979).
22. M. Cornet, C. Bertrand, and M. Da Cunha Belo, *Metall. Trans.* **13A**, 141 (1982).
23. R. M. Latanision and M. Kurkela, *Corrosion* **39**, 175 (1983).
24. N. R. Moody, S. L. Robinson, S. M. Myers, and F. A. Greulich, *Acta Metall.* **37**, 281 (1989).
25. Su-Il Pyun and R. A Oriani, *Corros. Sci.* **29**, 485 (1989).
26. N. Boes and H. Züchner, *J. Less Common Metals* **49**, 223 (1976).
27. R. A. Oriani, *Ann. Rev. Mater. Sci.* **8**, 327 (1978).
28. G. J. Thomas, in *Proc. Third Int. Conf. on Effect of Hydrogen on Behavior of Materials*, ed. I. M. Bernstein and A. W. Thompson, p. 77, The Metallurgical Society of AIME, Warrendale, PA (1981).

29. I. M. Bernstein and G. M. Pressouyre, in *Hydrogen Degradation of Ferrous Alloys*, ed. R. A. Oriani, J. P. Hirth, and M. Smialowski, p. 641, Noyes Publications, Park Ridge, NJ (1985).

30. K. W. Lange and H. J. Koning, in *Proc. Second Int. Conf. on Hydrogen in Metals*, ed. P. Azou, paper 1A5 (1973).

31. W. Beck, J. O'M. Bockris, M. A. Genshaw, and P. K. Subramanyan, *Metall. Trans.* **2**, 883 (1971).

32. G. M. Pressouyre, "Role of Trapping on Hydrogen Transport and Embrittlement, " Ph. D. Thesis, Carnegie-Mellon University (1977).

33. I. M. Bernstein and A. W. Thompson, in *Proc. Symp. AIME on Advanced Techniques for Characterizing Hydrogen in Metals*, ed. N. F. Fiore and B. J. Berkowitz, p. 89, AIME (1981).

34. M. T. Wang, Technical Rept. AFML-72-102, Part I (1972); Ref. 105 in "The Stress Corrosion and Hydrogen Embrittlement Behavior of Maraging Steels," *Proc. Conf. on Stress Corrosion Cracking and Hydrogen Embrittlement of Iron-Base Alloys*, p. 798, NACE, Houston, TX (1973).

35. P. Tison, R. Broudeur, J. P. Fidelle, and B. Hocheid, in *Proc. 2nd International Congress on Hydrogen in Metals*, Vol. 2, paper 1A4, International Assoc. for Hydrogen Energy, Pergamon Press, New York (1977).

36. D. P. Dautovich and S. Floreen, in *Proc. Conf. on Stress Corrosion Cracking and Hydrogen Embrittlement of Iron-Base Alloys*, ed. R. W. Staehle, J. Hochman, R. D. McCright, and J. E. Slater, NACE, p. 798, Houston, TX (1977).

37. T. J. McCaffrey, *Advanced Maters. Processes*, 1992, **9**, 47.

38 A. W. Thompson and I. M. Bernstein, in *Advances in Corrosion Science and Technology*, ed. R. W. Staehle and M. Fontana, p. 53, Plenum Press, New York (1979).

39. B. G. Pound, R. M. Sharp, and G. A. Wright, *Acta Metall.* **35**, 263 (1987).

40. D. H. Lassila and H. K. Birnbaum, *Acta Metall.* **35**, 1815 (1987).

41. T. M. Harris and R. M. Latanision, in *Proc. Fourth Int. Conf. on Hydrogen Effects on Material Behavior*, ed. N. R. Moody and A. W. Thompson, p. 133, The Minerals, Metals & Materials Society, Warrendale, PA (1990).

42. S. M. Bruemmer, R. H. Jones, M. T. Thomas, D. R. Baer, *Metall. Trans.* **14A**, 223 (1983).

Table 1. Alloy composition (wt%)

Element	X-750	18Ni (250)	18Ni (300)
Al	0.75	0.10	0.13
B	0.0045	0.003	0.003
C	0.04	0.002	0.009
Co	0.02	7.85	9.15
Cr	15.76	0.23	0.06
Cu	0.01	0.12	0.11
Fe	8.33	67.73	66.51
Mn	0.04	0.03	0.01
Mo	-	4.83	4.82
Nb	0.86	-	-
Ni	71.49	18.56	18.42
P	0.004	0.005	0.004
S	0.001	0.0005	0.001
Si	0.04	0.07	0.04
Ti	2.68	0.47	0.65
Other		0.050 Ca	0.05 Ca
		0.020 Zr	0.01 W
			0.02 Zr

Table 2. Values of k_a for alloy X-750

Condition	Test no.	η range (V)	No. of k_a values	k_a (s^{-1})
Unaged	1	-0.15 to -0.30	4	0.055 ± 0.001
	2	-0.10 to -0.15	2	0.060 ± 0.003
Aged	1	-0.20 to -0.25	2	0.058 ± 0.005
	2	-0.20 to -0.25	2	0.058 ± 0.003
	3	-0.25	1	0.059
	4	-0.25	1	0.062

Table 3. Values of k_a for 18Ni (250) maraging steel

Condition	Test no.	η range (V)	No. of k_a values	k_a (s^{-1})
Unaged	1	-0.15 to -0.30	3	0.033 ± 0.001
	2	-0.15 to -0.25	3	0.031 ± 0.002
Aged	1	-0.20 to -0.25	2	0.006 ± 0.000
	2	-0.10 to -0.20	3	0.006 ± 0.001

Table 4. Trapping parameters for Ni-containing alloys

Alloy	Condition	k_a (s^{-1})	D_L/D_a	k (s^{-1})
X-750	Unaged	0.057 ± 0.002	1.4 ± 0.3	0.080 ± 0.022
	Aged	0.059 ± 0.003	2.4 ± 0.6	0.142 ± 0.042
625	17% cold work	0.004 ± 0.002	3.6 ± 0.8	0.014 ± 0.010
925	Aged	0.006 ± 0.003	5.6 ± 0.6	0.034 ± 0.004
718	Aged	0.031 ± 0.002	4.0 ± 0.5	0.124 ± 0.024
18Ni (250)	Unaged	0.032 ± 0.002	4.0 ± 1.6	0.128 ± 0.059
	Aged	0.006 ± 0.001	167 ± 45	1.00 ± 0.43
18Ni (300)	Aged[a]	0.005 ± 0.002	294 ± 76	1.47 ± 0.97

[a] Aged at the same temperature (482°C) used for the 250 grade, but aging time was 6 h rather than 4 h.

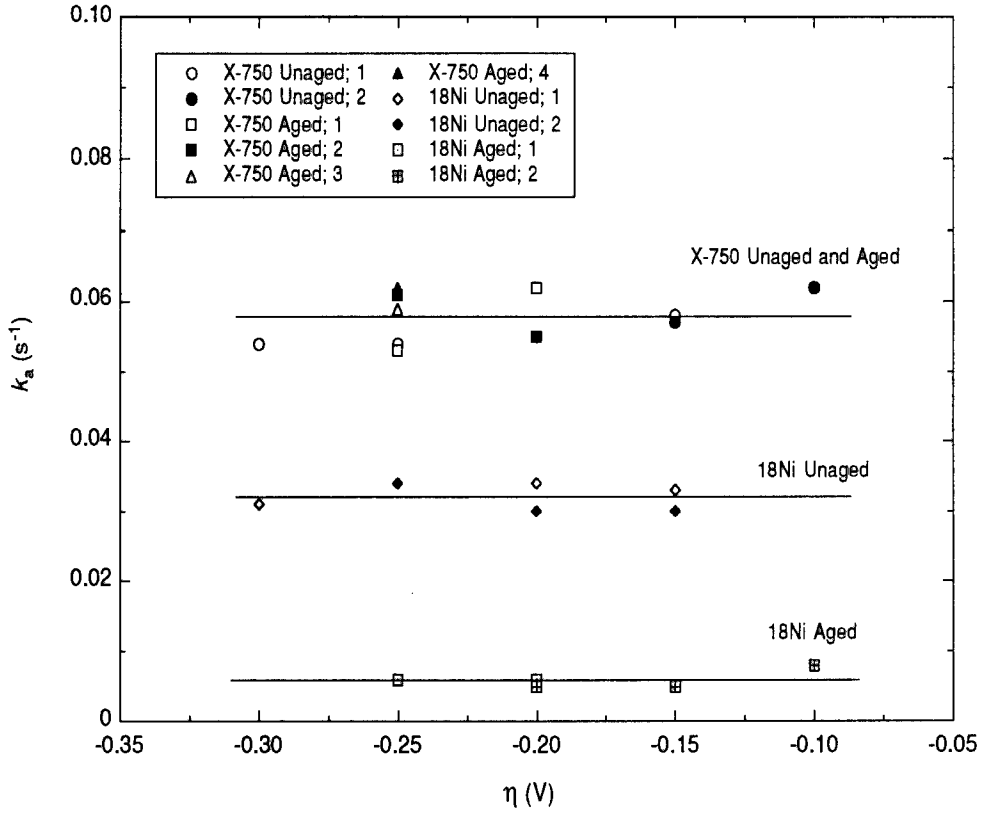

Figure 1. Values of k_a for alloy X-750 and 18Ni (250) steel at various overpotentials.
Each symbol is identified by the aged/unaged condition and a test number for that condition.

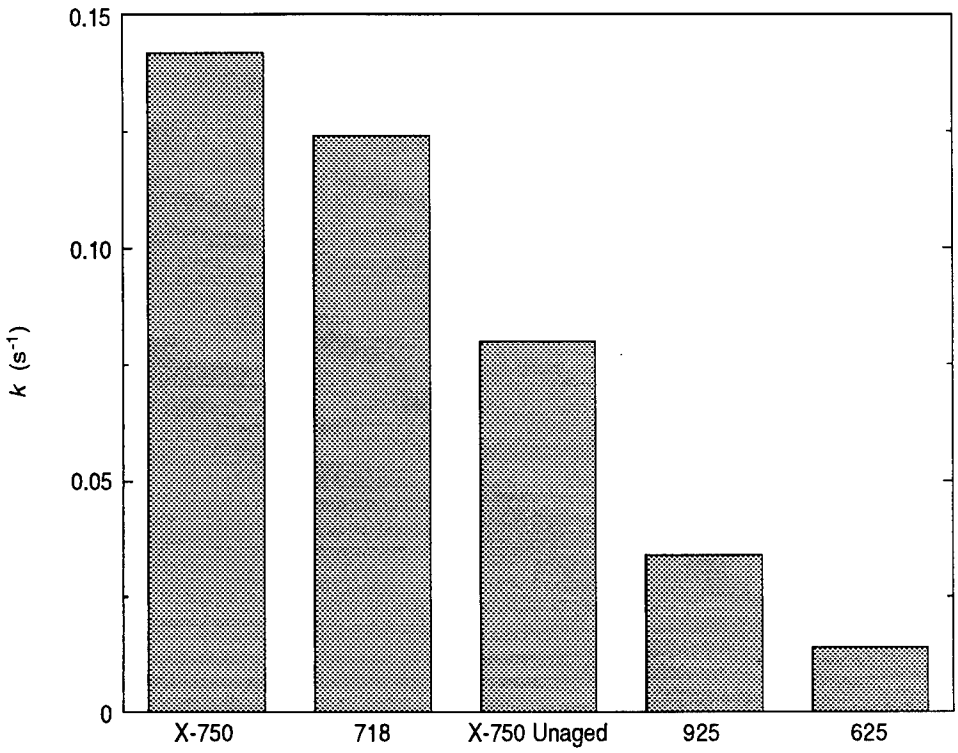

Figure 2. Variation in k for carbide-containing Ni-base alloys.

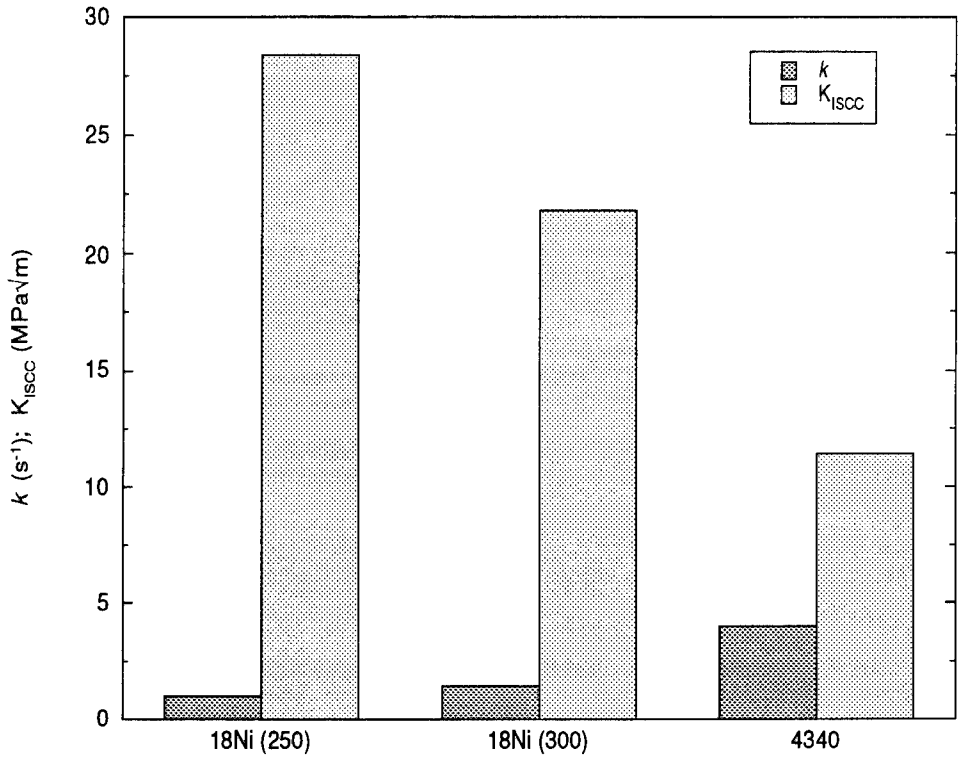

Figure 3. Comparison of k with K_{ISCC} for 18Ni steel and 4340 steel.
The K_{ISCC} data were taken from Refs. 36 and 37.

The Effect of Heat Treatment on Hydrogen Trapping in AerMet 100 and Alloy K-500*

ABSTRACT

The effect of heat treatment on irreversible hydrogen trapping was investigated for AerMet 100 and alloy K-500. A potentiostatic pulse technique was used to determine irreversible trapping constants (k) and H entry fluxes. Irreversible trapping in AerMet 100 varies with aging temperature. The order of k values for AerMet 100 and other high-strength steels inversely parallels their threshold stress intensities for stress corrosion cracking. The type of heat treatment used for alloy K-500 can also produce marked differences in irreversible trapping. The values of k for annealed-aged and direct-aged specimens were found to correlate with their observed resistances to hydrogen embrittlement.

INTRODUCTION

Various high-strength alloys are used by the Navy for fasteners and aircraft components such as landing gear and arresting hooks. These alloys must meet stringent requirements with respect not only to strength but also to resistance to environmentally assisted cracking. One of the alloys developed for aerospace applications is a martensitic steel—AerMet 100—that is strengthened by precipitation of M_2C carbides (M = Mo and Cr, with Fe also being identified in one study).[1,2] This steel is reported to have a higher resistance to hydrogen-assisted cracking in 3.5% NaCl than 18Ni maraging steel, 300M, and AISI Types 4340 and H11 steel.[3,4] However, precipitation-hardened, martensitic iron-base alloys as a group tend to be rather prone to hydrogen embrittlement (HE).[5,6]

Another type of alloy, the age-hardenable Ni-Cu alloy K-500, is used extensively for seawater applications where strength is a critical factor. However, aging can render the alloy more susceptible to HE, depending on the type of heat treatment.[7] Tests on cold worked alloy K-500 have shown that the ultimate tensile strength of annealed and aged (AA) specimens which were cathodically precharged for 16 days decreased by 35%, whereas the strength of the direct-aged (DA) alloy actually increased slightly. Thus, alloys, such as the high-strength steels and alloy K-500, that are of interest in their aged conditions continue to be of considerable concern regarding the possibility of HE.

The resistance of an alloy to HE is strongly affected by the interaction of hydrogen (H) with microstructural defects that act as H traps.[8] The local concentration of H trapped at a defect must reach some critical level (C_k) for cracks to be initiated.[8,9] The magnitude of C_k depends on factors such as the size and location of the defect. Thus, the type of defect can play a crucial role in determining an alloy's intrinsic susceptibility to HE, with large irreversible (high binding energy) traps typically imparting a high susceptibility.[9,10]

Over the last few years, H trapping in various high-strength alloys has been investigated at SRI by using a potentiostatic pulse technique.[11-15] The alloy of interest is cathodically charged with H at a constant potential for a given time. The potential is then stepped in the positive direction, so

* Published in *Proceedings of the 1997 Tri-Service Conference on Corrosion* (Wrightsville Beach, NC, 1997).

that H diffuses back to the entry surface and is reoxidized. The resulting anodic current transients obtained for different charging times are analyzed by using a diffusion/trapping model to determine values of the irreversible trapping constant (k) and H entry flux (J). The results show, for most of the alloys studied, a correlation between the intrinsic susceptibility, as represented by k, and the actual resistance to HE observed in mechanical tests. This correlation applies only to the specific alloys tested in their particular thermomechanical conditions and may not extend to these alloys at lower yield strengths or to other alloys. Exceptions to the correlation can occur, for example, when the entry flux is so low that it becomes the primary factor in determining the resistance to HE.

The correlation appears to apply to a range of alloys, including steels, Ni-base alloys, and Cu-Ni alloys. However, it has not been determined to what extent this correlation applies, particularly with respect to an alloy that is heat treated under different conditions. In the present work, the pulse technique was used to investigate the effect of heat treatment on irreversible trapping in AerMet 100 and alloy K-500. The variation in k was examined as a function of yield strength for AerMet 100 and type of heat treatment (direct aging versus annealing and aging) for alloy K-500. AerMet 100 extends the range of high-strength steels (4340, H11, and 18Ni) examined previously,[11, 12, 15] while alloy K-500 with different heat treatments provided a comparison with specimens of this alloy that had already been studied.[14, 15] The results were intended to characterize the intrinsic susceptibility of AerMet 100 and alloy K-500 to HE in terms of their irreversible trapping constants and to elucidate whether heat treatment has a large influence on the resistance of these alloys to HE.

ANALYSIS

Trapping Constants

The current transients obtained by the pulse technique were analyzed using a model that allows for the effect of trapping on diffusion for cases involving either a constant concentration or a constant flux at the input surface.[11, 16] In contrast, most, if not all, models for permeation methods are based solely on an input boundary condition of constant concentration. The permeation models thus strictly apply only for charging conditions without any entry limitation.

The constant flux model for analyzing the pulse data has been found to apply to all alloys studied to date. In this model, the rate of H ingress is controlled by diffusion, but the entry flux of H is restricted, which results in interface-limited diffusion control. Solution of the diffusion equation for a constant flux condition gives the following expression for the anodic charge (C m^{-2}):

$$q'(\infty) = FJ\, t_c\{1 - e^{-R}/(\pi R)^{1/2} - [1 - 1/(2R)]\mathrm{erf}(R^{1/2})\} \quad (1)$$

where F is the Faraday constant, J is the entry flux in mol m^{-2} s^{-1}, $R = k_a t_c$, and k_a is an apparent trapping constant measured for irreversible traps in the presence of reversible traps. The charge $q'(\infty)$ is equated to the charge (q_a) passed during the experimental anodic transients. q_a can be associated entirely with absorbed H, because the adsorbed charge is almost invariably negligible. For the constant flux model to apply, it must be possible to determine a value of k_a for which J is independent of charging time at each potential. Also, the model requires that k_a be independent of charging potential (except when a change in trapping behavior occurs), because the trapping

characteristics should be unaffected by electrochemical conditions unless the traps become filled to a significant extent.

Intrinsic Susceptibility to HE

k_a is related to the irreversible trapping constant (k) by kD_a/D_L, where D_a is the apparent diffusivity and D_L is the lattice diffusivity of H. The magnitude of k depends on the density of particles or defects (N_i) providing irreversible traps, the radius (d) of the trap defects, the diameter (a) of the metal atom, and D_L:[17]

$$k = 4\pi d^2 N_i D_L / a \qquad (2)$$

The term d^2N_i can be used to represent the trapping capacity and thus provides a basis for proposing k as an index of an alloy's intrinsic susceptibility to HE. It has long been recognized that the susceptibility is affected by a wide range of factors, but some of them would be expected to exert a greater influence than others and so be primarily responsible for determining the susceptibility. The correlation observed between k and the actual resistance to HE suggests that k contains enough key parameters to be effective as an index of susceptibility for the alloys studied to date at their respective yield strengths. Parameters other than those above may well assume a greater role at low yield strengths, such that k becomes inadequate as an index of susceptibility.

Trap size is a particularly important parameter because of the strong influence that it has on the critical concentration. At C_k, the trapped hydrogen causes enough of an increase in the induced and applied stresses and/or the hydrogen pressure to overcome the cohesive strength, which itself may be decreased.[18] The capability of large irreversible traps to impart a high intrinsic susceptibility results from their relatively high probability of being located in a crack-sensitive region and therefore of being associated with low values of C_k.[8] In contrast to large traps, irreversible traps that are finely and homogeneously distributed may delay the onset of cracking.[9] However, small irreversible traps can also be detrimental—that is, have a low C_k—if they lie in a vulnerable region such as a grain boundary.

Hydrogen is generally distributed within an alloy over a range of metallurgical sites with different interaction (and binding) energies.[19] However, these energies tend to fall into reasonably well-defined groups. In steels, for example, the interaction energy is ≤29.9 kJ/mol for most solute elements, dislocations, and grain boundaries; 53.1-58.9 kJ/mol for high angle grain boundaries; but somewhat higher for particle-matrix interfaces associated with MnS, Fe_3C, and TiC (up to 94.6 kJ/mol for incoherent particles). Thus, in terms of irreversible traps, only a few types of microstructural heterogeneities are usually important, these being primarily particle-matrix interfaces. More importantly, within a group of irreversible traps of similar interaction or binding energies, the relative contribution of each type of heterogeneity to k is determined by its size and density.

The effect of small irreversible traps on the value of k is a critical issue with respect to HE susceptibility. Homogeneously distributed, small particles (<<1 μm for α-Fe) that are irreversible traps can be beneficial in terms of delaying crack initiation, as noted above. Because of their small size, these particles are more likely to be associated with high values of C_k.[20] Moreover, the particles are supposedly small enough to limit their concentration of trapped H such that it cannot

reach C_k. Thus, the presence of small particles would not be expected to increase the intrinsic susceptibility (as determined by the irreversible traps) or, as a consequence, decrease the observed resistance to HE. Accordingly, k will not reflect the intrinsic susceptibility correctly when *only* small traps are present; the relationship between k and $N_i d^2$ implicitly applies to particles that are large enough for C_H to reach C_k. Neverthless, it should be noted that the presence of irreversible traps alone does not necessarily result in a high trapping constant; since k (and k_a) is proportional to d^2, small particles and other heterogeneities, even if numerous, may be associated with a relatively low value of k.

Previous results obtained with the pulse technique indicated that k is generally a reliable index of intrinsic susceptibility for engineering alloys containing a *range* of irreversible traps. In practice, most irreversible traps are characterized by large specific saturabilities, as noted by Gibala and DeMiglio.[21] The majority of the engineering alloys in the pulse tests contained carbides, carbonitrides, or sulfides that were in the form of large particles (>1 μm and typically several micrometers). Because of their density and size, these particles would be expected to have the predominant influence on the value of k. The trap density calculated using Eq. (2) was in fact found to be in good agreement with the actual concentration of particles for a number of the alloys, which indicated that it was these large particles that provided the *principal* irreversible traps.[13] Such particles are known to increase the extent of H damage in an alloy, particularly if they are distributed heterogeneously.[9] Thus, the addition of large traps gives a higher k value and is expected to cause a corresponding decrease in the actual resistance to HE, which fits with the observed correlation. Although a range of traps may be present in the alloys, the ability of the carbides and other particles to accumulate large amounts of H makes them likely sites for crack initiation.

The contribution of small particles to k in the case of most engineering alloys appears to be overwhelmed by that of larger particles, such that k correlates with the observed resistance to HE. However, this correlation may not hold for some alloys because the effect of large detrimental traps on the resistance to HE is delayed by a slow rate of H accumulation, which in turn is caused by either a restricted H entry into the alloy or the presence of a high density of small, homogeneously distributed, reversible or irreversible, trap heterogeneities.

EXPERIMENTAL PROCEDURE

Alloys

Table 1 shows the compositions of AerMet 100 and the other steels—4340, H11, and 18Ni. The AerMet 100 was supplied as 1.36-cm-diameter rod in an annealed/overaged (677°C/16 h) condition. A section of rod was subsequently solution treated at 885°C for 1 h, air cooled to 66°C over 1-2 h, further cooled to -73°C for 1 h, and finally aged for 5 h at temperatures of 270°, 370°, and 482°C, which is the standard aging temperature.

The microstructure of AerMet 100 was not examined in this study, because it has been investigated in detail by other workers.[1,2] The alloy has an Fe-Ni lath martensite structure. Fe_3C precipitates were found in alloy aged between 316° and 482°C but not at 204°C, which suggests that they can be formed somewhere in the range from 204° to 316°C. Aging at temperatures above 454°C causes precipitation of coherent M_2C carbides within the martensite, as noted above. Novotny found that the M_2C carbides produced by a 482°C/5 h age are well-dispersed, very fine,

rod-shaped precipitates with an average length of 9.1 nm.[2] Similar observations were made by Ayer and Machmeier, who reported the carbides as having a length of ~8 nm and a diameter of ~3 nm.[1] Ayer and Machmeier found that the M_2C carbides contained Cr, Mo, and Fe and that there was no Fe_3C, at least at the grain boundaries, in a 482°C-aged sample. In contrast, Novotny reported that only Mo and Cr constituted the metallic components in the M_2C carbides and that rod-shaped Fe_3C precipitates (40 nm long × 5 nm wide) were present. AerMet 100 also contains ~3 vol.% austenite as quenched and when aged for 5 h at temperatures from 93° to 468°C. Aging at 482°C increased the amount of austenite slightly to 4 vol.%. The austenite is present as a thin film (~3 nm) at the martensite lath boundaries.

Table 1 also gives the compositions of cold drawn (CD) alloy K-500 and the annealed and aged alloy (in two heats, denoted as AA-1 and AA-2)(1) used previously.[15] AA-1 and AA-2 were supplied as sections of bar that had been solution-annealed and aged at 607°C for 16 h to give a yield strength in the range 689-724 MPa. The alloys had a similar bulk composition, but the AA-2 alloy exhibited a moderate amount (~20%) of graphitic C at the grain boundaries, whereas the AA-1 alloy contained only a small amount (1-3%) of grain boundary C.[22]

The CD alloy K-500 was supplied as a 1.27-cm-diameter rod, which was direct aged (DA) in the previous work to give a yield strength of about 1096 MPa. The aging treatment followed the procedure recommended for CD rods ≤3.8 cm in diameter: Heat at 600°C for 8 h and then cool to 480°C at a rate of 11°C/h.[23] In the present work, the CD alloy was annealed at 982°C and, where relevant, aged at 600°C. The alloy was tested in four conditions: (1) annealed for 0.5 h, (2) annealed for 0.5 h and aged for 8 h, (3) annealed for 0.5 h and aged for 16 h, and (4) annealed for 0.25 h and aged for 8 h. These conditions are denoted as 0.5h-A, 0.5h-AA, 0.5h-AA-16h, and 0.25h-AA, respectively. During aging, particles of $Ni_3(Ti,Al)$ are precipitated throughout the matrix of alloy K-500.[23]

Electrochemical Tests

Details of the electrochemical cell and instrumentation have been given previously.[11] The test electrodes consisted of a 1.27-cm length of rod press-fitted into a polytetrafluoroethylene sheath so that only the planar end surface was exposed to the electrolyte. The surface was polished before each experiment with SiC paper followed by 0.05-μm alumina powder. The electrolyte contained 1 mol L^{-1} acetic acid and 1 mol L^{-1} sodium acetate (pH 4.8) with 15 ppm As_2O_3 and was deaerated continuously with argon before and throughout data acquisition. The potentials were measured with respect to a saturated calomel electrode (SCE). All tests were performed at 22° ± 1°C.

The test electrode was cathodically charged with H at a potential E_c for a time t_c, after which the potential was stepped anodically to a value 10 mV negative of the open-circuit potential E_{oc}. Anodic current transients were obtained over a range of charging times, typically from 5 to 60 s, at different overpotentials ($\eta = E_c - E_{oc}$). The open-circuit potential of the test electrode was measured immediately before each charging time and was also used to monitor the stability of the alloy surface.

(1) Provided by Dr. M. Natishan, University of Maryland, while at the David Taylor Research Center, Department of the Navy.

RESULTS

For alloy K-500 and aged AerMet 100, Eq. (1) could be fitted to the experimental data for q_a to obtain values of k_a and J where J was independent of charging time. For overaged AerMet 100, q_a increased linearly with t_c, indicating that $k_a = 0$ and therefore that irreversible trapping was negligible. Tables 2 and 3 show the number of tests and range of overpotentials used for AerMet 100 and alloy K-500, respectively. Also listed are the number of k_a values and the mean k_a obtained for each test.

The values of k_a for aged AerMet 100 are presented in Figure 1. In all the tests, k_a was independent of charging potential, as is required for the model to be valid. The aged alloy, in contrast to the overaged alloy, exhibited moderately high values of k_a, which were indicative of pronounced irreversible trapping. However, raising the aging temperature from 270° to 370°C did not have a significant effect on k_a, whereas it was increased considerably by aging at the standard temperature of 482°C. The overall mean value of k_a for each aging temperature is given in Table 4, which shows that k_a for the 482°-aging is 50% higher than the value for the two lower aging temperatures.

The values of k_a for alloy K-500 in each condition are given in Figure 2. k_a was independent of charging potential also for this alloy. Annealing increased k_a, with the unannealed DA alloy having the lowest value, followed by the 0.25-h-annealed alloy and then the 0.5-h-annealed alloy. The overall mean values of k_a listed in Table 4 show that k_a is more than doubled by a 0.25-h anneal and is tripled by a 0.5-h anneal. In contrast, k_a was essentially independent of aging time (such that it was the same within experimental uncertainty) for all conditions involving a 0.5-h-anneal.

DISCUSSION

Irreversible Trapping Constants

Irreversible trapping constants (k) were calculated from the mean values of k_a by correcting for the effect of reversible traps. The correction is made using diffusivity data for the "pure" alloy to obtain the lattice diffusivity (D_L) and for the actual alloy to obtain the apparent diffusivity (D_a). From the viewpoint of diffusivity, the "pure" alloys were assumed to be 65Ni-35Cu for alloy K-500 and Fe-11Ni-3Cr for AerMet 100. (Although Co is a prominent alloying element in AerMet 100, it is regarded as an anti-trap in Fe[8] and has been shown to have little effect on the diffusivity[24]). Minor elements (either in their atomic form or as intermetallics precipitated during aging) in the actual alloys were treated as reversible traps and in fact were assumed to be primarily responsible for reversible trapping.

For body-centered cubic (bcc) Fe, elements such as Cr can have a marked effect on the diffusivity of H.[25] For example, the addition of 5 at% Cr to Fe decreases the diffusivity by over two orders of magnitude at 27°C. Although AerMet 100 differs in having a martensitic lattice and in Cr being considered one of the its major elements, minor elements that act as reversible traps could also be expected to have significant but smaller effects in this alloy. Moreover, based on the case of Cr, even these reduced effects are likely to be large enough to dominate those from microstructural defects such as dislocations. The austenite present at lath boundaries may provide

reversible traps in the actual alloy, but the small amount (3-4 vol%) suggests that the effect of the austenite should be small enough to ignore, particularly for a martensitic lattice. The contribution of the martensitic lattice itself is discussed below.

For face-centered cubic (fcc) alloys, defects such as vacancies or edge dislocations were presumed to make a negligible contribution to reversible trapping, because the binding energy of H to such defects is considerably smaller than the activation energy for diffusion.[26, 27] Thus, reversible trapping in alloy K-500, which has an fcc lattice, should be influenced more by composition than by microstructural defects.

AerMet 100 — The diffusivity was not available for martensitic Fe-11Ni-3Cr, so a value was estimated for D_L from data for ferritic Fe-3Cr.[25] The diffusivity for Fe-3Cr is $(7.5 \pm 0.5) \times 10^{-11}$ $m^2 s^{-1}$, which approaches the diffusivities for quenched and tempered martensitic steels (even with reversible traps) such as 4340 (1.4×10^{-11} $m^2 s^{-1}$)[28] and thus suggests that the decrease caused by the Cr is enough to effectively incorporate that resulting from the martensitic lattice of AerMet 100. The effect of Ni on the diffusivity for Fe is much smaller than that of Cr; for example, 5Ni decreases the diffusivity by a factor of only 1.3 compared with ~140 for 5Cr.[25, 29] Hence, it was assumed that the effect of 11Ni on the diffusivity could be neglected. The presence of two phases (α and γ) in Fe-Ni alloys containing between 10 and 33% Ni[30] was ignored for the purposes of estimating data for a martensitic steel. Thus, D_L was taken simply as the diffusivity for Fe-3Cr.

Diffusivity data were also not available for AerMet 100. However, the diffusivity for another high-strength steel—D6AC with a yield strength of 1550 MPa—has been studied[28] and, although this steel contains only 1.08 Cr, was considered to provide the most appropriate value of D_a. The diffusivity obtained from electrochemical permeation measurements for D6AC is $(7.8 \pm 0.5) \times 10^{-12}$ $m^2 s^{-1}$. Thus, a value of 9.6 was obtained for D_L/D_a and was used to calculate values of k for AerMet 100, as given in Table 4. The same value of D_L/D_a was assumed to apply to the overaged alloy and the partially and standard (482°C) aged alloy, because the Fe_3C and M_2C particles precipitated during aging were considered irreversible traps[19] (discussed below) and therefore should not affect D_a as measured when only reversible traps are effective (irreversible traps being saturated).

Alloy K-500 — The lattice diffusivity was determined by interpolation of data for a range of binary Cu-Ni alloys and was found to be $(3.0 \pm 0.1) \times 10^{-14}$ $m^2 s^{-1}$ for 65Ni-35Cu at 25°C.[31] The level of Cu differs slightly between the 65Ni-35Cu alloy and actual alloy K-500 (30Cu), but the error in using the diffusivity of the 35Cu alloy for D_L was considered negligible. The apparent diffusivity for AA alloy K-500 (assumed to be at ambient temperature) is 1.90×10^{-14} $m^2 s^{-1}$, which is only slightly higher than the value of 1.48×10^{-14} $m^2 s^{-1}$ for the DA alloy.[7] These data were used to calculate values of k for the AA and DA alloys, as given in Table 4.

No data were available for the diffusivity for the annealed (unaged) alloy, so D_a was estimated from the values for the aged alloy. The intermetallic particles precipitated during aging appear to have little effect on D_a compared with that of the minor alloying elements in solid solution: D_a for the DA alloy was only about a factor of 2 smaller than D_L. Because most solutes introducing an electron vacancy provide reversible traps that could largely account for this factor, the intermetallics must be presumed to add little to the effect of the minor elements. Hence, it was assumed that D_a for the annealed alloy could be approximated to that for the AA alloy. By using this value and the D_L above, k was calculated for the annealed alloy (Table 4).

Susceptibility to HE

AerMet 100 — The trapping constants for AerMet 100 are compared with those for the three other steels (4340, H11, and 18 Ni) in Table 4. AerMet 100 has the lowest k value and is therefore considered to have the lowest intrinsic susceptibility to HE of the four steels. The order of the k values for these steels inversely parallels typical values of their threshold stress intensities for stress corrosion cracking (K_{ISCC}) in 3.5% NaCl[3,4] (Figure 3); that is, a lower value of k corresponds to a higher value of K_{ISCC}. This trend is underscored by the similarity in k values matching the similarity in K_{ISCC} values for the two most susceptible steels—4340 and H11. The k values indicate that the intrinsic susceptibility may actually be a little lower for H11. The order of this difference is consistent with test results showing that, for these two steels in distilled water, the failure times at various applied stress intensities were longer for H11.[32] Furthermore, the value of k for H11 is consistent with that for 18Ni steel in terms of the degree of embrittlement observed in electrolytic charging tests.[33]

The parallel between k and K_{ISCC} supports the general view that hydrogen plays the predominant role in stress corrosion cracking of martensitic steels.[34] Thus, for these four steels, k can be correlated with the observed resistance to HE, as represented by K_{ISCC}. This correlation provides additional support for the concept of k as an index of intrinsic susceptibility for high-strength alloys. In addition, it implies that the intrinsic susceptibility is a primary—possibly the predominant— factor determining the observed resistance of these high-strength steels to HE.

Figure 4 compares the dependence of k on aging temperature with a typical dependence of yield strength, as reported by the alloy producer.[35] k clearly follows the general trend in yield strength, exhibiting an initial increase before leveling off and then increasing more sharply. The changes in the two curves match reasonably well with respect to aging temperature, bearing in mind that the yield strength curve is not specific to either the form or size of alloy used in these tests. The increase in k with aging temperature, particularly between 370° and 482°C, implies that the observed resistance to HE should decrease based on the correlation between k and K_{ISCC}. Such a decrease would be consistent with the decreases in HE resistance observed for 4340 steel and 18Ni maraging steel as their yield strengths are increased.[6,36] Bernstein and Thompson have shown, however, the resistance to HE to be more directly an effect of microstructure than of strength.[34,37] Thus, k would not necessarily be expected to show a correlation with yield strength. Clearly, the more appropriate comparison is between k and the microstructural changes that occur during aging.

Figure 5 shows the variation in k and carbide size with aging temperature. The increase in k occurs in two stages. The first stage corresponds to Fe_3C precipitation and the second stage corresponds to M_2C precipitation. The arrest in k between 270° and 370°C coincides with the aging temperature range where the Fe_3C particles do not change in size. Furthermore, the subsequent steep increase in k occurs with the transition in carbides from Fe_3C to M_2C and evidently reflects the sharp increase in size of the M_2C particles. Possibly, the lath boundary austenite provides irreversible traps and hence that the higher k at 482°C resulted from the increase in austenite. However, the increase was only from 3 vol% to 4 vol%, and also k~0 for the unaged alloy with its 3 vol% austenite.(1) Another possibility is that impurities such as S and P segregate to grain boundaries during aging, thereby causing an increase in the irreversible trapping capability. Nevertheless, the M_2C particles remain most likely responsible for the increased k at

(1) Any additional reversible trapping caused by the slightly higher level (1 vol%) of austenite in the standard aged alloy would decrease D_a and therefore increase k. Hence, the effect of aging would appear even more pronounced.

482°C. Thus, irreversible trapping in AerMet 100 appears to involve the carbides primarily, with Fe_3C particles providing the principal traps for lower aging temperatures and M_2C particles filling that role for higher aging temperatures.

The M_2C particles in AerMet 100 aged at 454°C are coherent with the matrix,[(1)] but at least some of them appear to lose coherency at 482°C.[1] The particles are therefore expected to become more irreversible as traps for higher aging temperatures.[19] Lee has shown that stress corrosion cracking in AerMet 100 proceeds intergranularly,[38] which implies that the loss of coherency must occur preferentially at grain boundaries, if the resistance to HE is governed by irreversible trapping (as indicated by the correlation with k) and if the less coherent M_2C particles are the principal irreversible traps produced by aging at 482°C.

Alloy K-500 — The values of k for the different heat treatments are presented graphically in Figure 6. Clearly, alloy K-500 can exhibit a marked difference in irreversible trapping, depending on the type of heat treatment. Annealing caused a large increase in k for CD alloy K-500 and thus is deemed to greatly heighten the instrinsic susceptibility of this alloy. In fact, the values of k for all the 0.5-h-annealed specimens—unaged or aged—were more than twice as large as that obtained for the direct-aged CD specimen. Even halving the annealing time to 0.25 h resulted in a k double that of the DA alloy and only about 20% lower than the value obtained for the full (0.5-h) annealing time. Addition of the 0.5-h-annealing step before aging the CD alloy gave the same k values as those for the annealed and (16-h) aged alloy (AA-1 and AA-2) that was obtained from two other heats and tested previously. The effect of 8-h aging on k was negligible for the annealed alloy and relatively small for the unannealed alloy. Doubling the aging time to 16 h for the annealed alloy did not affect k. Thus, the annealed alloy had similar values of k in the unaged and the aged (at least up to 16 h) conditions.

The results show that differences in irreversible trapping observed previously between the DA specimens and the AA-1 and AA-2 specimens resulted from the differences in heat treatment. Moreover, they indicate that the key factor is the annealing step rather than the aging time and that annealing has quite a pronounced effect on the irreversible trapping characteristics of alloy K-500. Lee and Latanison have shown that graphite precipitation occurs at grain boundaries in Ni 200 (≤0.15 C) aged for 24 h at 450° to 650°C.[39] The AA-1 and AA-2 specimens, however, differed in heat treatment only with respect to annealing time yet exhibited different levels of grain boundary C, which implies that annealing renders alloy K-500 more prone to graphite precipitation during aging. Thus, the higher k values for the annealed and aged alloy appears to be determined by the amount of grain boundary graphitic C.

Tensile tests on alloy K-500, as noted above, showed a difference in ultimate tensile strength between DA and AA specimens cathodically precharged for 16 days.[7] The decrease (35%) in strength of the AA alloy together with the slight increase for the DA alloy indicated that the AA alloy is less resistant to HE. The order of the k values for the two types of aged alloy K-500 thus correlate with their observed resistances to HE, implying that the decrease in the resistance to HE produced by annealing is caused, at least in part, by changes in the irreversible H traps.

---

(1) Coherent particles are likely to be more reversible in terms of trapping.[19] If the coherent M_2C particles were reversible traps, D_a would be expected to decrease as the aging temperature is increased above 454°C, and so k would increase still more sharply with aging temperature.

The yield strength of alloy K-500 also varies with the type of heat treatment and should therefore be considered as a possible factor in the resistance to HE. However, the order of the yield strengths for the AA specimens (689-724 MPa) and the DA specimen (1096 MPa) was opposite to that of their k values, which suggests that the difference in HE susceptibility does not result from yield strength.

SUMMARY

- AerMet 100 exhibited a large difference in irreversible trapping between overaged (annealed) and aged specimens. In contrast to the overaged alloy, the aged alloy displayed significant irreversible trapping, which appears to be associated with Fe_3C particles at low aging temperatures and M_2C particles at high aging temperatures. The intrinsic susceptibility (as represented by k) of AerMet 100 to HE increases with aging temperature, particularly from 370° to 482°C.

- AerMet 100 in its standard aged (482°C) condition has a lower value of k than three other high-strength steels, 4340, H11, and 18Ni maraging steel. Hence, AerMet 100 has the lowest intrinsic susceptibility to HE of the four steels, whereas H11 and 4340 steel are the most susceptible. For these four steels, the observed resistance to HE, as represented by K_{ISCC}, can be correlated with the intrinsic susceptibility defined by k.

- Irreversible trapping in CD alloy K-500 can depend strongly on the type of heat treatment. Marked differences in k between DA and AA specimens can be attributed to the annealing step rather than to aging time. The intrinsic susceptibility to HE (k) is increased considerably by annealing, whereas aging has a negligible effect for the annealed alloy and only a modest effect for the unannealed alloy.

- The intrinsic susceptibilities for AA and DA alloy K-500 can be correlated with the observed resistances to HE. Thus, the decrease produced in the HE resistance by annealing appears to result to a large extent, if not entirely, from a change in the number or the type of irreversible traps. Differences in the grain boundary chemistry resulting from heat treatment could account for changes in the type of irreversible traps.

ACKNOWLEDGEMENT

Financial support of this work by the Office of Naval Research under Contracts N00014-91-C-0263 and N00014-95-C-0313 (Dr. A. J. Sedriks, Program Officer) is gratefully acknowledged.

REFERENCES

1. R. Ayer and P. M. Machmeier, *Metall. Trans.* **24A**, 1943 (1993).
2. P. M. Novotny, in *Proc. Gilbert R. Speich Symposium: Fundamentals of Aging and Tempering in Bainitic and Martensitic Steel Products* (ISS, Warrendale, PA, 1992), p. 215.
3. T. J. McCaffrey, *Advanced Mater. Proc.* **9**, 47 (1992).
4. P. M. Novotny and J. M. Dahl, in *Proc. 32nd Conf. on Mechanical Working and Steel Processing*, Vol. XXVIII (ISS, Warrendale, PA, 1991), p. 275.
5. A. W. Thompson, *Metall. Trans.* **4**, 2819 (1973).

6. D. P. Dautovich and S. Floreen, in *Proc. Conf. on Stress Corrosion Cracking and Hydrogen Embrittlement of Iron-Base Alloys*, eds. R. W. Staehle, J. Hochman, R. D. McCright, and J. E. Slater (NACE, Houston, TX, 1977), p. 798.
7. J. A. Harris, R. C. Scarberry, and C. D. Stephens, *Corrosion* **28**, 57 (1972).
8. I. M. Bernstein and G. M. Pressouyre, in *Hydrogen Degradation of Ferrous Alloys*, eds. R. A. Oriani, J. P. Hirth, M. Smialowski (Noyes Publications, Park Ridge, NJ, 1985), p. 641.
9. G. M. Pressouyre and I. M. Bernstein, *Acta Metall.* **27**, 89 (1979).
10. G. M. Pressouyre and I. M. Bernstein, *Metall. Trans.* **9A**, 1571 (1978).
11. B. G. Pound, *Corrosion* **45**, 18 (1989).
12 B. G. Pound, *Acta Metall.* **38**, 2373 (1990).
13. B. G. Pound, in *Proc. Fifth Int. Conf. on Hydrogen Effects on Material Behavior*, eds. N. R. Moody and A. W. Thompson (TMS, Warrendale, PA, 1996), p. 115.
14. B. G. Pound, *Corrosion* **50**, 301 (1994).
15. B. G. Pound, "Characterization of Hydrogen Ingress in High Strength Alloys," Final Report, Office Of Naval Research, Contract No. N00014-91-C-0263 (1995).
16. R. McKibbin, D. A. Harrington, B. G. Pound, R. M. Sharp, and G. A. Wright, *Acta Metall.* **35**, 253 (1987).
17. B. G. Pound, R. M. Sharp, and G. A. Wright, *Acta Metall.* **35**, 263 (1987).
18. G. M. Pressouyre and I. M. Bernstein, *Metall. Trans.*, **12A**, 835 (1981).
19. G. M. Pressouyre, *Metall. Trans.* **10A**, 1571 (1979).
20. G. M. Pressouyre, in *Current Solutions to Hydrogen Problems in Steels*, eds. C. G. Interrante and G. M. Pressouyre (ASM, Metals Park, OH, 1982), p. 18.
21. R. Gibala and D. S. DeMiglio, in *Proc. 3rd Int. Conf. on Effect of Hydrogen on Behavior of Materials*, eds. I. M. Bernstein and A. W. Thompson (TMS, Warrendale, PA, 1980), p. 113.
22. M. E. Natishan, E. R. Sparks, and M. L. Tims, in *ISTFA '90: Proc. Int. Symposium for Testing and Failure Analysis* (ASM, Materials Park, OH, 1990), p. 385.
23. Monel Nickel-Copper Alloys, 4th ed. (Huntington Alloys, Huntington, WV, 1981).
24. K. W. Lange and H. J. Koning, in *Proc. Second Int. Conf. on Hydrogen in Metals*, eds. P. Azou, paper 1A5 (1973).
25. J. O'M. Bockris, M. A. Genshaw, and M. Fullenwider, *Electrochim. Acta* **15**, 47 (1970).
26. W. D. Wilson and S. C. Keeton, in *Advanced Techniques for Characterizing Hydrogen in Metals*, eds. N. F. Fiore and B. J. Berkowitz (TMS, Warrendale, PA, 1981), p. 3.
27. J. Y. Lee and S. M. Lee, *Metall. Trans.* **17A**, 181 (1986).
28. C. S. Kortovich and E. A. Steigerwald, *Eng. Fract. Mech.* **4**, 637 (1972).
29. W. Beck, J. O'M. Bockris, M. A. Genshaw, P. K. Subramanyan, *Met. Trans.* **2**, 883 (1971).
30. R. E. Ogilvie, *Trans. TMS-AIME* **223**, 2083 (1965).
31. H. Hagi, *Trans. Jpn. Inst. Metals* **27**, 233 (1986).
32. W. D. Benjamin and E. A. Steigerwald, *Metall. Trans.* **2**, 606 (1971).
33. T. P. Groeneveld, E. E. Fletcher, and A. R. Elsea, *A Study of Hydrogen Embrittlement of Various Alloys*, Summary Report, Contract NAS8-20029 (NASA, Huntsville, AL, 1966).
34. A. W. Thompson and I. M. Bernstein, in *Advances in Corrosion Science and Technology*, eds. R. W. Staehle and M. Fontana (Plenum Press, New York, 1979), p. 53.
35. Alloy Data: AerMet 100 Alloy, Alloy Steels 6 (Carpenter Tech. Corp., Reading PA, 1992).
36. G. Sandoz, *Metall. Trans.* **3**, 1169 (1972).
37. I. M. Bernstein and A. W. Thompson, *Int. Met. Rev.* **21**, 269 (1976).
38. E. U. Lee, *Metall. Mater. Trans.* **26A**, 1313 (1995).
39. T.S.F. Lee and R. M. Latanision, *Metall. Trans.* **18A**, 1653 (1987).

Table 1. Alloy Composition (wt%)

Element	AerMet 100	H11	4340	18Ni	K-500 CD	K-500 AA-1	K-500 AA-2
Al	0.005		0.031	0.13	2.92	2.95	2.95
B				0.003			
C	0.24	0.41	0.42	0.009	0.16	<0.17	<0.14
Co	13.47			9.15			
Cr	3.00	4.88	0.89	0.06			
Cu		0.03	0.19	0.11	29.99	29.53	29.8
Fe	71.00	bal	bal	bal	0.64	<0.85	<0.74
Mn	0.01	0.30	0.46	0.01	0.72	<0.70	<0.58
Mo	1.19	1.32	0.21	4.82			
Ni	11.07	0.04	1.74	18.42	64.96	65.29	65.1
P	0.002	0.011	0.009	0.004			<0.002
S	<0.0005	0.003	0.001	0.001	0.001	<0.001	<0.001
Si	<0.01	0.88	0.28	0.04	0.15	<0.05	<0.15
Ti	0.009			0.65	0.46	0.46	0.44
Other	<0.0010 N	0.45 V	0.005 N	0.01 W			
	<0.0010 O		0.001 O	0.05 Ca			
				0.02 Zr			

Table 2. Apparent Trapping Constants for Aged AerMet 100

T_{age} (°C)	Test no.	η range (V)	No. of k_a values	k_a (s^{-1})
270	1	-0.05 to -0.20	4	0.044 ± 0.005
	2	-0.10 to -0.25	2	0.044 ± 0.001
	3	-0.10 to -0.15	2	0.049 ± 0.002
	4	-0.10 to -0.20	2	0.049 ± 0.002
370	1	-0.10 to -0.20	3	0.045 ± 0.005
	2	-0.05 to -0.20	4	0.047 ± 0.002
482	1	-0.10 to -0.25	4	0.069 ± 0.006
	2	-0.20 to -0.25	2	0.069 ± 0.001

Table 3. Apparent Trapping Constants for Alloy K-500

Condition	Test no.	η range (V)	No. of k_a values	k_a (s^{-1})
0.5h-A	1	-0.30 to -0.40	3	0.065 ± 0.002
	2	-0.30 to -0.45	4	0.063 ± 0.005
	3	-0.30 to -0.40	3	0.066 ± 0.001
0.5h-AA	1	-0.25 to -0.45	5	0.064 ± 0.002
	2	-0.25 to -0.40	4	0.064 ± 0.004
0.25h-AA	1	-0.25 to -0.55	7	0.052 ± 0.004
	2	-0.25 to -0.50	3	0.051 ± 0.004
0.5h-AA-16h	1	-0.30 to -0.40	3	0.061 ± 0.001
	2	-0.30 to -0.40	3	0.066 ± 0.003

Table 4. Trapping Parameters for High-Strength Steels and Alloy K-500

Alloy	Condition	k_a (s^{-1})	D_L/D_a	k (s^{-1})
Steels				
AerMet 100	Annealed	0.000 ± 0.001	9.6 ± 1.3	0.00
	270°C-aged	0.046 ± 0.003	9.6 ± 1.3	0.44 ± 0.09
	370°C-aged	0.046 ± 0.004	9.6 ± 1.3	0.44 ± 0.10
	482°C-aged	0.069 ± 0.004	9.6 ± 1.3	0.66 ± 0.13
4340	HRC 53	0.008 ± 0.001	500	4.0 ± 0.5
H11	HRC 51	0.080 ± 0.004	43.3 ± 6.2	3.5 ± 0.7
18Ni (2068)*	482°C-aged (4 h)	0.005 ± 0.002	300 ± 90	1.50 ± 1.05
Alloy K-500				
	0.5h-A	0.065 ± 0.003	1.6	0.104 ± 0.008
	0.5h-AA	0.064 ± 0.003	1.6	0.102 ± 0.008
	0.25h-AA	0.052 ± 0.004	1.6	0.083 ± 0.009
	0.5h-AA-16h	0.063 ± 0.003	1.6	0.101 ± 0.008
	AA-2 (aged 16 h)	0.063 ± 0.003	1.6	0.099 ± 0.008
	AA-1 (aged 16 h)	0.060 ± 0.006	1.6	0.095 ± 0.013
	DA	0.021 ± 0.003	2.0	0.042 ± 0.007
	CD-Unaged	0.017 ± 0.003	2.0	0.034 ± 0.007

* Nominal yield strength in MPa.

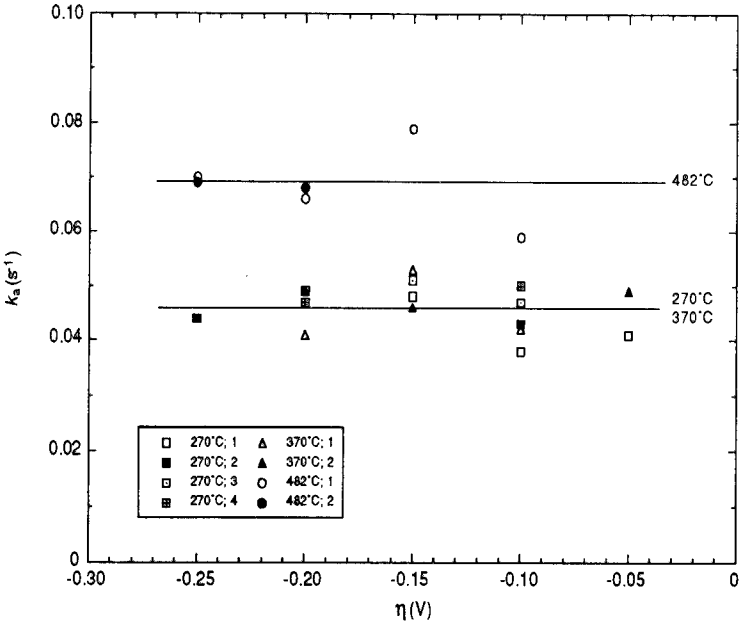

Figure 1. Values of k_a for aged AerMet 100 at various overpotentials.
Each symbol is identified by the aging temperature and a test number for that temperature.

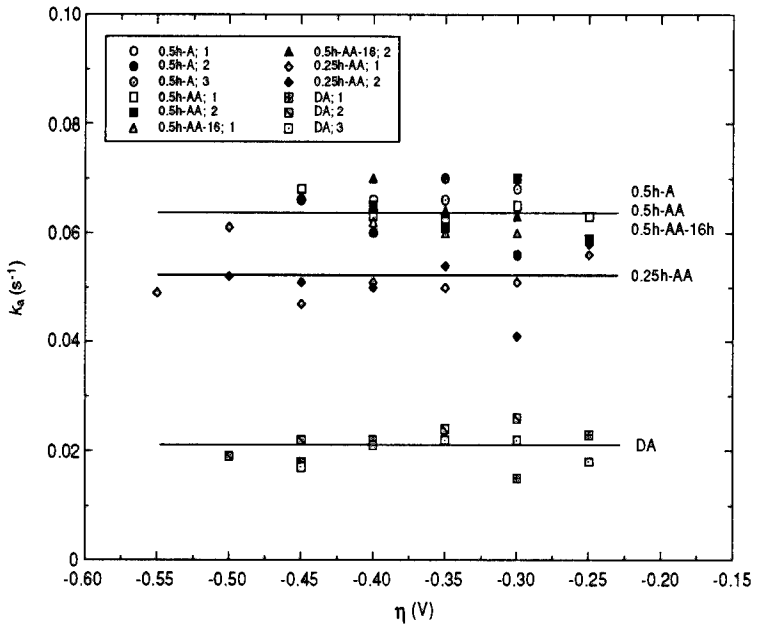

Figure 2. Values of k_a for alloy K-500 at various overpotentials.
Each symbol is identified by the heat treatment and a test number for that treatment.

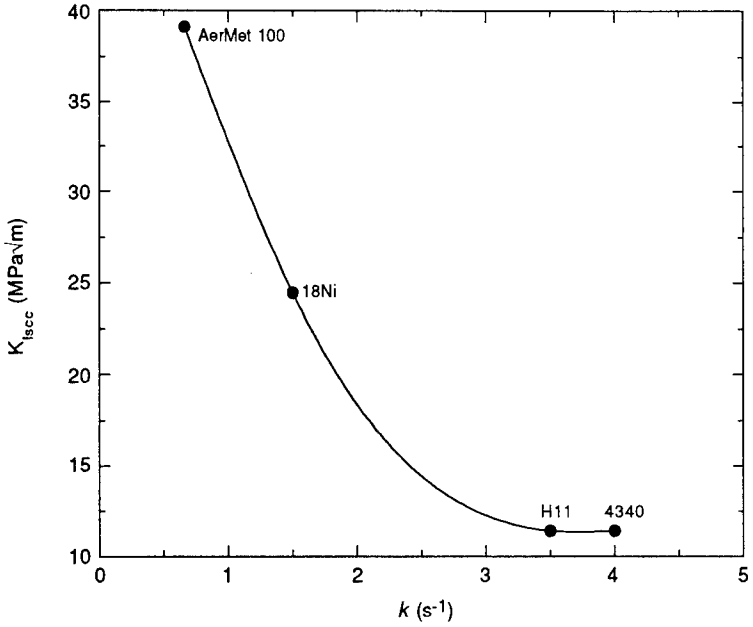

Figure 3. Variation of K_{ISCC} with k for high-strength steels. The value of K_{ISCC} for 18Ni pertains to the 1723 MPa (250 ksi) grade.

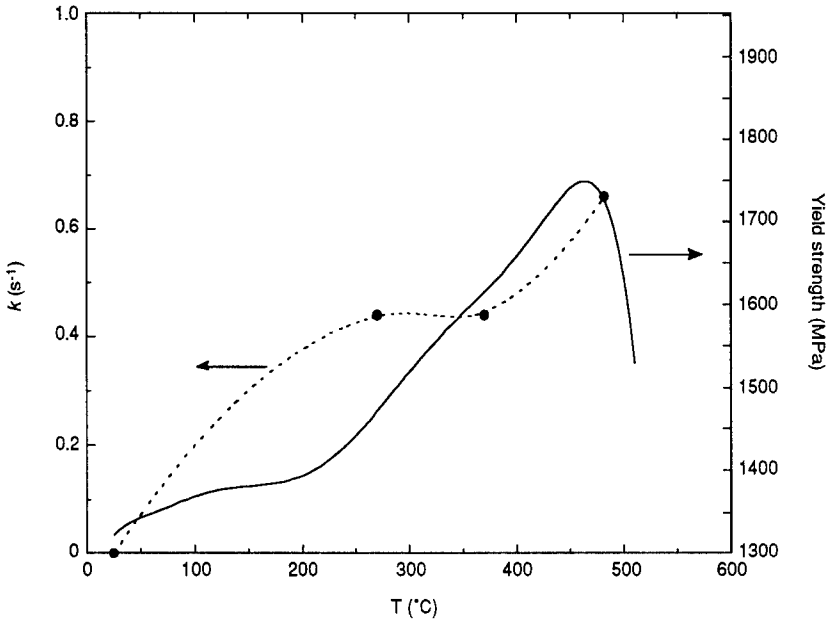

Figure 4. Variation of k and yield strength with aging temperature for AerMet 100.

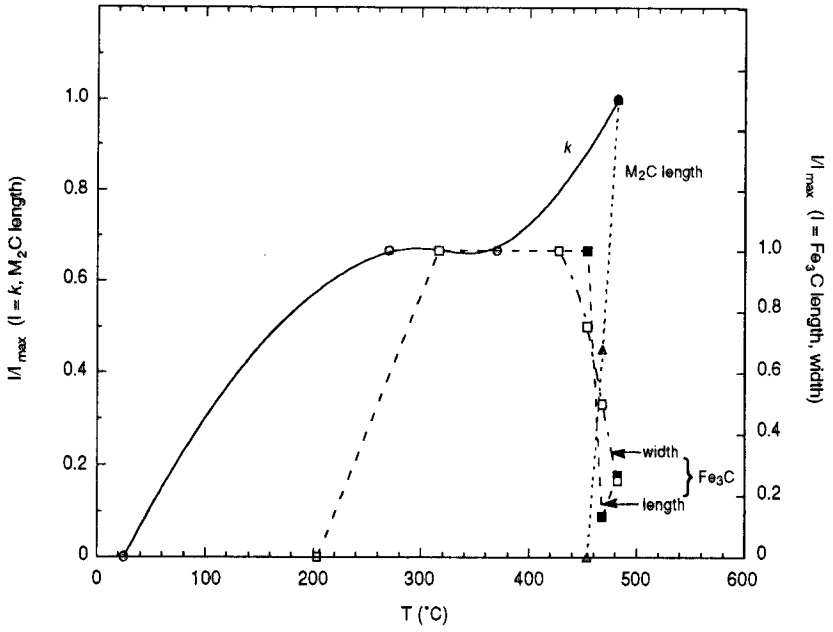

Figure 5. Variation of k and carbide size with aging temperature for AerMet 100.
The dimensions of the carbides were obtained from Ref. 2.

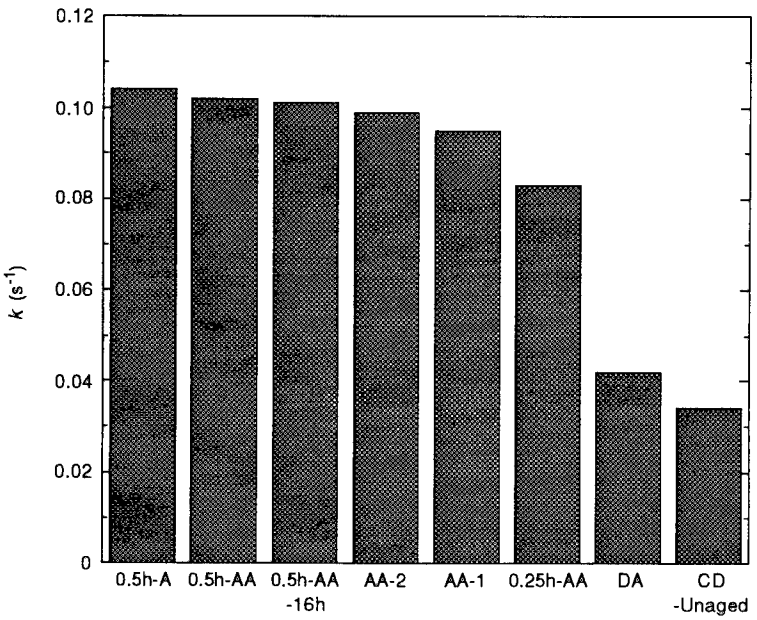

Figure 6. Variation in k for different heat treatments of alloy K-500.